CHALMERS
UNIVERSITY OF TECHNOLOGY

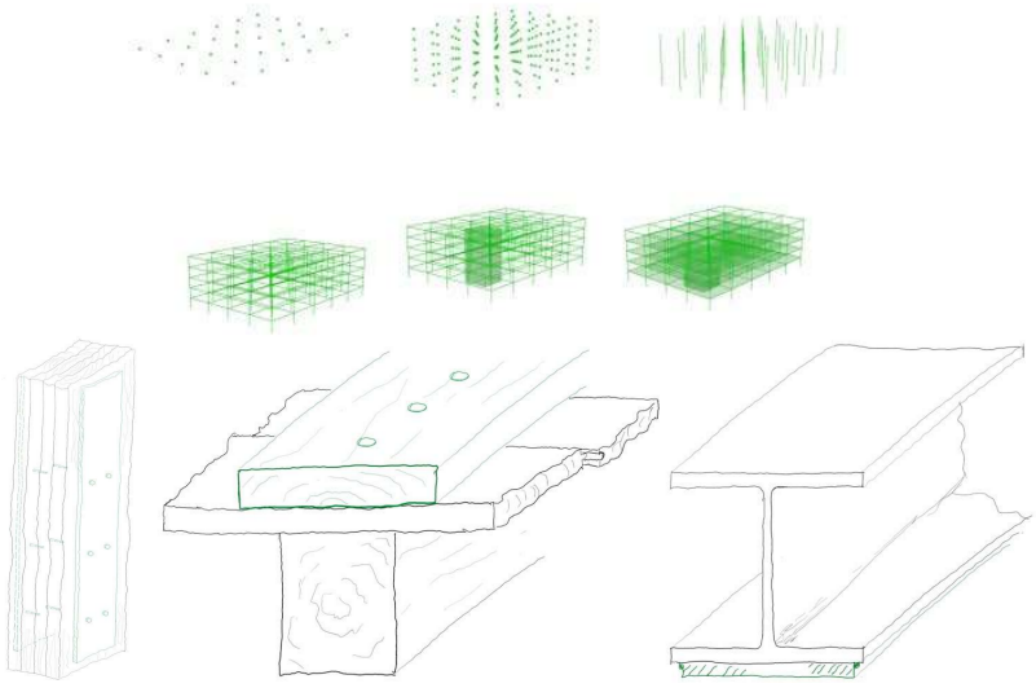

Optimisation of Structural Systems with Regards to Future Repurposiong

Current Practices and Suggestions for Improved Design Methods

Master's thesis in Master Programme Structural Engineering and Building Technology

JOHANNA NILSSON

DEPARTMENT OF ARCHITECTURE AND CIVIL ENGINEERING
CHALMERS UNIVERSITY OF TECHNOLOGY
Gothenburg, Sweden 2023
www.chalmers.se

Master's thesis 2023

Optimisation of Structural Systems with Regards to Future Repurposiong

Current Practices and Suggestions for Improved Design Methods

JOHANNA NILSSON

CHALMERS
UNIVERSITY OF TECHNOLOGY

Department of Architecture and Civil Engineering
Division of Structural Engineering
Chalmers University of Technology
Gothenburg, Sweden 2023

Optimisation of Structural Systems with Regards to Future Repurposiong
Current Practices and Suggestions for Improved Design Methods
JOHANNA NILSSON

© JOHANNA NILSSON, 2023.

Supervisor: Cecilia Hallgren, PE Teknik & Arkitektur
Examiner: Docent Ignasi Fernandez, Department Architecture and Civil Engineering

Master's Thesis 2023
Department of Architecture and Civil Engineering
Division of Structural Engineering
Chalmers University of Technology
SE-412 96 Gothenburg
Telephone +46 31 772 1000

Cover: Parametric modelling procedure together with strengthening techniques

Typeset in LaTeX
Printed by Chalmers Reproservice
Gothenburg, Sweden 2023

Optimisation of Structural Systems with Regards to Future Repurposiong
Current Practices and Suggestions for Improved Design Methods
JOHANNA NILSSON
Department of Architecture and Civil Engineering
Chalmers University of Technology

Abstract

As the climate situation becomes more critical, sustainable solutions and behavioural changes are required in all sectors and contexts. One sector that contributes significantly to greenhouse gas emissions is the building and construction sector. Therefore, it is necessary to start evaluating and rethinking how we can address the demand for new buildings in ways that are more environmentally sustainable and climate-smart compared to current methods. This involves assessing opportunities for repurposing, reuse, and refurbishment instead of demolishing and rebuilding.

The purpose of this master's thesis is to evaluate what influences the possibility of repurposing and how one can overcome these challenges in different ways. Is optimising for current purposes and later strengthening critical parts the best approach, or should one overdimension to enable future repurposing and increased flexibility?

Four different case studies were conducted to evaluate the common consequences of repurposing. The case studies were carried out for two different systems: a steel system with HDF floor slabs and a timber system with CLT floor slabs. To evaluate various situations, the studies were conducted using parametric design, with background information based on a literature review and insights from industry experts.

The results showed that there are good opportunities for strengthening measures in steel systems, making it a feasible alternative when choosing steel as a building material. It is recommended to optimise the use of materials in new constructions to apply suitable reinforcement methods during repurposing. The results also indicated that reinforcement methods for timber systems are somewhat more complicated, and there is not as much benefit in optimising current structures. Therefore, a combination of overdimensioning and subsequent reinforcement during potential repurposing is suggested.

Finally, a conclusion is drawn regarding the importance of constructing buildings in a way that allows for future reinforcement. This is crucial in determining potential future reinforcement measures' complexity, material and energy requirements.

Keywords: Sustainability, Repurposing, Optimisation, Strengthening technique, Beam-Column system

Acknowledgements

This thesis is in collaboration with the Department of Buildings at PE Teknik & Arkitektur in Gothenburg and the Department of Architecture and Civil Engineering at Chalmers University of Technology. Throughout the work of the thesis, I have had the opportunity to receive guidance from individuals to whom I would like to express my gratitude towards.

To Docent Ignasi Fernandez, I am very grateful for your involvement in this master's thesis and for the valuable feedback and guidance you provided throughout the entire process. Thanks for the opportunity.

To everyone at the PE office, thank you for your guidance and for providing important input. Thank you for sharing your valuable experiences in the field of buildings, materials, and the environment. I am extremely grateful for the opportunity to write my master's thesis with your organisation.

I would also like to extend my thanks to you, Simon Larsson and Fredrik Boman, for all the assistance with the parametric model and the programming behind it. Your help has been incredibly valuable in my work and has greatly contributed to the results I have achieved.

Finally, I would like to thank my supervisor at PE, Cecilia Hallgren, for your support throughout the work. From calculations and the development of optimisation procedures and parametric models to providing invaluable encouragement during challenging times, I am truly grateful. This work would not have been possible without you.

Johanna Nilsson

Gothenburg, June 2023

Contents

List of Figures

List of Tables

1
Introduction

Sustainability is a critical issue that requires attention. The latest report from the Intergovernmental Panel on Climate Change *(IPCC)* emphasizes the urgency of the situation and highlights the need for action across all sectors to reduce greenhouse gas emissions. Science plays a crucial role in achieving sustainability goals by providing the knowledge and technology necessary for implementing sustainable practices (Orr et al., 2021).

The construction and building sector significantly contributes to global CO2 emissions, accounting for nearly 40 % of world emissions (Orr et al., 2021). Moreover, this sector is a leading producer of waste. Designers and professionals in the field must find ways to reduce materials and resource use in order to meet the ambitious goals set by the Paris Agreement and mitigate the negative environmental impact of the construction sector.

One approach to achieve these goals is by following the waste hierarchy, which presents the preferred choices for waste reduction and sustainable decision-making. The waste hierarchy encompasses various strategies to minimize waste production and ultimately avoid building disassembly. Alongside the waste hierarchy, the report *Design for zero* presents a framework for carbon reduction potential, guiding decision-making in design and construction.

Based on this, this thesis explores the need for sustainable practices in the construction industry, particularly in relation to repurposing existing buildings. It examines the challenges and opportunities of retaining load-bearing systems in buildings during repurposing by strengthening, as this can lead to significant carbon reduction benefits by avoiding demolition. But strengthen a structural system is however far more complicated than demolishing the structural system and erecting a new one (Carolin, 2003). Hence, various strengthening techniques will be examined to identify the most suitable approach for improving future flexibility in terms of repurposing. Is over-dimensioning, design for strengthening, or material optimization the most effective solution?

1.1 Aim and Objectives

The thesis aims to examine the current design methods for structural systems of buildings and their consequences in future modifications due to repurposing. Based on this investigation, the target is to develop an enhanced design process that allows for greater flexibility in the future while still maintaining the current focus on optimization and cost-effectiveness.

To achieve the aim of the master thesis, some objectives have been defined.

1. Identify the area of study and collect general information.
2. Identify and review materials, structural elements and systems commonly used today.
3. Investigate and compare different strengthening techniques used today for:
   - Structural elements
   - Structural systems
4. Analysing the impact of repurposing due to changes of use, on structural systems and determining their performance under assumption:
   - Changes of imposed load.
   - Changes of geometry.
   - Changes of numbers of the floor.
5. Define and recommend a design procedure suitable for the design of new buildings.

1.2 Scope and Limitation

The analysis will be limited to isolated buildings in order to narrow down the scope and obtain an overall estimation of how to design for strengthening and repurposing. This limitation is implemented to achieve as similar ground conditions as possible. Additionally, the thesis will only examine the structural response to vertical loads and stabilization, while other loads such as horizontal or accident loads will be discussed briefly but not analyzed.

The study will be limited to the commonly used structure of today: beam-column system in steel with a hollow core slab and beam-column system in timber with CLT slab. The thesis only analyzes the response and evaluates strengthening techniques for the superstructure, the structural system above ground. Although the substructure has an important role, it won't be analyzed in depth and will only be briefly discussed.

Despite the ongoing global climate change, this master thesis will not take into account potential future increases in wind load or other impacts of extreme weather. Lastly, the work will be centred on developing rough models and concepts for new building design, with the goal of building a more sustainable future.

1.3 Method

The preparation work for the study includes conducting a comprehensive literature review and research on the topic studied. This is done by reading and analyzing relevant literature in the field to gain a deeper understanding. Additionally, information on the importance of actions in design processes is also investigated during the literature review. Based on this literature study, specific structural elements and systems are chosen for further research. A more detailed literature study is then conducted on these chosen elements and systems to gather information on the theory of structural design, strengthening techniques, building material performance and response to loads, and material properties.

The literature review will be supplemented by parametric studies to examine the effects of altering the building's usage, which can result in changes to the structure's imposed load, geometry, boundary conditions, and a number of floors, as well as the effectiveness of strengthening techniques. These studies will be conducted using commercial 3D computer graphics and design applications such as *Rhinoceros* and *Grasshopper 3D*. Additional tools, such as *Karamba 3D*, will be used to provide an accurate analysis of the performance of different systems and techniques under changing loads.

Based on the results of the analysis and literature review, an assessment and recommendation of design procedures will be made and discussed. The main steps of the master thesis include:

1. Conducting a general literature review on the topic studied.
2. Conducting a specific literature review on the chosen materials, elements, and structural systems.
3. Developing parametric models for structural elements and systems.
4. Analyzing the response of different systems and techniques to changes in imposed loads, geometry and numbers of floors.
5. Summarizing the necessary strengthening for different types of load changes on building elements.
6. Developing a recommended design procedure and way of thinking for future design.

2
Theory

2.1 Sustainability

Sustainability is an urgent matter that demands immediate attention. Accordingly, to an article published by Oxford University 2022, the world is at "code red" with deteriorating trends (Ripple et al., 2022). In 1992, over 1700 scientists signed the document "World Scientists' Warning to Humanity" expressing concern that humanity was surpassing the capacity of Earth's ecosystem (Ripple et al., 2017). Despite this warning, 30 years later in 2022, greenhouse gas emissions had risen by approximately 40% (Ripple et al., 2022). The following chapter will present regulations that have been adopted to counteract this and the present circumstances.

2.1.1 Current situation and regulations

Agenda 21, which was adopted in 1992 at the United Nations Conference on Environment and Development in Rio de Janeiro, is a long-term plan for sustainable development (*Agenda 21-kommittén*, 1995; Sitarz, 1993). Agenda 21 was created to act against the most urgent environmental, social and health challenges confronting the planet. The main object for agenda 21, regarding the environmental aspects, is to minimize and limit the dangerous human-induced climate change, and this was intended to do by stabilising the greenhouse gas concentration in the atmosphere (Falkner, 2016).

Based on Agenda 21, in December 2015, the Paris Agreement was established at the 21st climate conference. The agreement was a response to the lack of progress and insufficient reductions of green gas concentration. The Paris Agreement's main goal is to limit global warming to well below 2 degrees Celsius, compared to pre-industrial levels (UNFCCC, 2015). It is implemented by 196 parties and is the first legally binding agreement that brings together all nations to take ambitious actions to combat climate change and adapt to its impacts.

The urgent situation requires the need for action across all sectors to reduce greenhouse gas emissions. Science and engineering play an essential role in achieving this goal, as it provides the knowledge and technology needed to make sustainable practices a reality. It is vital that all sectors take responsibility for their emissions and actively work towards reducing them. By utilizing science, there is possible to establish sustainable solutions that will not only benefit the planet but also the society (Orr et al., 2021).

The construction and building sector plays a significant role in contributing to global CO_2 emissions, accounting for nearly 40% of world emissions. An all-time high where observed in 2021 regarding the operational energy-related CO_2 emission, after an increase of 5 % concerning 2020 emission levels (Programme, 2022). It is estimated accordingly to *Design for Zero* that 10 % of the total CO_2 emission is assigned to the decision-making of structural engineers (Orr et al., 2021). Additionally, the building and construction sector is also a leading producer of waste. Given this, it is projected that in the next 40 years, an area of 230 billion square meters of new buildings will be constructed over the world. These statistics highlight the demanding need for designers to find intelligent and sustainable solutions for materials and resource use in the construction industry. This is essential to meet the demanding goals set by the Paris Agreement and to mitigate the negative impact of the construction sector on the environment.

Laws, regulations, and more stringent limit values serve as instruments to promote the enhancement of companies, thereby leading to a reduction in their environmental footprint (Hasth, 2022). Consequently, the Swedish National Board of Housing enacted new legislation, effective from January 1, 2022, which mandates the inclusion of climate declarations for new buildings. Under the new law, developers are required to submit a climate declaration to the Housing Authority, which registers and tracks the climate impact resulting from the construction phase (Boverket, Accessed on 2023-06-12). The climate declaration serves to emphasize the environmental impact and must be submitted to the Housing Authority's registry for climate declarations. Proposed limit values for the climate impact of buildings have been introduced since 2022, with their actual implementation scheduled for July 1, 2025.

2.1.2 Repurposing

The conversation concerning repurposing and usage of buildings has grown into an essential and highly significant topic for achieving sustainability goals (Viola & Diano, 2019). As the construction industry utilizes large parts of the world's resources, there is an international ambition to establish a sustainable development of the sector through adaptive reuse of existing building stocks and by embracing the principles of circular economy (Owojori, Okoro, & Chileshe, 2021). *Design for zero* introduces the carbon reduction potential concept, which is a concept that applies circular economy principles in the building sector. As previous mention, in chapter 2.1.1, decisions made during the design process can greatly impact the carbon reduction potential, as demonstrated in the following list (Orr et al., 2021).

1. Built nothing:
   Potential of carbon saving is 100 % and questions to be answered are: Is a new building the right approach and why is it necessary to build a new building? Can a reframing of the problem itself solve the problem?
2. Built less

Can the existing building be reused, get repurposed or refurbished? Reduce and minimize the demand for producing newly built

3. Built clever
   How can the solutions be more low-carbon? Which technologies materials and production methods are most beneficial from a CO_2 emission perspective? Specify enough material and no more
4. Built efficiently
   Minimize and reduce the resource consumption in the construction

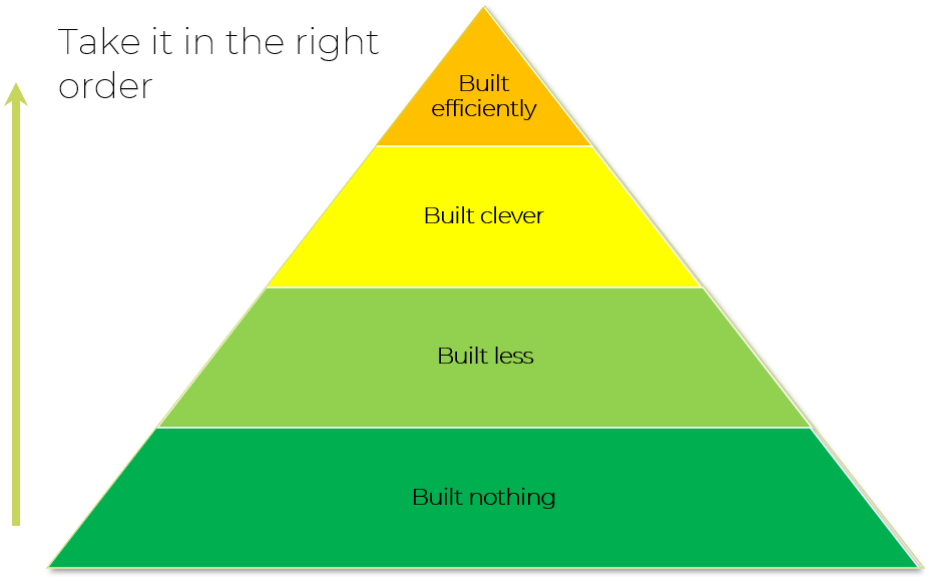

Figure 2.1: *The carbon reduction potential hierarchy, by Johanna Nilsson 2023*

The definition of repurposing is accordingly to Cambridge: *"To find a new use for an idea, product or building"* and for buildings, repurposing correlate lead to several outcomes (University, n.d.-c). Modification of building usage leads to changes in the load situation, as the design values for the new imposed loads are adjusted (CEN, 2002). Therefore, when evaluating the structural integrity of a building, it is essential to take into account the intended usage and the corresponding imposed loads.

Structural changes due to repurposing can also be caused by removing or relocating columns as a result of a desire to create a different floor layout. This measure can affect the boundary condition and the load distribution which also needs to be accounted for in the evaluation of the accuracy of the load-bearing system. A frequent result of repurposing is to take the opportunity to increase the number of floors as well.

2.1.3 Material Optimization

A central part of any problem involving decision-making is optimisation, regardless of whether it is engineering or economic problem-solving. Optimization is the act of making something as good as possible, based on one or several given objective functions (Chong & Zak, 2013; University, n.d.-b), and regarding material optimization adopted in the construction industry, it is the process of designing a structure specifically for a known purpose, aiming to use as little material as possible. The practice of optimization generally, has the past decade become increasingly recognized, primarily as a result of the progress in computer technology and for material optimisation also due to the need for limiting resource use.

2.1.4 Flexibility

When discussing flexibility, the concept aims to create systems that have *the ability to change or be changed easily according to the situation*, as defined by Cambridge (University, n.d.-a). Accordingly, to *Design strategies to increase building flexibility*, three key changes are covered by the need for flexibility in a building (Slaughter, 2001).

1. Changes in function, modifications made to activities or components to meet a specific objective.
2. Changes in capacity, the changes in the building's ability to fulfil performance requirements, in either loads/conditions or volume.
3. Changes in flow, refer to movements within and around a building, taking into account the user population and the surrounding environment. The flow of people, air, or other elements can be influenced by both internal factors, such as the physical environment within the facility, or external factors, such as the climate or surrounding environment.

Corresponding to these possible future changes, and when designing for flexibility, there are three corresponding design approaches (Slaughter, 2001). The objectives for the first approach are principles of *physically separating*, directing separation of the main building system, so that changes in one region, do not affect the entire system. The second approach covers the *prefabrication* of the components of the main system, aiming for making it easier to replace certain components later on. This approach aims to make maintenance and upgrades to the system more efficient and convenient. The last approach is a strategy for designing the structural system with *overcapacity*. The intention is to be able to accommodate by building systems that have more capacity than is currently required, sufficient for adjustment as needs change. These three strategies increase the flexibility of the building system in different ways to accommodate future growth and development.

2.2 Material

One of the variables in structural design is the choice of use and implementation of building materials. Different building materials come with various behaviour, material properties, advantages and disadvantages. Consequently, the structural system, building and strengthening techniques are therefore different for each material, all to enhance the advantages and minimize the disadvantages of the choice of the specific material. The following chapter will treat the material properties and state the benefits and consequences of the chosen materials: Steel and timber and concrete.

2.2.1 Steel

At the beginning of construction, the structures were mainly built in stone, brick and wood (Isaksson, Mårtensson, & Thelandersson, 2010). The structures made in stone and brick were mainly designed to carry the applied loads in compression due to the preferable compression material properties and large timber structures used similar reasoning. Steel was only used for connections between the structural elements constructed by traditional materials.

In the middle of the 19th century, new methods for effective steel production enabled load-bearing structures made in steel (Isaksson et al., 2010). This entailed changing construction principles, where the structures now could bear the loads more efficiently both in compression and in tension.

Steel is one of the strongest building materials available, which makes it ideal for tall or heavy structures (Al-Emrani, Engström, Johansson, & Johansson, 2013). Steel has a high strength-to-weight ratio compared to concrete and wood, which allows for more efficient use of material and reduces the overall weight of the structure. This has also come as an effect of that humans' understanding of the structural steel's behaviour and material properties has been improved since now the material is more used in situations where it is suitable (Moynihan & Allwood, 2014).

The material properties of steel are often described as the relationship between stress and strain, illustrated in the stress-strain curve below (Liang, 2015). In the initial state, steel has a linear elastic relation between stress and strain, following Hookes law, up until approximately the yielding strength f_y. From the yielding strength, the material behaviour differs slightly depending on whether the steel is hot rolled or cold rolled, where hot rolled steel experiences plastic deformation without any increase of stress (Liang, 2015; Al-Emrani et al., 2013). The material response is now plastic, and the deformations are irreversible. When reaching the hardening strain ε_{st} the stress continues to increase until the ultimate tensile strength f_u is reached.

Unlike wood and concrete, steel mechanical material properties have similar characteristics for compression and tension, which enables the possibility to design a structural system using both compression and tension, as previously mentioned (Isaksson et al., 2010; Al-Emrani et al., 2013).

2.2.2 Concrete

In the category of structural systems and elements made of concrete, there are two fundamental approaches, cast-in-situ and partly or fully precast concrete. One of the advantages of using structural systems and elements made in concrete is that concrete as a material is long-lasting and has generally good durability (Mather, 2004). It is also relatively economical and easy to work with. Additionally, concrete has a high thermal mass, which means that it can help to regulate the temperature inside a building, keeping it cool in the summer and warm in the winter (Shafigh, Asadi, & Mahyuddin, 2018).

Cast-in-situ concrete is a building technique where concrete is poured and cured on-site. This method is mainly categorized into two different systems: beam-column and load-bearing walls, where the facades and/or inner walls serve as load-bearing structures(Agrawal, Sanghai, & Dabhekar, 2021). Load-bearing systems in cast-in-situ offer advantages like homogeneous conditions, connections, and structural redundancy. The flexibility of shape is possible with appropriate formwork(Colombo, Ferrara, Negro, & Toniolo, 2004). However, cast-in-situ concrete has drawbacks, including long curing times that can cause construction delays and potential issues during or after casting.

Prefabricated concrete systems are similar to conventional concrete built up on similar principals, load-bearing walls and beam-column systems. Prefab enable high-quality controls and short erection time and minimized use of scaffolding (Wang, Cheng, & Sohn, 2015). This design choice also allows large spans. But choosing prefabricated elements has its drawbacks also. The design for the building needs to be stated in the early stages, unlike the case with cast in-situ concrete.

Concrete is a strong material in compression but weak in tension, which leads to the frequent occurrence of cracks in concrete structures even under low load levels and can for plain concrete lead to collapse (Hu, 2022; Engström, 2011). To avoid collapse, reinforcement steel bars can be applied to transfer tensile force across the cracks, but for structural elements loaded in bending or tension, or for columns loaded with an eccentricity, the cracks will occur under small loads, often already during service limit state. Even though the load-bearing capacity can be accounted for by the reinforcement steel, the cracks cause some problems.

When flexural cracks appear, an extensive part of the cross-section will become inactive. This affects the sectional rigidity, causing a decrease in the rigidity, and this part can't be accounted for by the reinforcement steel (Engström, 2011). This decrease results in increasing in deflection which can be limiting of the maximum

span of the reinforced concrete structural element. The ratio between the depth and the length, of the beam element or slab, is limiting for the maximum allowed deflection. The requirements are:

$$\left(\frac{l}{h}\right)_{beam} \approx 20 \tag{2.1}$$

or

$$\left(\frac{l}{h}\right)_{slab} \approx 24 \tag{2.2}$$

This value is based on *SS-EN 1992-1-1* and the boundary conditions

- (2.1) Simply supported beam and 2- or 4-side pinned slab
- (2.2) Slab supported on pillars without beams (pillar decks)

Other negative effects of cracking in reinforced concrete structures are corrosion of the reinforced steel and fatigue, due to cycling loading, caused by a large variety of strain (Engström, 2011; Almusallam, 2001).

2.2.2.1 Prestressed concrete

Prestressing concrete is an effective way to overcome the disadvantages of cracking in reinforced concrete structures. Prestressing is preparing a structure to receive a load by applying a proactive counteracting load. This means that a compression force is applied to the concrete during the production stage, and later on when the structure is loaded, the compression stress will decrease. Tensile stresses will not occur in the structure before a considerable load is applied (Benaim, 2007; Engström, 2011). This enables higher tensile stresses and flexural stresses before cracking appears.

In fully prestressed concrete structures, cracking is prevented, while in partly prestressed structures the cracking is limited under a high load level in a service limit state. By using the principles of prestressing, the mechanical properties of concrete are used in the best suitable way, by letting the concrete work in compression. Prestressing is a good way to create larger spans since the corresponding ratio for prestressed concrete elements is

$$\left(\frac{l}{h}\right)_{slab} \approx 45 \tag{2.3}$$

The value is determined from *Design and analysis of prestressed concrete structure*. Comparing the correlation between the span width and the cross-section height for reinforced concrete and prestressed concrete structural elements, with the requirements for deflection in SLS (CEN, 2005b),

$$\left(\frac{l}{h}\right)_{slab} \leq \left(\frac{l_{slab}}{250}\right) \tag{2.4}$$

it can be stated that, by using prestressed concrete, it is possible to create thinner slabs with smaller amounts of material, members that can span longer or a combination of these.

$$\left(\frac{l_r}{h}\right) \approx 24 \rightarrow \frac{l_r}{24} = h$$

$$\left(\frac{l_p}{h}\right) \approx 45 \rightarrow \frac{l_p}{45} = h$$

$$\Rightarrow l_p = \frac{45 \cdot l_r}{24} = 1.875 \cdot l_r \tag{2.5}$$

2.2.3 Glulam and CLT timber

Timber is the building material that has been used for the longest period, primarily since it is lightweight which makes handling and transporting with limited resources easier (Al-Emrani et al., 2013; Isaksson et al., 2010). Traditionally wood has been used for small and low buildings but in the last years, the construction of multi-story buildings in timber has become more common. This is a result of better understanding and because of benefits from the combination of the low self-weight, high strength and good thermal insulation. Primary it is also been used since it is a sustainable resource and an aesthetically pleasing material (Jack Porteous, 2013).

Wood differs from steel and concrete in its characteristics and properties, as wood is an *anisotropic material*, where the physical properties are determined by the grain direction. Therefore, in structural design, it is assumed to act orthotropic with three main axes, Longitudinal plane along the fibre direction, L, radial in relation to the growth rings, R and tangential in relation to the growths rings, T (Jack Porteous, 2013; Svenskt trä, 2015). The mechanical properties parallel to the grains and the cellular structure, L-direction, are considerably stronger and stiffer than the properties in the other two directions. Therefore in structural timber, both the loading direction and the mode of action, compression or tension, need to be considered.

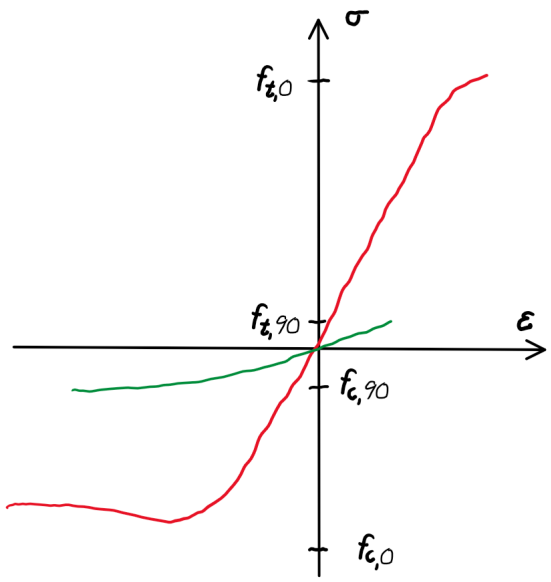

Figure 2.2: *Strengthproperties wood, by Johanna Nilsson 2023*

One of the limiting consequences of using wood-based structural elements is the size and quality of the sawn section of softwood (Jack Porteous, 2013). This is because timber is a non-homogeneous material and the material properties can vary greatly due to growth irregularities causing size and material defects (Blaß & Sandhaas, 2017). To resolve these limitations, Engineered Wood Products can be applied, *EWPs*, and by using EWP various types of structural elements can be created. Glued-laminated timber is the oldest type, and the technique was developed in Germany in the 20th century (Svenskt trä, 2015).

Glued-laminated timber, glulam, is produced from adhesive laminates that together create a static combined unit (Isaksson et al., 2010; Svenskt trä, 2015). The lamellas are sections between 33-50 mm thick and placed randomly, creating either totally straight members or slightly curved ones, and for significantly curved ones, the laminates can be a bit thinner. The benefit of using glulam elements is that it has been stated that the strength of the wood section has smaller variations. For solid timber products, the material properties can vary markedly over the section as a result of material defects and size defects.

During the 21 century, another wood-based product was established, Cross-laminated timber, *CLT* (Svenskt trä, 2015). Using an odd number of layers, a minimum of three, of orthogonally bonded laminates, CLT has improved dimensional stability in relation to solid timber products (Jack Porteous, 2013). As a result of that the layers are perpendicular to each other, and the strength and stiffness properties in the longitudinal and transverse directions are improved which creates the capacity of two-way spanning. To minimize waste and offcuts, coordination between design and manufacturing is important when producing panels with their outer layers oriented. For walls, the outer layers of CLT panels should be oriented vertically, while

for floors and roofs, they should be oriented in the direction of their major span (Jack Porteous, 2013).

2.3 Structural systems

The structural system of a building has primly two functions to fulfil. Firstly, it should be able to resist the permanent self-weight, as well as any loads associated with climate and imposed actions. Secondly, it should provide protection for the building's contents and building components (Lindberg, 2013; Al-Emrani et al., 2013). The load-bearing system is designed to ensure that its load-bearing parts have adequate strength and rigidity to resist the required loads and that it meets the necessary safety requirements to prevent collapse. In many cases, the structural system is often a significant contributor to the aesthetic design of a building and is therefore essential that it is both functional and visually appealing.

The structural system can be divided into a primary load-bearing system and a secondary load-bearing system (Isaksson et al., 2010). The primary system is responsible for carrying the load down to the ground, while the secondary system consists of structural elements that transfer the load to the primary system. Overall, the structural system plays a crucial role in the safety, stability, and durability of a building, and must be designed and constructed with precision, regarding material strength properties to resist failure modes such as tensile/compression failure or shear/flexural failure. Additionally, the system should be dimensional for the phenomenon of instability, which can be divided into three main groups:

- Buckling: A phenomenon that occurs in elements subjected to compressive axial forces, causing them to bend from the equilibrium position, generally pillars.
- Plate Buckling: A phenomenon that only affects steel elements and is distinct from buckling, as it is two-dimensional.
- Lateral-Torsional Buckling: A phenomenon that is specific to beams with low lateral stiffness compared to the direction of the load. This results in the beam twisting and bending outwards laterally.

The elements are commonly classified into two categories: Vertical load-bearing elements and horizontal load-bearing elements together these elements conform to the structural systems (Isaksson et al., 2010). The primary role of vertical load-bearing elements, such as columns, walls, and panels, is to transfer the self-weight and imposed loads down to the ground. Occasionally, these elements may also play a stabilizing role and are thereby subject to horizontal loads which create shear forces in the elements (Lindberg, 2013). In such cases, it is important to consider any misalignment of the elements.

Horizontal load-bearing elements, including beams, plates, and slabs, are responsible for bridging the space between, and transferring the load, to the vertical-bearing elements. It is important to design these elements to handle both vertical and hor-

izontal loads, both individually and in combination.

The design of a structural system can vary greatly and be constructed using a variety of materials. There are numerous combinations to choose from, and each has its advantages and disadvantages. In the following sections, different commonly used systems will be discussed in greater detail and the properties and applications of different materials will be examined.

2.3.1 General Beam-column system

One of the most frequently used load-bearing philosophies is a beam-column structural system since this technique enables bigger flexibility due to the possibility of large floor areas (Rezaei, 2022). The columns are often placed in the facades and supplementary rows if needed. This results in that no internal or external wall need to be load-bearing as the vertical loads are transferred to the ground through the beams and columns, and often is the system a part of the stabilisation of the structure (Lindberg, 2013). The simplest way to incorporate beam-column principles is by a simply supported beam on two columns, but even continuous beams could be used.

Columns' primary responsibility is to handle and transfer the applied load in the vertical direction. However, the definition is not strict, as the boundary between what is classified as a beam and what is responding like a column can be vague(Isaksson et al., 2010). A structural element is typically considered a column when the bending stresses are subordinated, while a beam is a structural element where the normal stresses are secondary. Note that this is a general guideline and may not always be true.

Furthermore, beams carry the applied load perpendicular to its length, where the dimension of the spanning is considerably larger than the cross-section dimensions, thickness, and width. The load is transferred from the beam, through bending and shear forces and the reactions are thus transferred to the column and down to the foundation. Depending on if the beam is simply supported or pinned or if the beam is continuous, the moment distribution varies, which gives results on the individual load that each column must handle. In subsections 2.3.2 and 2.3.3, more material-specific information will be provided for both beams and columns.

2.3.2 Steel system & prestressed concrete

Steel together with composite construction represents more than 60% of the market percentage of the building and construction sector in several countries in Europe (Davison & Owens, 2012). This is a result of the advantages such as long spans, the possibility of a fast construction sequence, the chance of integration of technical systems in and between the structural system, and improved product quality.

The basic principles of load-bearing steel systems are primary; either beam-column

systems with bracing that provides stability, or a mixed system where the beam-column system is connected to a rigid concrete core, that offers stability (Davison & Owens, 2012). The core is often incorporated in vertical services such as lifts and stairs and when using this principle, it is assumed that the beam-column system only accounts for the vertical loads.

Steel load-bearing systems mainly operate the combined effects of vertical and horizontal loads with *Moment resisting frame system* or *braced frame system*. Moment resisting frame system, using fixed frame action and can resist the axial, bending, and shear action without any bracing members. Observe as previous mention, that the beam-column connection tends to be quite advanced due to the need to transfer the horizontal load from the beam to the column. The system is therefore quite expensive but can be preferable due to high redundancy.

Bracing-frame system unlike moment-resisting frame systems uses hinges connections, which are simply produced connections. The interaction between the bending moment and axial forces is also limited. This stabilisation system uses the principles of separating the load-bearing system in the vertical direction from the system resisting the horizontal action. This is the fundamental form using a beam-column system connected to a rigid concrete core (Davison & Owens, 2012). The beams and columns transfer the main vertical load to the foundation, while the floor uses diaphragm action transferring the horizontal load to the core. This system, similar to a two-way frame system, gets large forces in the foundation, as well as great eccentricity for the load application in some cases.

For steel columns, it's common to use rolled profiles, such as HEA, HEB, and HEM together with HSS profiles, while IPE profiles often are used as beams (Bength Strandberg, 2015; Isaksson et al., 2010). As floor elements, it is common to use hollow core slabs, which is a prefabricated prestressed concrete element. The element type has great advantages in the form of low self-weight due to the longitudinal channels, the possibility for long-span widths, and cost-efficiency. HD/F 120, a homogeneous slab element, are commonly used and can span around 18 m.

2.3.3 Timber system

The benefit of choosing timber structures is that it is highly promoted for the future and have ductile behaviour. Investing in timber systems can be seen as a favourable choice for the future, primarily due to their significantly lower environmental impact. Timber has an emission rate of 0.133 kg CO_2e/kg, whereas materials like steel have a much higher emission rate of 3.15 kg CO_2e/kg (Boverket, Accessed on 2023-06-13). But in contrast with beams made of concrete or steel, the timber has a shorter maximum distance that it can span. The two most common principles for load-bearing timber systems are lightweight construction technology and solid wood technology (Fernandez, 2021).

Similarly to the structural system in steel, when aiming for open-purpose flexible

spaces, the load-bearing timber system using beam-column principles is preferable. In these timber buildings, the governing factor is often the deflection of the flooring and beams. The main building approaches that are used for timber buildings are either continuous columns or simply supported beams and floors, where the advantages are fewer columns which save time (Athanasiadis & Al Sahi, 2018). By using continuous beams supported on floor-height columns, the deflection can be reduced compared to simply supported beams and smaller among material usages.

The vertical timber load-bearing system is combined different elements and often also a mix of materials. It is common to use core elements in concrete or stabilisation trusses in steel. In these cases, it is important to pay attention to the different properties and limits restraining the components. As previous mention, timber is highly moisture sensitive, especially perpendicular to the grain, which affects the shrinkage of the element.

The horizontal load's transferred to the ground using bracing units or stabilisation members using diaphragm action. Using moment rigged connections in combination with stiff columns and beams, also framework can be used to stabilisation the structural system. Timber columns are mainly generated from structural timber or glulam, and for columns with a high-load appliance, it is preferable to use glulam products (Isaksson et al., 2010). Svenskt trä provides manufacturing ranges for glulam beams and columns (trä, 2015).

Floorings in timber are a bit more complicated than slabs in concrete. The primary bearing in a timber floor structure usually consists of simply supported timber beams made of construction timber or glulam (Isaksson et al., 2010). These beams are spaced at a specific centre distance, most commonly 600 mm. The secondary support, the actual floor, often consists of timber planks or some form of panel material. These components are preferably prefabricated. The floor is laid on the beams and bears perpendicular to them.
Since the introduction of CLT slabs, they have become a viable alternative, as explained in section 2.2.3 (Svenskt trä, 2019). In its most common configuration, a CLT structure involves panels supported by two supports. The supports may extend along the entire length of the panel or be point supports at regular intervals. For floor structures or similar applications with relatively short spans, panels with a uniform thickness are preferred. However, there may be economic reasons to reinforce the panels with glulam beams, for example, to create a T-cross-section.

2.3.4 Stabilisation system

As a supplement to the beam-column system, as previous mention, a stabilising system is implemented. The fundamentals for the stabilisation system are to handle the horizontal loads and axial action that the structural system is exposed to (Isaksson et al., 2010). These loads primarily originate from wind load and initial imperfection as a result of real pillar behaviour. The horizontal load can also derive from seismic loads. The stabilisation can be managed with favourable three different principles of systems, that often combine, aiming for the best system solution, Bracing system, Frame action, and Diaphragm Action.

2.3.4.1 Stabilisation with trusses

Stabilisation with trusses transfers the horizontal load through a diagonal bracing unit down to the foundation (Isaksson et al., 2010). The trusses are commonly implemented in the roof and wall structure and spans often across a whole section, illustrated in figure 2.3. The columns are considered pendulum columns, which refer to pinned connection both at the foundation and the connection beam to the column. The bracing unit is primarily made in steel profiles since steel is favourable considering its material properties in tension.

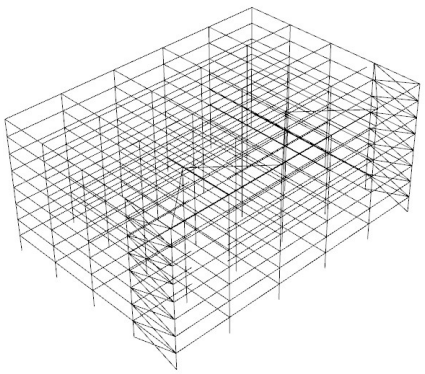

Figure 2.3: *Illustration of stabilisation with trusses, by Johanna Nilsson 2023*

2.3.4.2 Stabilisation with Frame action

Frame action resists the horizontal actions through moment distributions between the horizontal and vertical members, by ridged element connections or fixed support conditions in the foundation (Isaksson et al., 2010). Frame action encompasses three principles, two-way frame, three-way frame, and ridged frame (Lindberg, 2013; Isaksson et al., 2010). Two-way frameworks manage the axial force and bending moment in the foundation using fixed support conditions and simply supported beams.

Figure 2.4: *Defined from left to right, Two-way, Three-way and Ridged frame, by Johanna Nilsson 2023*

The three-way frame is a statically determined structure and is instead using moment rigid corners and pinned support conditions and a joint in the roof structure, to handle the bending and axial force. In Ridged frame there are similar to the three-way frame, moment rigid corners, but no joint in the roof structure. This generates a stabilising frame with high redundancy, but using this type of frame action has some requirements for the system. Complicated connections and joints since they need to be ridged, which can be hard in practice. Since the axial forces and bending moment are managed by the columns, this can be covered for the design of the column size.

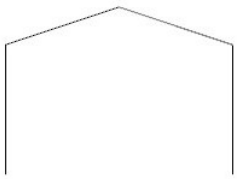

Figure 2.5: *Ridged frame, no joints in corners, by Johanna Nilsson 2023*

2.3.4.3 Stabilisation with Diaphragm action

Diaphragm action can be accomplished using both walls and slabs in concrete, timber, and steel. Common for all types of diaphragm is that they are stiff in the plane, while orthogonal to the plane the rigidity is significantly lower.

2.4 Strengthening of members

Although strengthening a structure can seem like a simple task, it is far more complicated than demolishing the structural system and erecting a new one (Carolin, 2003). In difference with creating a new building, concerns regarding the existing material and its condition, and the operative geometry, together with the dimensional aspects for structural systems, such as loads. Also, when strengthening for one failure mode, there is crucial to evaluate the other failure modes, since the strengthening can cause failure in another part.

There are several techniques for strengthening existing structural members, some are more traditional while others are newer and in the phase of research or greater emphasis on experimentation. Commonly, when strengthening structural systems is often increasing the dimensions of the critical areas or adding supporting elements to the existing structure (Carolin, 2001). Since the strength of a member is highly dependent on the cross-section dimensions, by modifying the dimension, a higher capacity can often be achieved. This can, for example, be achieved by incorporating plates on beams and columns, or intuitively by adding elements, that enhance the overall capacity of the system. More about how this is implemented in the following sections.

By using these traditional methods, the structure often becomes more cost-effective compared to alternative modern solutions. These methods ensure reliable structural safety since they often have been tested for a long time, and in the case of utilizing steel, they also offer the added benefit of future steel recycling possibilities. Despite these benefits, there are some disadvantages, mostly connected to the changes in cross-section. When the cross-section dimensions are increased, it leads to a corresponding increase in the self-weight of the elements. Additionally, additional loads are applied to the global system, which can result in higher loads being transferred to other parts of the system that have not been strengthened (Karlsson, 2007).

2.4.1 Steel columns and beams

For steel members such as columns and beams, there are, as previously mentioned, several techniques that can be used. Enlargement of the members' cross-section is often done with plates and rolled sections to fulfil higher load-bearing capacities. The plates are commonly welded to the cross-section to provide reinforcement and can be placed in many different configurations, especially for steel beams (American Institute of Steel Construction, 2018)

When strengthening steel columns, symmetrical reinforcement plates are the most common (American Institute of Steel Construction, 2018). When it's possible, a symmetrical strengthening configuration is beneficial to use since the columns section remains doubly symmetrical, see figure 2.6 and 2.7. By introducing additional steel plates the cross-section area will increase and consequently to the moment of inertia, resulting in enhanced strength.

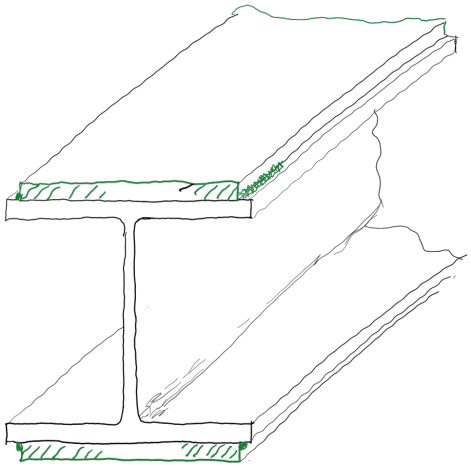

Figure 2.6: *Double symmetrical flange plates, by Johanna Nilsson 2023*

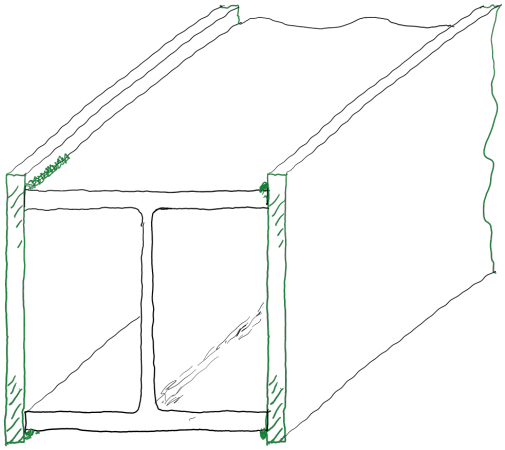

Figure 2.7: *Double symmetrical web plates, by Johanna Nilsson 2023*

In situations where double symmetrical plate reinforcement is not feasible, for example, when a column is embedded in a wall and access to only one side is possible, it is crucial to acknowledge that performing welding on only one side of the column increases the risk of welding distortions. Welding distortions are consequences of expansions and contractions of the weld and the surrounding base material, introduced by the heating and cooling process during welding (Deng & Murakawa, 2008). This can create or enhance the secondary moment in the column, causing even larger problems, see figure 2.8. Therefore, whenever possible, it is advisable to weld on both sides to mitigate potential distortions and maintain structural integrity(American Institute of Steel Construction, 2018).

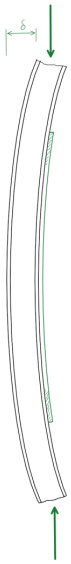

Figure 2.8: *Illustration of consequences of welding distortion, by Johanna Nilsson 2023*

Particularly for the strengthening of columns with welded plates to enlarge the cross-section, the American Institute of steel construction has presented some possible strengthening designs. In these examples, it is shown that by only reinforcing the middle half of a column in compression, approximately, the same load-bearing capacity can be assumed as if the whole length of the column should be reinforced. This is beneficial knowledge, as one of the disadvantages of strengthening with welded plates, is limited access sometimes.

Another possible strengthening strategy is changing the static system. By changing the connections and support conditions of the structure, a considerable reduction of the maximum stress can be obtained and the changes are generally easy to perform. As a consequence of this strategy, the static system is modified and the strength and behaviour of the structure must be analysed to ensure that the new load situation is resisted properly. However, the decrease in stress in some locations is associated with an increase in stress at other locations

Regarding the strengthening of beams, plates can also be utilized for the purpose of strengthening. Similar to columns, limited accessibility is one of the main challenges that prevent the possibility to weld plates at both flanges. The limitation, combined with the preference to avoid overhead welding since it is the most difficult welding position, often ends in built-up shapes that are single symmetric (Dowswell, 2014; Dwivedi & Dwivedi, 2022). Illustrated in figure 2.9, built-up profiles are shown for strengthened results, where the simplest and most economical when strengthening for higher resistance of bending in the strong axis, is the single flange plate. This approach allows for horizontal welding, as the plate is larger than the flanges, which is beneficial considering the economic and time aspect.

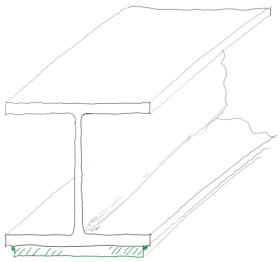

Figure 2.9: *Single flanges plate, by Johanna Nilsson 2023*

Strengthening with a tee profile, illustrated in figure 2.10, provides increased strength and stiffness but requires, as can be seen overhead welding. For higher bending resistance along the weak axis, the cap channel is effective.

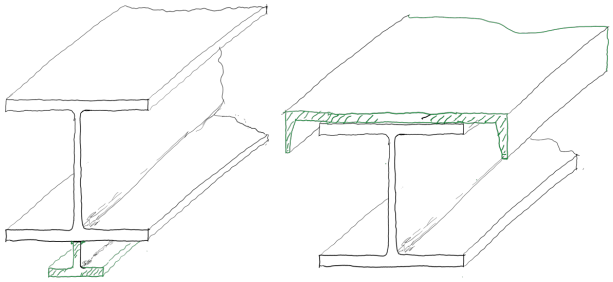

Figure 2.10: *Illustration of Tee and Cap profile, by Johanna Nilsson 2023*

When aiming for strengthening to resist torsional and lateral torsional buckling, closed sections are preferred since to their high efficiency against these failure modes. Figure 2.11 demonstrates two reinforcing configurations that effectively address these concerns, double web plates, and double angel (Dowswell, 2014). As mentioned earlier, welding can lead to distortion, but in the case of beams, single-side reinforcement does not pose a problem. In fact, in the presence of welding distortion, it can even be advantageous for overall deflection behaviour (American Institute of Steel Construction, 2018).

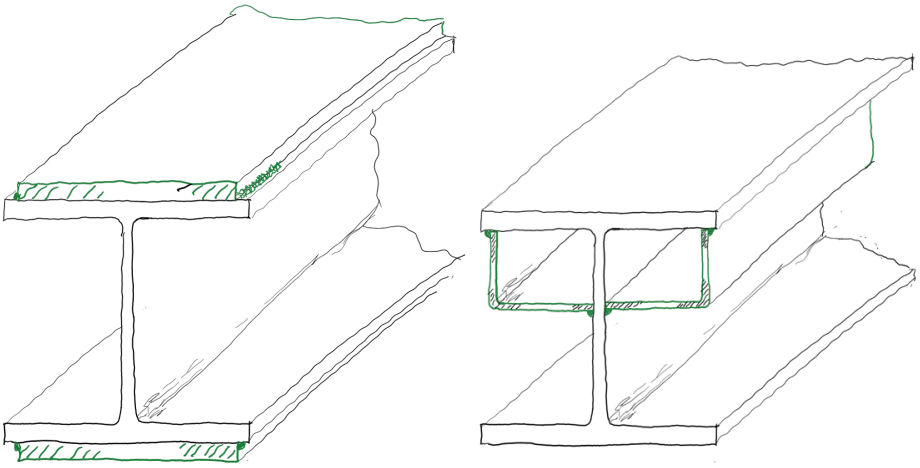

Figure 2.11: *Illustration of double web plates and double angel profile, by Johanna Nilsson 2023*

Besides the traditional techniques and strategies, new modern techniques have also developed. The most noticed one is *Fiber-reinforced polymer*(Teng, Yu, & Fernando, 2012). The fibres commonly consist of carbon, glass, aramid, and basalt where glass fibre (*GFRP*) and carbon fibre (*CFRP*) are the most used ones. FRP has several advantages compared to the traditional method, where the most significant is the high strength-to-weight ratio and corrosion resistance. Further on, the adhesive bonding technique provides multiple pros, among ease of application and refined fatigue performance (Linghoff, Haghani, & Al-Emrani, 2009).

When strengthening steel beams and columns with CFRP there are mainly two different products that are used today, laminate and fabric (Karlsson, 2007). The laminates consist of unidirectional fibres, creating an anisotropy property relation, strong in the longitudinal direction and weaker in the transversal direction. Laminates are mainly used for strengthening the bending and flexural moment (Karlsson, 2007). While this approach has been extensively tested and employed with success for various building materials, current research is being conducted specifically for steel elements. Accordingly, to research done by Chalmers University of Technology, the increase of moment capacity when strengthening with CFRP is limited by the yielding in compression of the steel member (Linghoff et al., 2009). Amplification of 20 % can be achieved for double symmetrical I-sections, but by also strengthening the compression zone, a higher moment capacity can be obtained.

Regarding the strengthening with CFRP fabric, the method is primarily used for strengthening for improved shear strength. However, it can also be utilized to strengthen bending moments, are applied on beams and columns, with various building materials (Karlsson, 2007). The fabric is produced from fibres in one or two directions and is advantageously applied to beams and columns. This method is similar to the strengthening for an increase in bending moment, an ongoing research field, but also here, an increase in the ultimate load for a column can accede (Keykha, Nekooei, & Rahgozar, 2015).

2.4.2 Concrete elements

As mentioned in subchapter 2.4.1, CFRP laminates can be used for strengthening the bending and flexural moment and are a well-established approach for concrete elements, especially considering the relatively low tensile strength of concrete (Karlsson, 2007). To improve the flexural moment resistance, the strengthening process involves applying laminates on the side that experiences tension. As carbon fibre laminates are characterised by high tensile strength, the strengthening technique is preferable for elements in static or dynamic bending such as beams, slabs, roofs and walls.

Strengthening for improved shear capacity is frequently more challenging than reinforcing for bending moments in concrete structures. However, it is often necessary

to address shear strengthening when reinforcement for bending has already been implemented. The widely employed method entails the application of CFRP fabric, which facilitates cooperation between the existing reinforcement within the concrete element and the bonded nets. This approach effectively enhances shear capacity and ensures structural integrity.

2.4.3 Glulam elements and CLT floor

The primary issue affecting the structural behaviour of timber beams and floors is the limiting bending and in-plane stiffness due to mechanical properties (Valluzzi, Garbin, & Modena, 2007). Similar to steel structural elements, here there are several available techniques for strengthening the elements, some more proven, while others are more innovative. Some of these techniques are for example additional members, implementing strengthening FRP strips or bars on the tension side of the beam/ floor or creating T-sections, using the original timber as a web, and creating a flange by applying and connecting a new element on the top of the floor.

Reinforcing glulam beams with steel has been a successful method for a long time (Jacob & Barragán, 2007). By strategically positioning the steel in the outer regions of the glulam beam, particularly in the most exposed areas, the objective is to enhance both the strength and stiffness of the beam. This approach serves to safeguard against premature beam failure. Leveraging the high strength and stiffness properties of steel allows for optimal utilization of the wood material.

Comparably to steel sections, the use of FRP laminates or strips has become an innovative and promising strengthening technique also for timber beams and floors, when aiming for increased capacity for tensile stress due to bending (Valluzzi et al., 2007; Karlsson, 2007). However, research has demonstrated that the local bond between the FRP and the wood is affected highly by the relative humidity of the wood. Consequently, the relative humidity becomes the critical factor that directly affects the mechanical properties and as a result, determines the extent to which the strengthening measures can effectively improve the structure. Therefore appropriate preparation for the material at the interface and regulating the relative humidity, preferably around 12 %, is required for achieving a good result of the reinforcement measures.

One of the covering factors, when designing a timber system, is deflection. CFRP-laminates can also be used to reduce the deflection of a timber beam by milled laminated into the beam preferably before the beam is loaded but can be done afterwards (Karlsson, 2007). Another alternative is to employ prestressing in the laminated material, aiming to mimic a behaviour similar to prestressed concrete. This approach aims to achieve the same outcome: reduce deflection and minimise structural deformation.

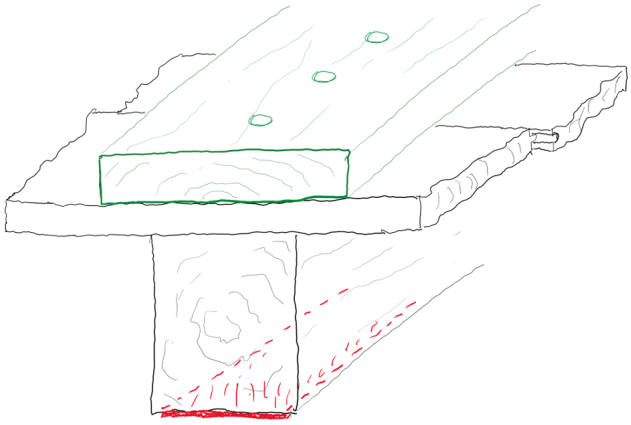

Figure 2.12: *Possible use of CFRP, where the red colour illustrates the laminates, by Johanna Nilsson 2023*

The concept of creating a T-section involves connecting a steel beam or reinforced concrete slab to an existing wooden beam (Valluzzi et al., 2007). This technique has been refined to incorporate timber for both the flange and web, to reinforce and maintain the existing wooden floor. This is achieved by adding a new plank and connecting it to the original structure using dry wood dowels. Test results have shown that, on average, dry beech wood dowels outperform steel dowels, likely due to different failure modes. Dry wood dowels primarily experience shear-flexural failure, while steel dowels primarily fail through the bending of the hole before the deformation of the steel dowels occurs. By combining T-sections made of wood and using dry dowels, the strengthened member can support approximately 3.5 times higher ultimate load.

The strategy of creating a T-section is originally performed by connecting a steel beam to the existing beam or reinforced concrete slabs integrating with the existing beams (Valluzzi et al., 2007). This approach has been elaborate aiming for constructing both the flange and web in timber to maintain and reinforce the current wooden floor. This by applying a new plank and connect to the original structure using dowels. Tests have shown that on average dry beech wood dowels perform better than steel dowels, where the difference can be motivated by the different failure modes. The dry wood dowels failure is covered by shear-flexural mode, while the steel dowels were mainly represented by bending of the hole before the deformation of the steel dowels occurred. By applying the combination of T- sections made of wood and dry dowels, the strengthened member can carry around 3.5 times higher ultimate load. Figure 2.13 provides an illustration of the built-up of a T-section.

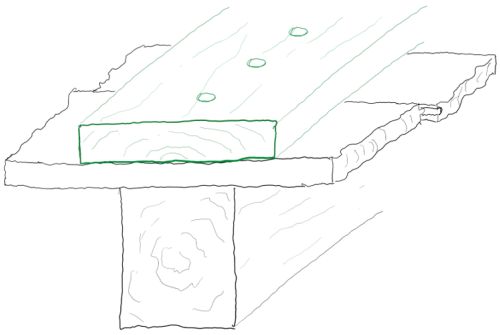

Figure 2.13: *Possible configuration of T-section, by Johanna Nilsson 2023*

Similarly, just like top glulam beams, timber columns have traditionally been strengthened by incorporating steel bars and plates (Chang, 2015). These steel elements provide support to the timber column, enabling it to bear and transfer loads effectively. Additionally, they serve the purpose of preventing cracks and subsequent splitting. Frequent configurations of steel reinforcement include steel plates fastened with nails or screws, perforated metal plates, and steel rods bonded with adhesive. Buckling tests have demonstrated that steel reinforcing plates exhibit a load-carrying capacity that is at least 2.5 times greater than that of unreinforced columns. Figure 2.14 shows a column reinforced with plates.

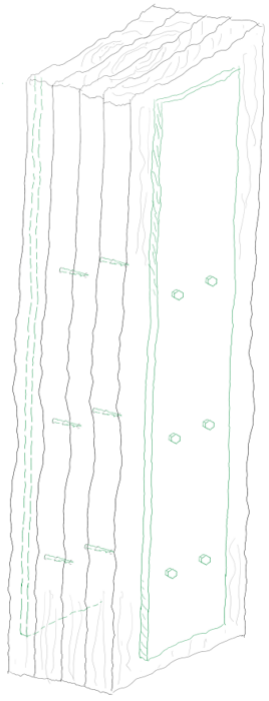

Figure 2.14: *Configuration column reinforced with steel plates, by Johanna Nilsson 2023*

Expanding the cross-sectional area of a column can effectively mitigate stress within the column, thereby reducing the likelihood of buckling and material yielding under compression (Chang, 2015). This can be beneficial in terms of lateral load resistance, as columns with substantial cross-sections offer enhanced restoring forces. This reinforcement helps the column return to its original position after undergoing displacement.

Strengthening of glulam columns can also be done with FRP laminates. A study done by Dalhousie University indicates that the utilization of FRP strengthening methods can potentially result in improved strength and stiffness of glulam columns. This method acts to counteract and prevent column buckling and thereby improve the overall structural performance (Taheri, Nagaraj, & Khosravi, 2009).

2.5 Loads

When dimensioning a structure, there are several loads that need to be accounted for. According to *EN 1991-1-1*, the loads are divided into permanent and variable loads, and depending on this, there are treated differently. This chapter will explain Eurocode definitions and how the considered loads are addressed.

2.5.1 Imposed load

The load on a building generated by its intended usage are referred as imposed load or live load (Liang, 2015). According to *EN 1991-1-1*, the imposed load is defined as a quasi-static action, which means it is a dynamic force represented by an equivalent static force in a static model (CEN, 2002). The category covers normal usage of people, furniture and movable objects, vehicle operations, and preparation for limited scenarios such as crowding of furniture or movement of objects during reorganization or redecoration. The imposed load on a structure can vary greatly in both magnitude and distribution, depending on the structure's intended usage and occupancy. The amount of imposed actions on a structure can range from zero to maximum values, which are infrequent and considered to be the highest loads a structure may encounter during its design life (Liang, 2015). The most critical load situation should be considered when an area is subjected to different categories, eg the highest value should be applied.

The imposed load for buildings is specified as a characteristic free variable load in the table below. The correction factor α_n can be used for the reduction of the imposed load, accounting for multiple storeys in the design of columns and walls. The reduction can be made since there are unlikely that several floors is loaded with the highest load, at the same time.

$$\alpha_n = \frac{2 + (n-2)\psi_0}{n} \tag{2.6}$$

ψ is a correction factor used in load combination calculations.

The imposed load should also be reduced for the areas that support the member, as can be calculated according to the equation below, and the reduction factor should be applied to the g_k, stated in Table 6.2. This factor is only used for beams, floors and slabs. α_n and α_A are not to be combined.

$$\alpha_A = \frac{5}{7}\psi_0 + \frac{A_0}{A} \leq 1,0 \tag{2.7}$$

When the imposed load is treated as an accompanying action, defined in EN 1990, only one of the two factors, either ψ from Tabel A.1.1 in EN1990 or α_A, α_n, from section 6.3.1.2(10) and (11), shall be used.

Table 2.1: Classifications of Application

Category	Specific use	Exampel
A	Area for domestic and residential activities	Rooms in residential buildings and houses; bedrooms and wards in hospitals; bedrooms in hotels and hotels kitchens and toilets
B	Office areas	
C	Areas where people may congregate (with the exception of areas defined under categories A,B, and D[1]	C1: Areas with tables, etc. c.g. areas in schools, cafés, restaurants, dining halls, reading rooms, and receptions. C2: areas with fixed seats, e.g. areas in churches, theatres or cinemas, conference rooms lecture halls, assembly halls, waiting rooms, and railway waiting rooms. C3:Areas without obstacles for moving people, e.g. areas in museums, exhibition rooms, etc. and access areas in public and administration buildings, hotels, hospitals, and railway station forecourts. C4: Areas with possible physical activities, e.g. dance halls, gymnastic rooms, and stages. C5: areas susceptible to large crowds, e.g. in buildings for public events like concert halls, sports halls including stands, terraces and access areas and railway platforms.
D	Shopping areas	D1: areas in general retail shops. D2:areas in department stores

Table 2.2: Corresponding values for each imposed action category

Category of loaded areas	q_k $[kN/m^2]$	Q_k $[kN]$
Category A		
-Floor	1,5 to 2,0	2,0 to 3,0
-Stairs	2,0 to 4,0	2,0 to 4,0
-Balconies	2,5 to 4,0	2,0 to 3,0
Category B	2,0 to 3,0	1,5 to 4,5
Category C		
-C1	2,0 to 3,0	3,0 to 4,0
-C2	3,0 to 4,0	2,5 to 7,0(4,0)
-C3	3,0 to 5,0	4,0 to 7,0
-C4	4,5 to 5,0	3,5 to 7,0
-C5	5,0 to 7,5	3,5 to 4,5
Category D		
-D1	4,0 to 5,0	3,5 to 7,0 (4,0)
-D2	4,0 to 5,0	3,5 to 7,0

Table 2.3: Corresponding values for reduction factors for each load

Load	ψ_0	ψ_1	ψ_2
Imposed			
-Category A	0,7	0,5	0,3
-Category B	0,7	0,5	0,3
-Category C	0,7	0,7	0,6
-Category D	0,7	0,7	0,6

2.5.2 Snow load

The vertical load-bearing system is influenced not only by self-weight and imposed loads but also by the snow load. In accordance with the guidelines provided by *EN-1991-1-3* (CEN, 2003), the snow load is classified as a variable fixed load. Calculating the snow load requires consideration of several parameters:

- S_k - Characteristic value of snow load on the ground for a given location
- C_e - exposure coefficient, should be taken as 1,0 unless otherwise specified for different topographies
- C_t - Thermal coefficient, recommended value 1.0, for all cases except high thermal transmittance surfaces, ($> 1\ W/m^2K$)
- μ_i - Shape coefficient

The characteristic snow load data is obtained from the European Ground Snow Load Maps, which are the outcome of scientific research conducted under contract to OGIII/O-35 of the European Commission by a dedicated research group. This information can be found in *EN 1991-1-3* and other relevant standards.
Table 2.4 illustrates the reduction factors that are applied to different load cases. These factors are used to adjust the snow load accordingly.

Table 2.4: Corresponding values for reduction factor for snow load

Load	ψ_0	ψ_1	ψ_2
Snow			
-$S_k \geq 3,0 kN/m^2$	0,8	0,6	0,2
-$2,0 \leq S_k \leq 3,0 kN/m^2$	0,7	0,4	0,2
-$1,0 \leq S_k \leq 2,0 kN/m^2$	0,6	0,3	0,1

2.5.3 Wind load

According to *EN-1991-1-4* is the wind load defined as a variable tied load that acts perpendicular to surfaces or individual coating elements (CEN, 2005a). The load acts directly as a pressure or suction on the outer surfaces of closed buildings along with the inner surfaces of an open building. Due to leaks in the building envelope, it has an indirect action on the inner surfaces. As a result of sweeping past larger surfaces, tangential frictional forces can be introduced. The wind loads can be treated as the result of dynamic effects but since most buildings have high natural damping, the response can be calculated using the static external wind load, according to the equation below.

$$w_e = q_e(z_e) \cdot c_{pe} \tag{2.8}$$

q_e refers to peak velocity pressure, which is based on the reference wind speed, v_b, describing the wind condition in the region. The speed varies over Sweden between 21m/s to 26 m/s depending on area-specific value (CEN, 2005a).

The peak velocity pressure is highly dependent on the height of the building and therefore, the reference speed multiplies with the reference height, commonly the same as the height of the structure. Supplementary to the reference wind speed and reference height, exposure factors are applied, considering the size and geometry of the building's envelope, together with the direction of the wind. The aerodynamic pressure against a wind-loaded surface varies significantly across the area, but it has been chosen that the exposure factor be based on the subjected area (Isaksson et al., 2010).

2.5.4 Unintendent inclination

For load-bearing systems, the phenomenon of unintended inclination and geometrical imperfections needs to be considered in the analysis of the ultimate limit state (CEN, 2005b). For load-bearing elements exposed to axial pressure and for elements with vertical load, Eurocode has provided some requirements and strategies to calculate the horizontal force that is generated from this phenomenon. The philosophy is similar between both steel members and timber members, but the imperfection differs between materials. For timber beam-column structures,

$$H = \alpha_{md} \sum V_i \tag{2.9}$$

Where

$$\alpha_{md} = \alpha_0 + \frac{\alpha_d}{\sqrt{n}}$$

$$\sum V_i = V_i \cdot n$$

V_i - Total vertical load on each column (from self-weight, roof, imposed load etc.
n - Numbers of columns
α_0 - Systemic part of inclination angle
α_d - Random part of inclination angle

For steel and concrete beam-column system, the equation differs a bit but is built up in a similar way.

$$H = \phi \sum N_i \tag{2.10}$$

$$\phi = \phi_0 \cdot \alpha_h \cdot \alpha_m$$

Where
N_i - Total vertical load on each column (from self-weigth, roof, imposed load etc.
ϕ_0 - is the basic inclination value: $\phi_0 = \frac{1}{200}$
α_h - is the reduction factor for height h applicable to columns:

$$\alpha_h = \frac{2}{\sqrt{h}} but \frac{2}{3} \leq \alpha_h \leq 1,0$$

h - is the height of the structure in meters
α_m - is the reduction factor for the number of columns in row:

$$\alpha_m = \sqrt{0.5 \cdot \left(1 + \frac{1}{m}\right)}$$

m - the number of columns in a row including only those columns which carry a vertical load N_{Ed} not less than 50 % of the average value of the column in the vertical plane considered

2.6 Parametric model

A parametric model is a computer-based approach to modelling that enables the alteration of parameters to shape, and thereby change the model's behaviour (Fu, 2018). This makes it useful in disciplines such as architecture and engineering, where designs must be adjusted and analyzed under various conditions. By using programming code to specify dimensions and geometry, a parametric model can be visualized in 3D drawing programs to simulate the objectives' real behaviour under different conditions.

Before parametric modelling, the scheme design stages were very difficult for engineers, since the design tends to change frequently. Parametric modelling enables designers to modify the entire shape of a model, not just individual elements in a quick and effective way. The technique was in the beginning only adopted by architectures to enable the possibility to draw complex structures, but have the past years also been adopted by structural engineers (Fu, 2018).

2.6.1 Rhinoceros 3D

Rhinoceros 3D was developed in 1980 by Robert McNeel & Associates and was the first parametric model program (Fu, 2018). The program is based on AutoCAD drawings and data derived from business processes(Associates, n.d.). The program can create analyses, and documents, animate and translate Nurbs curves and surfaces for example and especially enable the possibility of drawing complex structures.

2.6.2 Grasshopper

Grasshopper 3D is a graphical algorithm editor that operates as a plug-in for Rhino 3D modelling software (Davidson, n.d.). This tool was created to enhance the capabilities of Rhino in areas where it falls short, providing users with even more design possibilities (Sawantt, n.d.). One of the key benefits of using Rhino with Grasshopper is that it eliminates the need for programming or scripting, making it a user-friendly option for individuals with varying skill levels in these areas (Associates, n.d.).

This powerful combination of Rhino and Grasshopper has become a popular choice among designers and engineers looking to streamline their design processes and bring their ideas to life in a fast and efficient manner. The flexibility and versatility of Grasshopper, combined with the robust features of Rhino, make this a top choice for professionals in a wide range of industries, including architecture, engineering, product design, and more

2.6.3 Karamba

Karamba3D is a unique finite element program, specifically designed for use in the parametric design environment of Grasshopper(Preisinger & Heimrath, 2014). Unlike traditional finite element programs, Karamba3D is geared towards interactive use in the parametric design environment, making it ideal for architects, engineers, and designers who want to quickly and easily analyze the structural behaviour of trusses, frames, and shells (*Karamba 3D*, n.d.). The program provides accurate analysis of these structures, taking into account a variety of loading scenarios, and provides clear and actionable feedback to help users refine their designs. Karamba can also perform the structural design of steel structures according to EN-1993-1-1.

2.6.4 Beaver

Similar to Karamba 3D, the software tool *Beaver* provides structural design of timber structures according to EN-1995-1-1 (Food4Rhino, Accessed 2023). Beaver was founded by Poålytechnic School of the University of Sâo Paulo in Brazil, and was initially designed to cooperate with Karamba 3D, but has now been developed also to be applicable to any FEA plug-in inside Grasshopper environment. By using this workflow, it's possible to create a parametric design process that encompasses everything from architectural conception to structural detailing within a single software interface. This approach proves advantageous for complex parametric structures as well as conventional modular structures, as it grants users the ability to optimize structural arrangements, sections, and connections while ensuring compliance with established safety limit state codes.

3
Methods

The master thesis began with a comprehensive literature review and research on the studied field. This was done by carefully selecting and analysing relevant literature in the field to gain a deeper understanding of the topic and identify areas that required investigation

Additionally, information on the importance of actions in design processes was also investigated during the literature review. Based on this literature study, specific structural elements and systems were chosen for further research. A more detailed literature study was then conducted on these chosen elements and systems to gather information on the theory of structural design, strengthening techniques, building material performance and response to loads, and material properties.

The literature review was supplemented by parametric studies to examine the effects of altering the building's usage, which was represented in this thesis by changes to the structure's imposed load, geometry, boundary conditions, and several floors as well as the effectiveness of strengthening techniques. The parametric studies were performed using commercial 3D computer graphics and design applications such as *Rhinoceros* and *Grasshopper 3D*. Additional tools, such as *Karamba 3D*, were adopted to provide an accurate analysis of the performance of different systems and techniques under changing loads.

Based on the result from the computational model and literature review, improvement methods and strengthening techniques were recommended. In the following section, the method for the different parts will be covered.

3.1 Literature studie

To increase knowledge and gain a fundamental understanding the thesis started with a qualitative literature study. A literature review assists with identifying hypotheses, reaching questions, contributing, and contextualizing the research (Rowley & Slack, 2004). Literature consisting of a sustainability framework, building techniques, structural systems, and lastly how to strengthen elements, parts, and systems, was consumed.

The literature consumed was found online,*Google Scholar*, standards, and books. In table 3.1 a summarising of the different keywords and tapering words are listed.

Table 3.1: Keywords and tapering words

Keywords	Tapering word	Tapering word
Framework	Sustainability Climate declaration	FN Paris agreement Building and Construction sector
Design for zero	Hierarchy	
Repurposing	Buildings	Steel Timber
Structural system	Load-bearing	Steel Timber
Building material	Pros and cons	Steel Concrete Timber
Steel structural system	Beam-column	Vertical load Horisontal load
Timber structural system	Beam-column	Vertical load Horisontal load
Strengthening techniques	Columns	Steel Timber Buckling
Strengthening techniques	Beam	Steel Timber LT-buckling Lateral stability Deflection

3.2 Parametric model

To be able to use and validate the gained knowledge obtained from the literature research, the collection of data was required. Therefore, a model was developed to accumulate results and observations concerning structural behaviour under altering variables and situations. Since this master's thesis aims to test different changes in the load situation, to conclude how this affects the structural system and how an insufficient system can be strengthened, the creation of a parametric model was crucial. For further explanation of the methodology for the parametric model, see chapter 4.

3.3 Triangulation

Since the studied field of this master thesis constantly evolving, new research is published, and knowledge and conclusions are acquired and recognized ongoing, there is a possibility of contradicting information. There for, the use of triangulation was applied since it is beneficial to establish validated sources and verify the information. Triangulation refers to confirming the information and facts with multiple sources and validating the gathering results from the literature review through various methods (Bekhet & Zauszniewski, 2012). The triangulation mainly consisted of validation using comparisons of different sources, but also through dialogue and discussions with experienced and seniors in the industry.

The parametric model was also triangulated, to verify the result and the accuracy of the model. This was done through hand calculations and is more detailed explained in section 4.8.

4

Parametric model procedure

This chapter covers the generation of the parametric model and outlines the essential information and presumptions made during the model's development. The objective was to create a model that depended on a few parameters and that had a short routine time, with easily interpreted results.

Consequently, the initial step in the modelling process involved determining the intended purpose of the model and the specific outcomes desired, as for this reaches, analyse of the sectional forces and deflections in the beam and column elements. Based on this, the visual programming started using Grasshopper 3D with Rhinoceros 3D as displaying program. To derive a structural analysis from the model, the plug-in tools for grasshopper, *Karamba 3D* and *Beaver* was incorporated. In the following subchapter, the building up of the parametric model will be accounted for.

4.1 Geometry

As mentioned previously, the model consists of a few parameters that through the process will be changed in an iterative approach. This iterative approach allows for refining and optimising the model based on specific requirements and desired outcomes. The geometry was therefore built up on a grid, where all variables are changeable through sliders. Consequently, this creates a possibility of analysing different span lengths, numbers of floors, positions of core, and the building's total length and width. Observe that the floors are in direct correlation to each other and are replicas of the first floor.

The columns were generated first and based on the column's coordinates, the beams in X- and Y-direction create. This is performed to preserve a relationship between all the elements in the simulation. The columns and beams are verified to ensure they do not intersect with the core, thereby ensuring that the two components do not occupy the same location. Furthermore, the slabs are formed from the beams and are also controlled against intersecting with the core. The roof was set to a flat roof. Figure 4.1 illustrate the built-up process of the geometry.

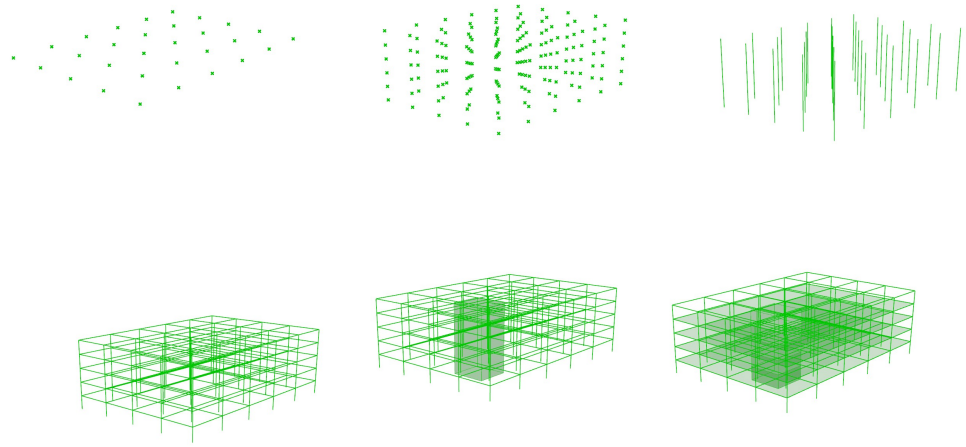

Figure 4.1: *The built-up process of the geometry, by Johanna Nilsson 2023*

Figure 4.2 shows an illustration of which beams that further on will be called X-beams. It is the X-beams that support the slabs, as they are chosen, both for the steel and timber system to carry the load in one direction. Figure 4.3 displays two different configurations of beams in the Y-direction, known as Y-beams, marked with green and yellow.

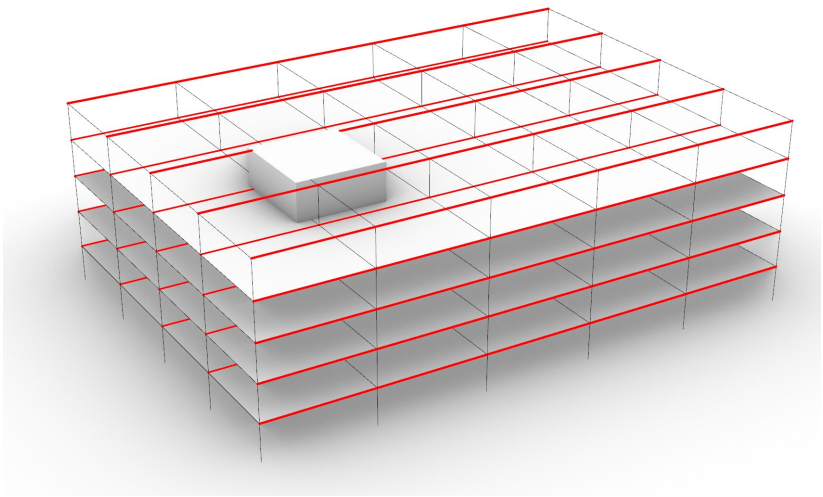

Figure 4.2: *Illustration of X-beams, marked with red colour, by Johanna Nilsson 2023*

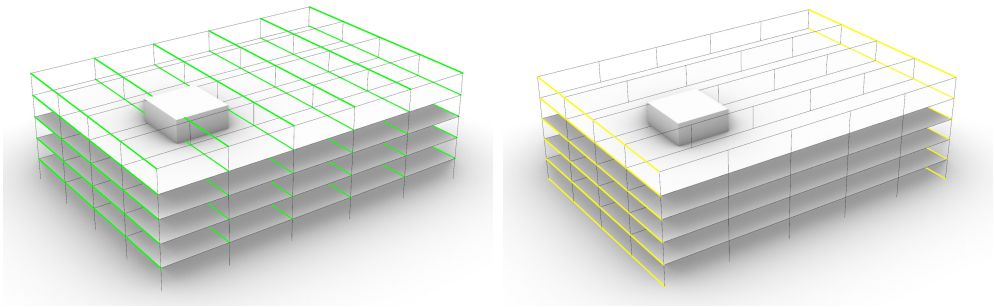

Figure 4.3: *Possible configuration for Y-beams, by Johanna Nilsson 2023*

This model includes all necessary elements, and its level of detail can be easily adjusted to include specific components for analysis. For instance, the model generates beams in both X and Y directions, but for this study, only the X-directed beams and edge beams in the Y-direction are being analyzed, see yellow beams in figure 4.3. Also, the possibility of bracing units is created and incorporated into the model, to the extent of the stabilising effect. Although the two systems possess individual properties and benefits, they have both been analyzed using the same geometry. This decision was made to enable a more precise comparison and handling of the data.

Figure 4.4 illustrates an example of geometry that can be analysed, while figure 4.5 shows the structural elements that actually will be analysed for this thesis. Further explanation of the analysis procedure will be covered in section 4.6

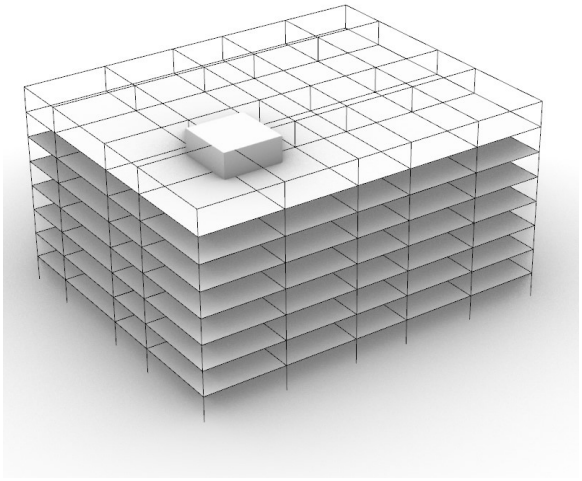

Figure 4.4: *Example of geometry that can be analysed, by Johanna Nilsson 2023*

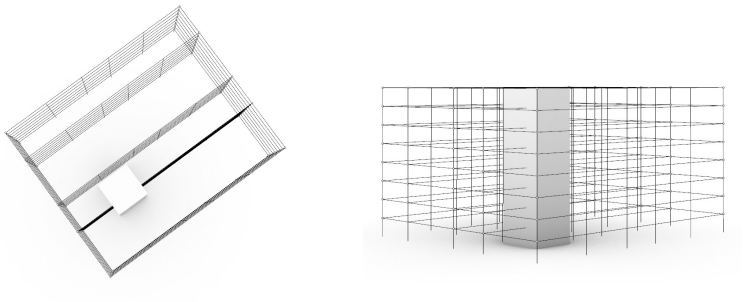

Figure 4.5: *Skeleton structure for beam-column system, by Johanna Nilsson 2023*

4.2 Material and Cross-section

As previously described, the two studied structural systems consist of steel columns and beams together with hollow core slabs, and the alternative one, timber columns and beams with CLT floors. Provided within Karamba 3D, there are defined material components that supply the material properties for the different materials. This can be seen in figure 4.8. The timber system utilised both Karamba 3D and beaver to create the cross-sections.

4.2.1 Mixed system

For the steel columns and beams, steel S355 was chosen, since it is standardised. The modulus of elasticity is set to $E = 2100\,kN/cm^2 = 210\,GPa$ by default for steel in Karamba 3D, see figure 4.8 below (Karamba3D, 2021). These prerequisites apply to both the columns and beams in X-and Y-direction.

Cross-sections were chosen for the columns to HEA and HEB, based on common approaches and profiles, explained in subchapter 2.3.2. This is done through the Karamba 3D component Cross section Range Selector, which selects from the cross-section library, ranging between HEA/HEB100-HEA/HEB1000. Similarly, IPE80-IPE600 was selected for the beams in X-and Y-direction. For beams in X-directions, X-beams, cross-section HEA was also included in the selectable profiles, due to its resistance to moments and to avoid overly high profiles that restrict ceiling height, etc.

The selectable profiles for each element were then sorted based on area, progressing from the smallest to the largest cross-section and consequently sorted on mass to produce a ranking of the most beneficial. This can be seen in the schematic illustration, figure 4.6. Note that the shown profiles are the profiles chosen for the columns, but the same procedure was implemented for the X-beams. This will further be explained in the section 4.6 and when outlining the steps of the optimization process. Figure 4.8 illustrates the identification and assignment of material and cross-section.

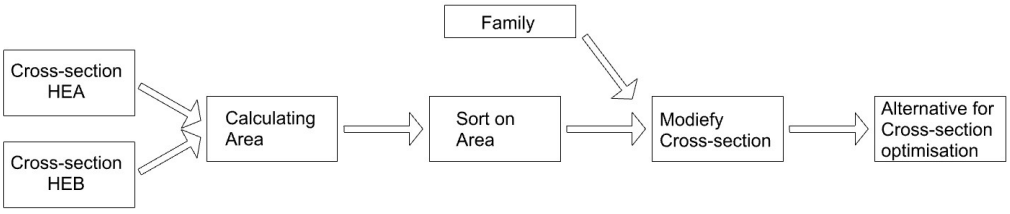

Figure 4.6: *Illustration of the sorting process, by Johanna Nilsson 2023*

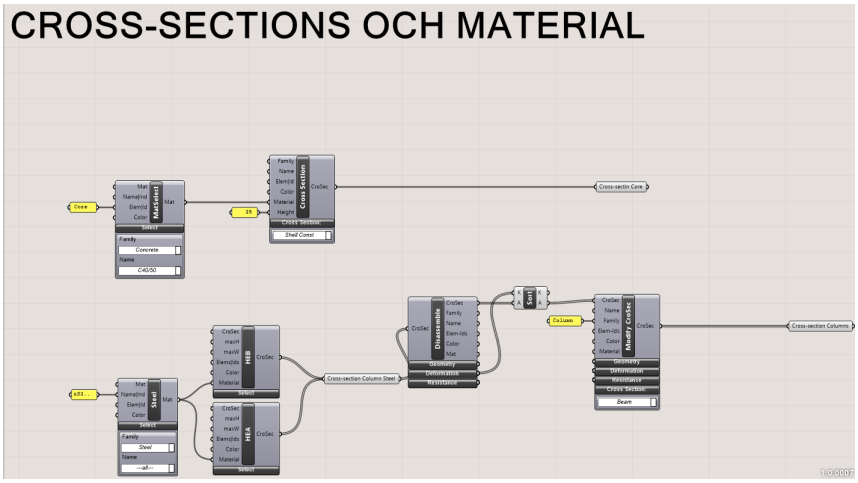

Figure 4.7: *Components for steel material and cross-sections, by Johanna Nilsson 2023*

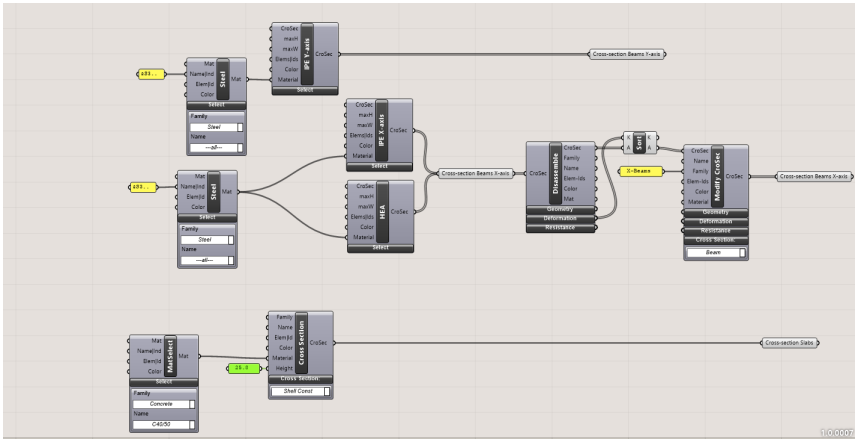

Figure 4.8: *Components for steel material and cross-sections, by Johanna Nilsson 2023*

The hollow core slab was defined as HD/F120/27, according to strängbetongs manufacturing range (Strängbetong, 2015). Since the built-in cross-section component in Karamba 3D, does not have HDF as a cross-section input choice, an effective height

was calculated for a homogeneous rectangular concrete cross-section. The concrete class were defined as C40/50, also based on the manufacturing range. See Appendix C for calculations of the effective height. It should be noted that this cross-section is only used for the general analysis of the stabilisation. For other analyses, HDF was represented as a permanent load on the beams.

4.2.2 Timber system

Since Beaver, more detailed explained in 2.6.4, is developed for timber structures, the software has been utilized in the analysis of the timber system. The material properties were therefore provided through Beavers' special material file, see appendix D instead of Karamba's built-in library. This can be seen in figure 4.9. The strength class was chosen to GL30c founded on the manufacturing range for glulam columns and glulam beams manufactured in Sweden (trä, 2015).

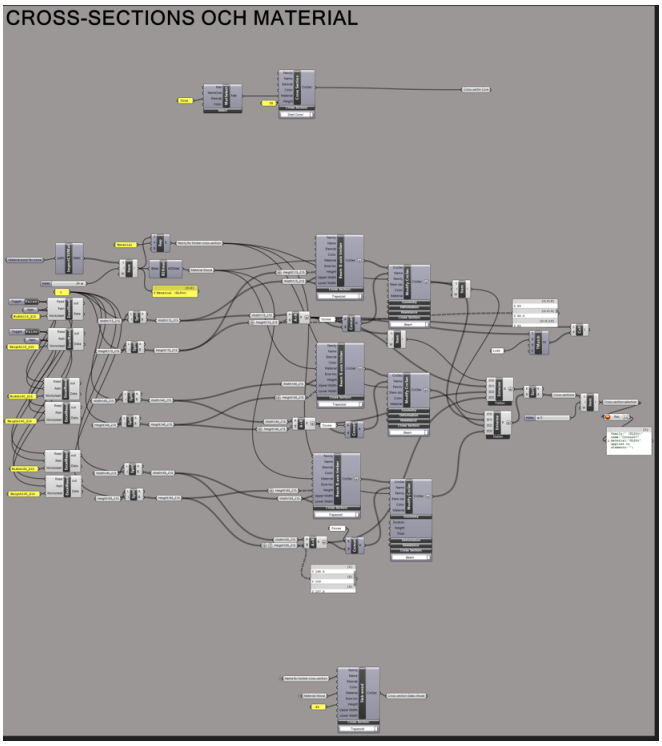

Figure 4.9: *Cross-section choice and sorting procedure, by Johanna Nilsson 2023*

Sourced from the same manufacturing range, the heights ranging from 18-162cm, and widths, 11.5-215cm, are implemented, to create a diversity of combinations, for possible cross-sections for the timber elements. For specific components, see Figure 4.10 and 4.11. Considering the CLT slab, the material was also provided with beaver, together with the mechanical properties. The thickness of the CLT flooring was chosen to be 0.25 m.

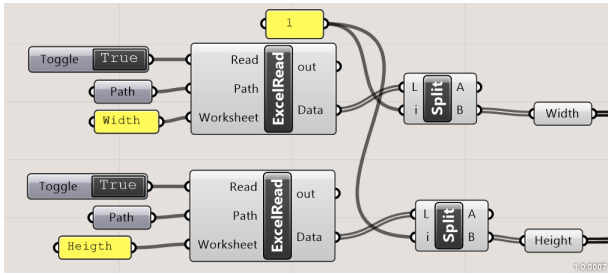

Figure 4.10: *Creating dimensions in Excel and implement them into Grasshopper, by Johanna Nilsson 2023*

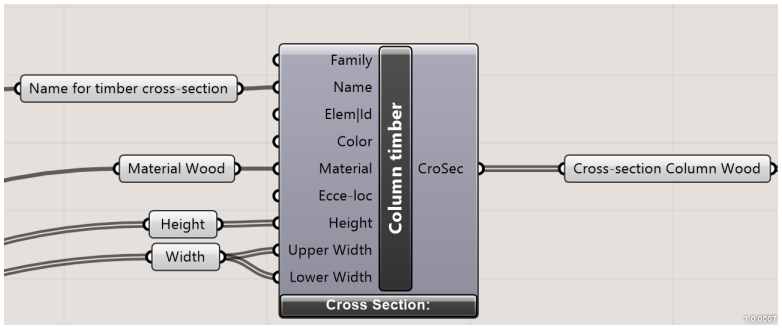

Figure 4.11: *Component creating the timber elements cross-section, Cross-section, by Johanna Nilsson 2023*

The prerequisites for the core, are the same for both systems and were modelled as a concrete shell with a thickness of 35cm, derived from a similar project and experience on PE Teknik and Arkitektur. The concrete class was set to C40/50 using the same Karamba 3D components as for the steel beams and columns.

4.3 Mesh and beam elements

To generate structural beam elements, that can be analysed through Karamba 3D, the component *Line to beam* was used. Input such as *Line*, *Identifier* and *Cross-section* was given to pair polylines with different cross-sections and names. Using this approach, the elements are organised into groups to ensure that those on the same level, and for the X-beams additionally, those in the same row, are dimensioned uniformly. This applies to all members defined as beam elements, i.e. columns, and beams parallel to the X- and Y-axis. These elements were modelled as beam elements since they describe failure and response caused by bending and axial force effectively, but don't require equal computing strength as modelling them as shell elements (Plos, 2008). The grouping of columns and X-beams are illustrated in figures 4.12 and 4.13. Please note that the illustration of grouping of X-beams is only done for some beams, the same approach applies to all X-beams.

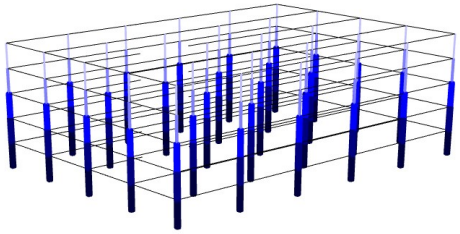

Figure 4.12: *Grouping of columns for optimisation, by Johanna Nilsson 2023*

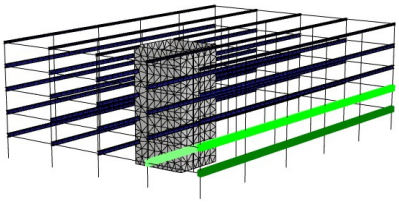

Figure 4.13: *Grouping of X-beams for optimisation, by Johanna Nilsson 2023*

The core, on the other hand, was modelled as shell elements, since the core is working as a stabilisation element and therefore, the shear failure and torsional stiffness were desired to be described. The detail level for beam elements is insufficient to describe these parts in a good way in a FEM analysis. Below, in figure 4.14, an illustration of how modelling of the different elements has been done. The main components that were used were *Line To Beam* to create the beam elements, *Element Set* used for grouping, and *Mesh Brep* and *Mesh To Shell* for creating the core.

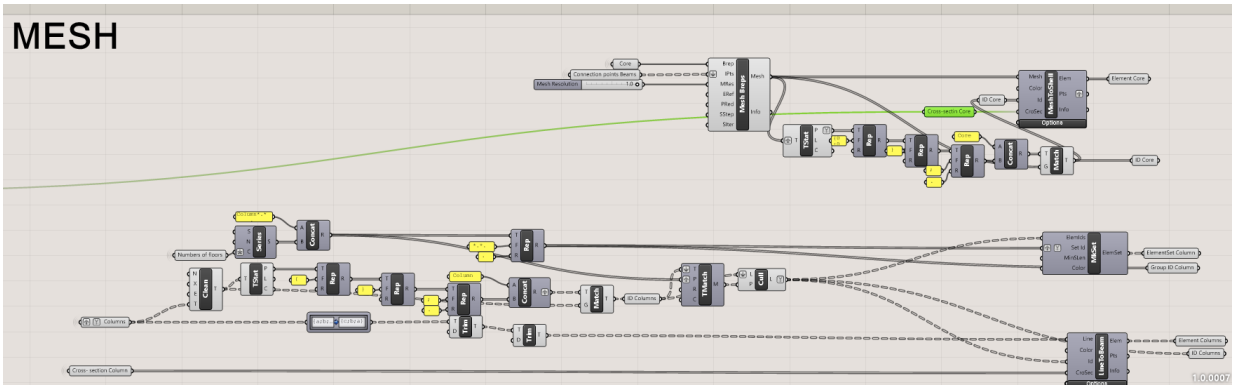

Figure 4.14: *Exampel of modelling of different elements, by Johanna Nilsson 2023*

Since one of the model's intentions was to create an accurate and valid but simple

model with limited routine time, the slabs and roof were decided to only be modelled as a mesh that distributes the imposed load respective snow load. This decision was also made based on the connections between the slab and the vertical load-bearing elements that didn't quite represent reality in a good way. To account for and to be able to model the elements and especially the connections for these elements, the model needed to be more detailed and consequently heavier with a longer routine time.

Although, a separate model was created to provide a general understanding of how the horizontal load affects the overall outcome. In this model, the slab elements were modelled, similar to the core, as shell elements. A discussion about the floorings impact and especially how it distributes the loads and stabilises the building can be found in subsection 6.2.5

4.4 Support and connections

In order to establish a consistent reference point, all models and analyses shared the same support conditions. As the core was supposed to act as a stabilisation element, using diagram action, the support conditions for the core were modelled as fixed to the foundation, except for allowing rotation around the z-axis. The columns, however, were instead structured as pendulum columns. This was done by modelling the supports for the columns on the ground floor as fully fixed, and then modelling the connections as hinged between the different floors. The X-beams and Y-beams are modelled as continuous, supported by the columns and core.

4.5 Loads and Load combinations

For the design and analysis of the two structural systems, the considered load are categorised into two groups, permanent and variable loads.

4.5.1 Load combinations

The load combinations were chosen to incorporate a collection of dimensional values according to EKS, the Swedish National Board of Housing, and their applications of Eurocode EN 1990. This was used to verify the structural reliability of a limit state under the simultaneous influence of different loads. The values and equations are presented below.

Derived from these equations, the resulting seven primary load combinations are further explained and a more detailed explanation of how the different loads have been defined in the model.

- 6.10a (STR): Used for verifying the internal failure och excessive deformation (ULS)

$$1.35G$$

G=Self-weight and other permanent loads, see section 4.5.2

- 6.10b Imposed (STR): Applied to check the internal failure och excessive deformation, with the imposed load as the leading variable action and snow load as the accompanying variable load. (ULS)

$$0.89 \cdot 1.35 \cdot G + 1.5 \cdot a_n \cdot Q_{imp} + 1.5 \cdot \psi_{0,i} \cdot Q_S$$

$$= 1.2 \cdot G + 1.5 \cdot a_n \cdot Q_{imp} + 1.5 \cdot 0.6 \cdot Q_S$$

G=Self-weigth and other permanent loads, see section 4.5.2
Q_{imp}= Imposed load, Variable load
Q_S= Snow load, Variable load

- 6.10b Snow load(STR): Applied to check the internal failure och excessive deformation, with the Snow load as the leading variable action and imposed load as the accompanying variable load. (ULS)

$$0.89 \cdot 1.35 \cdot G + 1.5\psi_{0,i} \cdot Q_{imp} + 1.5 \cdot Q_S$$

$$= 1.2 \cdot G + 1.5 \cdot 0.7 \cdot Q_{imp} + 1.5 \cdot Q_S$$

- 6.15b Imposed load (FREQ): Frequent load combination, used often to analyse the reversible limit states, and the constructions deformation. Imposed loads are acting as the main load, accompanied by the snow load. (SLS)

$$1.0 \cdot G + 1.0 \cdot \psi_{1,i} \cdot Q_{imp} + 1.0 \cdot \psi_{2,i} \cdot Q_S$$

For load $2kN/m^2 - 4kN/m^2$

$$1.0 \cdot G + 1.0 \cdot 0.5 \cdot Q_{imp} + 1.0 \cdot 0.1 \cdot Q_S$$

For load $5kN/m^2 - 7kN/m^2$

$$1.0 \cdot G + 1.0 \cdot 0.7 \cdot Q_{imp} + 1.0 \cdot 0.1 \cdot Q_S$$

- 6.15b Snow load (FREQ): Frequent load combination, used often to analyse the reversible limit states, and the constructions deformation. Snow loads are acting as the main load, accompanied by the imposed load (SLS).

$$1.0 \cdot G + 1.0 \cdot \psi_{2,i} \cdot Q_{imp} + 1.0 \cdot \psi_{1,i} \cdot Q_S$$

For load $2kN/m^2 - 4kN/m^2$

$$1.0 \cdot G + 1.0 \cdot 0.3 \cdot Q_{imp} + 1.0 \cdot 0.3 \cdot Q_S$$

For load $5kN/m^2 - 7kN/m^2$

$$1.0 \cdot G + 1.0 \cdot 0.6 \cdot Q_{imp} + 1.0 \cdot 0.3 \cdot Q_S$$

G=Self-weight and other permanent loads, see section 4.5.2
Q_{imp}= Imposed load, Variable load
Q_S= Snow load, Variable load

4.5.2 Self-weigth

The self-weight was modelled as a gravity load, using a load component, provided within Karamaba 3D. The gravity load are assigned by default to all structural elements, i.e. columns and beams in this model. However, since the self-weight of the integrated system was relevant, the slab self-weight was applied manually, represented as a mesh load.

For the hollow core slab, the self-weight was estimated from the manufactured product and prestandard documentation from strängbetong.Since the chosen HDF, HD/F120/27 has two dimensions on their ducts, resulting in two different area loads, a mean value from these two, where assumed and can be seen below. For detailed calculations, see Appendix C.

$$g_{HDF.slab} = 5.34 \ \frac{kN}{m^2} \tag{4.1}$$

Regarding the timber systems flooring, designed to be composed of CLT, the magnitude of the self-weight becomes, as predicted, much smaller. The CLT floor was chosen, as stated before, to have a thickness of 0.25m, and together with the Beavers density for timber, the self-weight assumes to be:

$$g_{CLT.slab} = 1.275 \ \frac{kN}{m^2} \tag{4.2}$$

For detailed calculations, see Appendix C

4.5.3 Imposed load

The imposed load are, as previously stated, an important part of evaluating changes correlated to repurposing. The magnitude of the load was set as a variable parameter, to be able to investigate how the load influence the structural system and if any conclusions or observations can be made.

The imposed load was applied as a mesh load on all slabs, to reflect the behaviour of how the imposed load is distributed. In theory, the imposed load should be distributed as a line load along the X-axis beams only, since the slabs only carry the load in one direction in this model. Therefore the loads could have been modelled as beam loads instead of mesh load, but since the core also carry the load, the mesh alternative provides a more accurate result. As seen in figure 4.15, the load component is shown, where the upper one shows the line load on the beams, while the lower one shows the point loads acting on the core. This requires more computer power but fewer hand calculations for each change. As explained in subsection 2.5.1, the reduction factor for number of floors was applied for every load combination in ULS, where the imposed load acts as the main load.

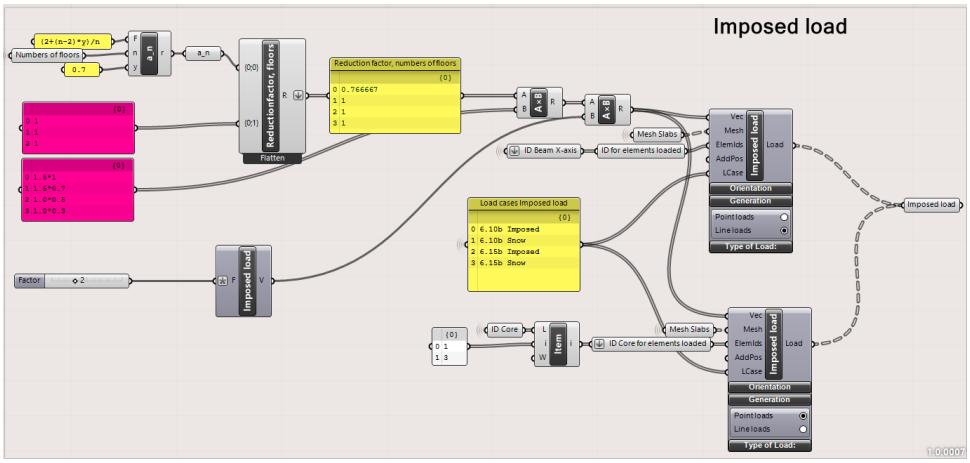

Figure 4.15: *Imposed load modelling, by Johanna Nilsson 2023*

4.5.4 Snow load

The snow load is applied similarly to the imposed load, as a mesh load, on the roof. For the analysis, the building was assumed to be located in Gothenburg, Sweden, and modelled as a flat roof. The magnitude of the snow load was calculated accordingly to EN-1991-1-3 (CEN, 2003), with a characteristic snow value $S_k = 1.5\ \frac{kN}{m^2}$ and a roof shape coefficients $\mu = 0.8$ as its stated for flat roofs. This resulted in a uniformly distributed load of $Q_S = 1.2$ and the calculations can be seen below in the equation

$$Q_S = S_k \cdot \mu = 1.5 \cdot 0.8 = 1.2\frac{kN}{m^2} \tag{4.3}$$

4.5.5 Load cases

To investigate the influence of the variable load on the support moment, three different load cases were simulated. This was done by dividing the slabs into 5 sections and applying the imposed load on one, two respective all five slabs. This study focused on a specific case study described in detail in 4.7.1.

One of the objectives of the parametric study was to create a general model with limited routine time, the decision was made to prioritise one load case for further analysis and other case studies. The chosen load case was the imposed load to all spans, as it represented the dimensional characteristics of most load situations. Therefore, the other three case studies were based on this particular load case. Figure 4.16.

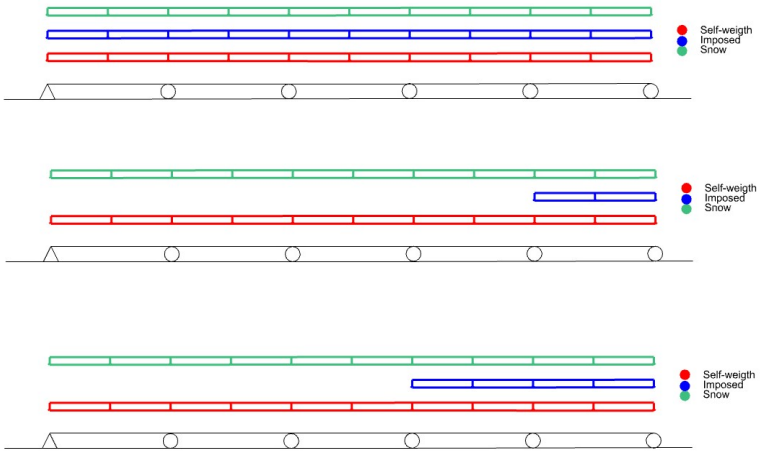

Figure 4.16: *Load cases, by Johanna Nilsson 2023*

4.5.6 Beaver: Load combination

The load combinations for analysing the timber system were generated using the built-in function in Beaver, which created load combinations based on their names. Therefore, it was essential to name the different loads in a specific manner. For instance, the permanent load was named *P* and the snow load was named *Snow*. However, this naming created a challenge when it came to the imposed load, which had to be referred to as the snow load due to the author didn't find any other solution.

By default in Beaver, the partial factor for the permanent load was set to 1.35, while for the variable load, it was 1.5. To align with the partial factors used in the EKS, the permanent partial factor was divided by 0.89, resulting in a value of 1.2.

4.6 Analysis

Both structural systems were analysed in a similar manner, with the exception of the optimisation of their cross-sections. The primary approach involved assembling the model, optimising the columns and beams' cross-sections, analysing the structure, and finally monitoring utilisation to ensure it remains below 80% for ultimate load and 100 % for displacement. Figure 4.17 shows a schematic illustration of the method for the analysis.

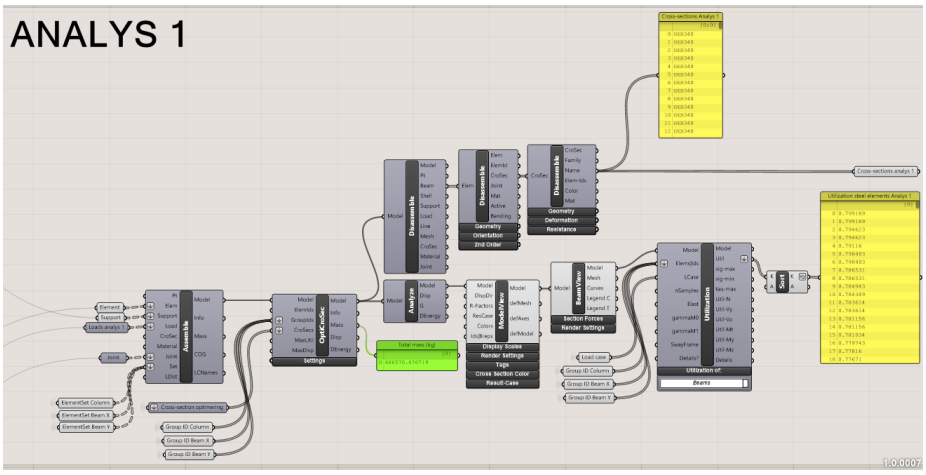

Figure 4.17: *Schematic illustration of primary approach for analysis of the structures, by Johanna Nilsson 2023*

After the initial analysis, a second analyst makes alterations to the input data, recording the overall mass, mass for each element group, and number of modified elements. These values were then compared to the data from the initial analysis. The ensuing outcome is elaborated upon in subsequent chapters.

4.6.1 Optimisation of steel elements

As described in subsection 2.3.2, the input from the cross-section was defined as a list of different cross-sections. For the optimisation of the steel columns and beams, Karamaba 3D optimisation components were used, to select the most suitable cross-sections. The design is done by going through the provided list of cross-sections until it's sufficient for the sectional forces for each element. The cross-sections are arranged in order of mass, with the one having the lowest mass first in the list, representing the most preferable choice.

The optimization aimed to use grouping as its fundamental basis, such as location and floor level. This allowed for the use of the same cross-section for elements within each group, not only did it replicate current practices, but it also optimized the model for improved efficiency.

The steel elements are optimized to achieve maximum utilization of 79% during ultimate limit state (ULS) conditions. This value is carefully chosen to avoid rounding up to the nearest value and instead focuses on optimization against 0.79999. Initially, the target limit was set at 80%, but that would allow results up to 0.89, which is undesirable. Under ULS, deflection is not considered and therefore has no upper limit. Consequently, the maximum iteration for finding the best solution is ten times for utilization and one time for deflection.

Additionally, in conjunction with optimizing for maximum utilization of 79%, the serviceability limit state (SLS) load combinations are also examined and optimized. In this case, the goal is to achieve a maximum deflection of L/300 and utilization of 100%. As this analyst considers both utilisation and deflection, but primarily optimises to fulfil the deflection condition, the number of iterations to achieve the limit was set to five maximum running for utilisation and ten for deflection. The option requiring the largest amount of material is then selected to ensure its validity under both ULS and SLS conditions.

For the steel system, it should be noted that the deflection is checked globally, as this is how Karamba components calculate the deflection by default.

4.6.2 Optimisation of timber elements

In difference to the optimisation for the steel elements, Karamaba 3D does not currently offer an optimisation component for timber. As a result, a manual optimization procedure was developed. This procedure involves individually analysing the various cross-sections described in section 4.2. Each cross-section is checked to ensure that its utilisation is below 79% under ULS conditions and 100% under SLS conditions. During this phase, all elements are assigned the same cross-section.

The cross-sections that meet the utilisation requirements are then extracted and grouped, similar to the steel system. Within each group, the largest required cross-section is applied to all the elements. Subsequently, a comprehensive analysis is performed to evaluate the structural system globally, considering the selected cross-sections and groupings. Below an illustration of the procedure is shown, figure 4.18, together with the definitions.

For the steel system, the deflection is calculated locally, in difference from the steel system. This approach was adopted because the initial analysis performed the examination of each element separately. A more comprehensive exploration of this distinction between the two systems will be conducted in Chapter 6.

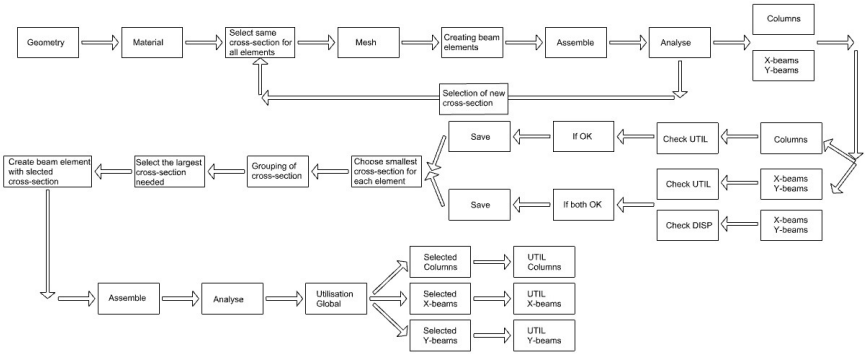

Figure 4.18: *Schematic illustration of manual optimisation procedure, by Johanna Nilsson 2023*

4.7 Result

The result was lastly contained from the model inform of four main tests. The main categories were: Modification of the magnitude of imposed load, Geometry alternations, changes in the number of floors and changes in utilisation. Further details and explanations of these four studies can be found in Chapter 5, where each case study and its corresponding input data are elaborated upon. The structure of the results from both models was aimed to be as closely aligned as possible, ensuring that they could be effectively compared and discussed in relation to each other.

The steel system analysis primarily relied on Karamba 3D's components, namely *Analyze* and *Utilisation*. The obtained results were mainly compared between the reference load of 2 kN/m^2 and various scenarios of interest, which were thoroughly examined and discussed. For the timber model, the software Beaver was employed instead. Since Beaver relatively new program without a user manual, this aspect presented some challenges. Consequently, to the best extent possible, the results obtained from Beaver were cross-validated with components in Karamba, and a thorough analysis of the outcomes was conducted. Therefore, some results were decided to not be included, since they could be treated as not vailed. This will further be discussed in section 5.2.

4.7.1 Case study: Modification of imposed load

To ensure relevant results when analysing changes in the applied load magnitude, a fixed geometry is chosen as a reference point. This geometry is selected based on experience and commonly used span widths. However, the need for a consistent reference point for both systems imposes some limitations on the geometry, especially to manage the long running time for the calculations of the timber system.

In this case study, a 5-floor structure is chosen to represent a typical residential or office building, taking into account computational efficiency. The span widths are set to 8 m in the X-direction and 7 m in the Y-direction. The only variable in this study is the magnitude of the imposed load, ranging from 2 kN/m to 7 kN/m^2. These different loads are applied to the structural system, and optimisation is performed either through Karamba 3D's optimisation tool for steel members or the optimisation procedure for the timber system, developed by the author.

4.7.2 Case study: Altering of geometry

Following the same principles as for modification of the imposed load, the case study investigates the effects of altering the geometry while keeping a fixed base of study. Due to that the geometry in this study is the variable one, the load magnitude and number of floors are instead the preset conditions. The load is defined as the reference load, 2 kN/m^2, illustrating residential/ office building accordingly to *EN 1991-1-1*, see figure 2.2.

The number of floors is, similar to the previous case study, which established to 5 floors. The X- and Y-spans are altering between 6 m-12 m, with beams in the same directions having consistent dimensions. In total, there are 49 unique combinations of span widths. The cross-section optimisation is iteratively performed for the different geometries.

4.7.3 Case study: Varying of the numbers of floors

In the process of analysing a structure with varying numbers of floors, a consistent geometry and load magnitude are applied. The previously defined reference load of 2 kN/m^2 is also applied in this particular case study. The span widths are specified as 8 m for the X-spans and 7 m for the Y-spans.

The intention was to create a wide range of floor numbers, alternating between 4.00 m and 15.00 m, in order to mimic the characteristics of a typical residential or office building. Similarly to the previous case study, *Modification of imposed load* and *Altering number the geometry*, the cross-section optimisation is iteratively performed for the different numbers of floors.

4.7.4 Case study: Changes in utilisation

A similar procedure as described for the case study *Modification of imposed load* assessed the potential for strengthening the structure, excluding the optimisation component. The applied load was increased, and a comprehensive analysis was conducted to determine the extent of the difference and the final utilization of each element during the load increase. The cross-sections and the geometry chosen for the reference load were applied for all the different load scenarios and under the variable loads. Based on this, a more thorough examination was conducted on the most exposed column and X-beam, focusing on their critical aspects.

4.8 Model verification

As described in section 3.3, hand calculations were performed to validate the model. The validation process focused on one X-beam and one column, and the calculations were categorized into two subcategories: *Structural Analysis* and *Structural Design*.

Under the section on Structural Analysis, the calculations involved determining the maximum moment and reaction forces for both systems. On the other hand, the Structural Design section entailed assessing the resistance to lateral torsional buckling and buckling for the steel X-beam and column. Additionally, it encompassed evaluating the resistance to lateral-torsional instability and buckling for the timber X-beam and column.

4.8.1 Verification of structural analysis

The following section is an explanation and summary of the calculation of the structural analysis conducted for both the steel and timber systems. For the complete set of calculations, please refer to Appendix A.

4.8.2 Moment verification

The beam analysed was Beam X0.0.0.4, which is located at the end-span of a continuous facade beam system. The specific position of this beam is illustrated in Figure 4.19. Within the overall system with a total length of 40.0 m, Beam X0.0.0.4 covers a span of 8.0 m.

The maximum span moment obtained from both the hand calculations and the parametric model is presented below, see equation 4.4 and 4.5. Since the beam is continuous, elementary cases were applied to determine the maximum span moment manually. In the steel system, the profile of the beam is HEA400.

$$M_s = k_s \cdot q_d \cdot s_{x-axis} = -365.33kNm \tag{4.4}$$

$$M_{s.model} = -351.65$$

$$\eta_{Steel} = \frac{M_s}{M_s.model} = 1.039$$

A 4% difference between the maximum span moment obtained from the hand calculations and the moment from the model can be seen as tolerant. The hand calculations can be seen as more conservative. The same theory was applied to the verification of the timber systems' maximum span moment, exclusive of the material properties, that were changed to timbers. The cross-section are 115x585 mm GL30c

$$M_s = k_s \cdot q_d \cdot s_{x-axis} = -240.8kNm \tag{4.5}$$

$$M_{s.model} = -224.4$$

$$\eta_{Timber} = \frac{M_s}{M_s.model} = 1.073$$

A slightly higher ratio of 7% between the hand calculations and the model was observed, which can still be considered acceptable. This discrepancy may be attributed to the fact that the Karamba 3D module, specifically the "Beam force" function, is primarily adapted to steel elements. Consequently, manual adjustments to the load combinations and partial coefficients were necessary due to Karamba's unique approach to creating them.

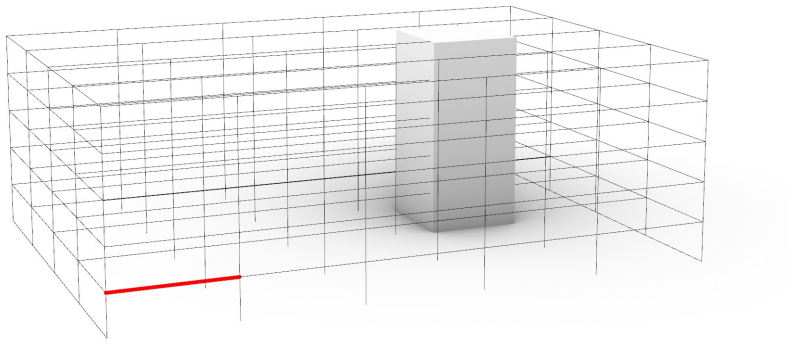

Figure 4.19: *Position of Beam X0.0.0.4, by Johanna Nilsson 2023*

4.8.3 Reaction forces verification

In a similar vein, the verification of reaction forces was conducted by performing hand calculations on Column 4.2.0, as depicted in Figure 4.20. The column is situated between the ground floor and the 1st floor, with a height of 2.7 m and being hinged.

The hand calculations and corresponding values obtained from the model are presented below. Since the beams supported by the column are continuous, elementary cases were utilized to determine the reaction forces. In the steel system, Column 4.2.0 is composed of a HEB240 profile.

$$R = (k_h + k_v) \cdot N = 4276kNm \tag{4.6}$$

$$R_{model} = 3869.33kN$$

$$\eta_{timber} = \frac{R}{R_{model}} = 1.108$$

The timber column consisted of 215x450 mm GL30C and was calculated using the same approach.

$$R = (k_h + k_v) \cdot N = 2715kNm \tag{4.7}$$

$$R_{model} = 2513kN$$

$$\eta_{Steel} = \frac{R}{R_model} = 1.08$$

Considering the slight variations observed between the models and the manual calculations, they can still be deemed acceptable. These differences could potentially be attributed to the calculation of element weights, which is performed within a built-in component of Karamba 3D in the models.

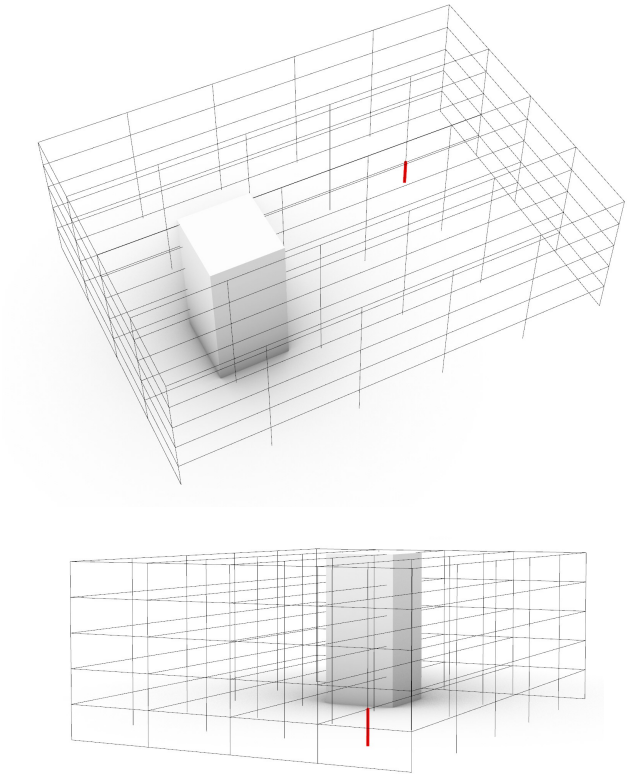

Figure 4.20: *Position of Column 4.2.0, by Johanna Nilsson 2023*

4.9 Verification of structural design

The subsection *Verification of structural design* treats the calculation of the buckling resistance and lateral torsional buckling resistance, for the two systems. The calculations are according to EN 1993-1-1 for steel and 1995-1-1 for timber. See Appendix B.

4.9.1 Column buckling resistance verification

The buckling verification consists of the calculation of the buckling resistance of the same column as was analysed in structural analysis. For the steel element, the column's resistance against buckling has been calculated in accordance with section 6.3 of EN 1993-1-1. The obtained values are presented below.

$$\begin{gathered} N_{Ed} = 4276kN \\ N_{Rd} = \chi \cdot \frac{f_y}{\gamma_{M1}} \\ \eta_b = \frac{N_{Ed}}{N_{Rd}} = 1.28 \\ \eta_{b.model} = 1.27 \\ \eta_{Steel} = \frac{\eta_b}{\eta_{b.model}} = 1.01 \end{gathered} \tag{4.8}$$

The discrepancy of 1% can be considered acceptable. The buckling resistance of the timber columns was calculated in accordance with section 6.3.2 of EN 1995-1-1. Also here, the variance can be considered reasonable.

$$\begin{gathered} N_{Ed} = 2715kN \\ N_{Rd} = f_{c0d} \cdot k_c \cdot A \\ \eta_b = \frac{N_{Ed}}{N_{Rd}} = 1.87 \\ \eta_{b.model} = 1.78 \\ \eta_{Timber} = \frac{\eta_b}{\eta_{b.model}} = 1.05 \end{gathered} \tag{4.9}$$

4.9.2 Lateral torsional buckling resistance verification

Lateral torsional buckling calculations were performed on Beam X0.0.0.4. For the steel system, the beam was, as previously stated, of profile HEA400 and the cross-section data is taken from standards. Lateral torsional buckling for steel members can be calculated with a general case, where the critical moment is calculated but also with a simplified approach since lateral torsional buckling of an I-beam mainly involves lateral displacement of the compressed upper flange. To verify the model, both methods have been used, but below, the result from the general case is presented as this is more exact, together with the values obtained from the parametric model.

$$\begin{gathered} M_s = 365.33kNm \\ M_{b.Rd} = \chi_{LT.mod} \cdot W_y \cdot \frac{f_y}{\gamma_{M1}} = 641.026 \\ \eta_{LT} = \frac{M_s}{M_{b.Rd}} = 0.57 \\ \eta_{LT.model} = 0.54 \end{gathered} \tag{4.10}$$

$$\eta_{Steel} = \frac{\eta_L T}{\eta_{LT.model}} = 1.06$$

The discrepancy, 6 % can be considered acceptable. However, it is important to note that the complete calculations involve several parameters that are assumed or intentionally conservative compared to real-world conditions. For instance, when determining the critical moment, the constant C_1 accounting for loading and restraint conditions was assigned the value for simply supported beams, which is a conservative assumption. Additionally, the value of $\chi_{LT.mod}$ was used as stated, considering Karamba 3D's utilization in the calculations

The lateral-torsional stability for the timber system was performed using section 6.3.3 in 1995-1-1. The simplified approach could be used, since the material was glulam and due to that the cross-section is rectangular. The produced values are provided below. These values can be considered identical since they only differ by 8 %.

$$\begin{gathered} \sigma_m = 24,483 MPa \\ f_{m.d} \cdot k_{crit} \\ \eta_{LT} = \frac{\sigma_{m.crit}}{f_{m.d} \cdot k_{crit}} = 1.675 \\ \eta_{LT.model} = 1.82 \\ \eta_{Steel} = \frac{\eta_L T}{\eta_{LT.model}} = 0.92 \end{gathered} \tag{4.11}$$

5

Results

In the following chapter, the result obtained from the parametric studies will be presented and explained. The results will be analysed together with the theory in chapter 6,*Discussion* and summarised in chapter 7,*Conclusion*. First, the result from imposed load variations will be presented through comparisons between different load scenarios. Second, the result from the investigation of changes in geometry, in the form of span lengths will be stated, followed by the consequences of adding floors will be illustrated. Lastly, the changes in utilisation will be examined, to investigate different strengthening possibilities.

5.1 Modification of the imposed load

Section 4.7.1, presents the case study that investigates the effects of modifying the magnitude of imposed load. The results of this analysis are compared to a reference load of 2 kN/m^2. Table 5.1 and table 5.2 provide a summary of the analysis of the total difference in weight between the optimised cross-sections for the reference load and for different magnitudes of imposed load. Figures 5.1 and 5.2 illustrate these observed differences and the obtained results are later discussed in chapter 6.2.1

Table 5.1: Total difference in weight between reference load, 2 kN/m^2, and the new magnitude for imposed load, Steel system

Imposed load **Steel system**	Difference in weight [ton]	Number of elements that changes
Imposed load 2 kN/m^2	0,00	0
Imposed load 3 kN/m^2	3,93	83
Imposed load 4 kN/m^2	14,09	187
Imposed load 5 kN/m^2	24,35	216
Imposed load 6 kN/m^2	29,54	216
Imposed load 7 kN/m^2	30,88	216

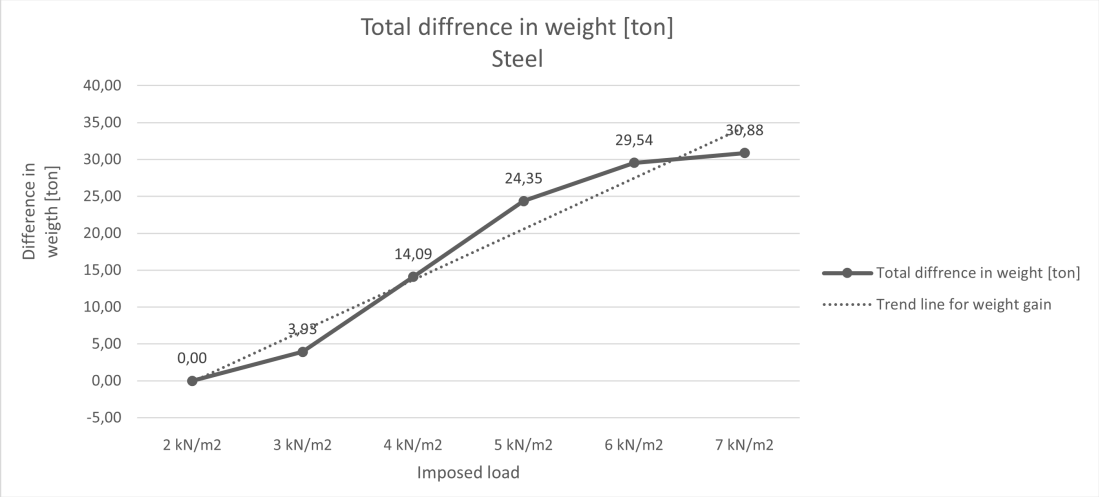

Figure 5.1: *Illustration of how the total difference in weight changes with amplitude of imposed load, Steel system, by Johanna Nilsson 2023*

Table 5.2: Total difference in weight between reference load, 2 kN/m^2, and the new magnitude for imposed load, Timber system

Imposed load **Timber system**	Difference in weight [ton]	Number of elements that changes
Imposed load 2 kN/m^2	0,00	0
Imposed load 3 kN/m^2	9,48	221
Imposed load 4 kN/m^2	19,14	221
Imposed load 5 kN/m^2	30,10	221
Imposed load 6 kN/m^2	39,71	221
Imposed load 7 kN/m^2	49,84	258

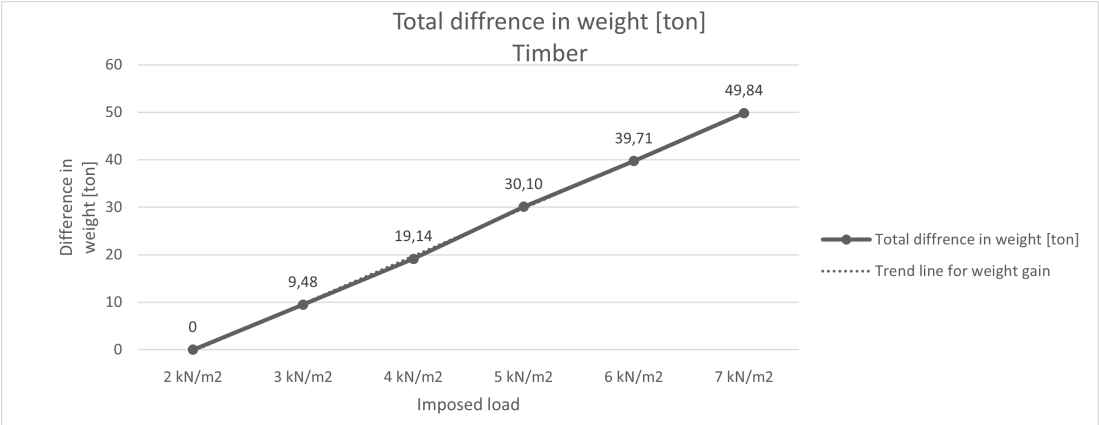

Figure 5.2: *Illustration of how the total difference in weight changes with amplitude of imposed load, Timber system, by Johanna Nilsson 2023*

As the outcome obtained from the comparison between the total difference in weight only gives a general overview of the consequences when varying the imposed load,

a group-specific analysis is also performed, to break down it further. As explained before, the two systems are built up on columns, X-beams Y-beams and a core. As the core isn´t optimised, the weight of the core is disregarded. This leaves three main groups, where the result is assembled and presented in a similar way as for the whole structure, but this time, specific for each group.

The result is presented below, and are grouped for the steel system in two groups: Columns and X-beams. The Y-beams, carrying only the facade load, did not changes through the varied loads, and therefore the result for Y-beams is neglected. For the timber system, on the other hand, the analysis revealed that the Y-beams adjust for the last load iteration, 7 kN/m^2. The timber system will therefore be presented in three groups instead, Columns, X-beams and Y-beams.

It is worth noting that, similar to the methodology applied for analysing the overall weight difference, the quantities of elements and the weight discrepancy are interconnected with the two structural systems under consideration, specifically in relation to the reference load. Table 5.3 and 5.4 present the resulting numbers from the analysis of the steel system, together with the illustrations 5.3 and 5.4. It is worth emphasizing the somewhat surprising change in the number of elements for an imposed load of 5 kN/m^2. This will be further discussed in 6.2.1

Table 5.3: Total difference in weight and number of elements that changes, for columns between reference load, 2 kN/m^2, and the new magnitude for imposed load

Imposed load **Steel system**	Difference in weight **Columns** [ton]	Number of Columns that changes
Imposed load 2 kN/m^2	0,00	0
Imposed load 3 kN/m^2	1,04	58
Imposed load 4 kN/m^2	2,54	87
Imposed load 5 kN/m^2	5,75	116
Imposed load 6 kN/m^2	6,14	116
Imposed load 7 kN/m^2	7,48	116

Table 5.4: Total difference in weight and number of elements that changes, for X-beams between reference load, 2 kN/m^2, and the new magnitude for imposed load

Imposed load **Steel system**	Difference in weight X-beams [ton]	Number of X-beams that changes
Imposed load 2 kN/m^2	0,00	0
Imposed load 3 kN/m^2	2,89	25
Imposed load 4 kN/m^2	11,55	100
Imposed load 5 kN/m^2	18,60	125
Imposed load 6 kN/m^2	23,40	100
Imposed load 7 kN/m^2	23,40	100

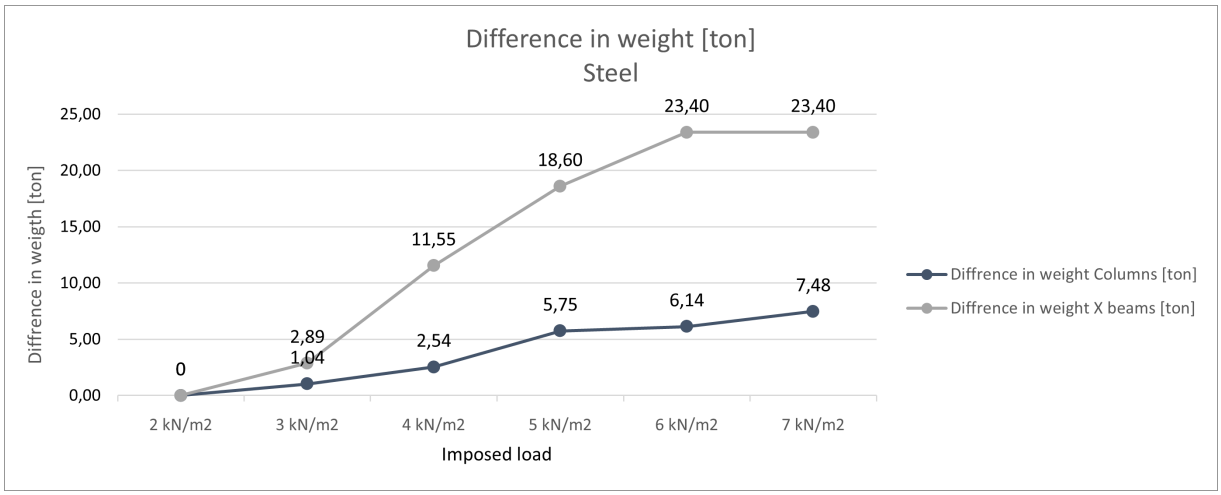

Figure 5.3: *Illustration of how the difference in weight for columns and X-beams changes with amplitude of imposed load, Steel system, by Johanna Nilsson 2023*

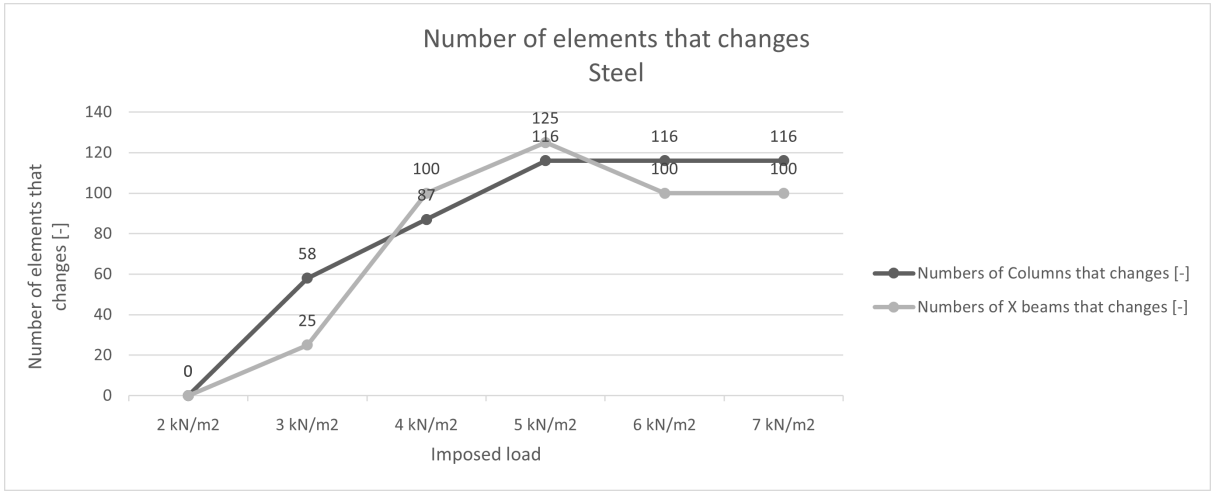

Figure 5.4: *Illustration of how the number of columns and X-beams that needs to be changed, with amplitude of imposed load, Steel system, by Johanna Nilsson 2023*

Below the result from the timber system analysis are presented. As previous mention, the timber system got changes in the Y-beams also, therefore, the result is presented in three different tables, 5.5, 5.6 and 5.7, accompanied by the illustrations 5.5 and 5.6

Table 5.5: Total difference in weight and number of elements that changes, for columns between reference load, 2 kN/m^2, and the new magnitude for imposed load

Imposed load **Timber system**	Difference in weight **Columns** [ton]	Number of Columns that changes
Imposed load 2 kN/m^2	0,00	0
Imposed load 3 kN/m^2	9,50	116
Imposed load 4 kN/m^2	11,48	116
Imposed load 5 kN/m^2	13,44	116
Imposed load 6 kN/m^2	15,51	116
Imposed load 7 kN/m^2	17,60	116

Table 5.6: Total difference in weight and number of elements that changes, for X-beams between reference load 2, kN/m^2, and the new magnitude for imposed load

Imposed load **Timber system**	Difference in weight **X-beams** [ton]	Number of Columns that changes
Imposed load 2 kN/m^2	0,00	0
Imposed load 3 kN/m^2	36,98	105
Imposed load 4 kN/m^2	44,77	105
Imposed load 5 kN/m^2	52,80	105
Imposed load 6 kN/m^2	60,47	105
Imposed load 7 kN/m^2	69,83	110

Table 5.7: Total difference in weight and number of elements that changes, for Y-beams between reference load, 2 kN/m^2, and the new magnitude for imposed load

Imposed load **Timber system**	Difference in weight **Y-beams** [ton]	Number of Columns that changes
Imposed load 2 kN/m^2	0,00	0
Imposed load 3 kN/m^2	0,00	0
Imposed load 4 kN/m^2	0,00	0
Imposed load 5 kN/m^2	0,00	0
Imposed load 6 kN/m^2	0,00	0
Imposed load 7 kN/m^2	3,16	32

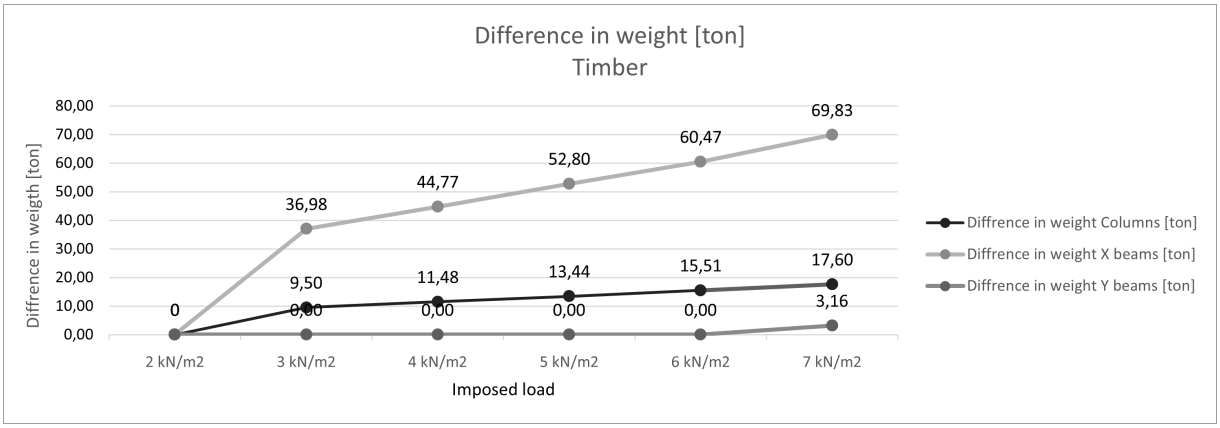

Figure 5.5: *Illustration of how the difference in weight for columns, X-beams and Y-beams changes with amplitude of imposed load, Timber system, by Johanna Nilsson 2023*

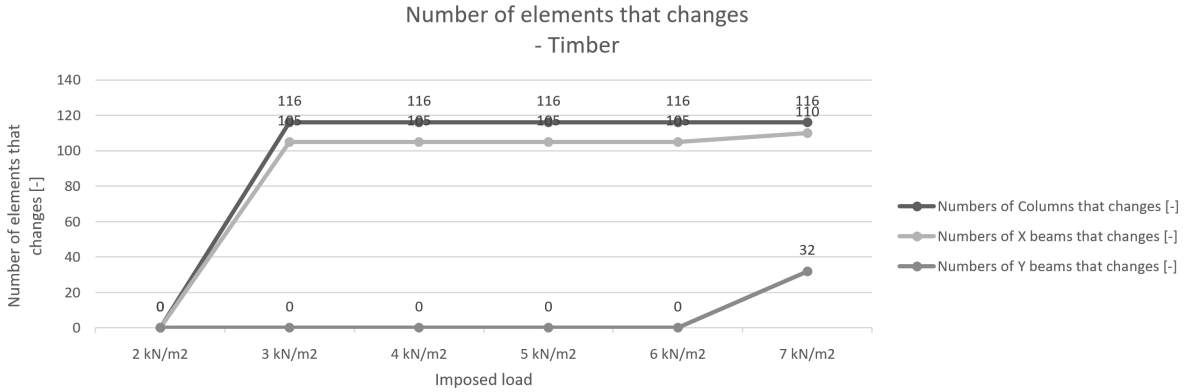

Figure 5.6: *Illustration of the number of columns, X-beams and Y-beams changes with amplitude of imposed load, Timber system, by Johanna Nilsson 2023*

5.2 Result from altering of geometry

Below is the result obtained from the analysis of the case study investigating the impact of geometry alterations. For a detailed description of the case study, see 4.7.2. The results from the 49 unique combinations applied for the steel model are presented in table 5.8 and illustrated in figure 5.7.

Table 5.8: Result for altering the span widths in X-and Y-direction

Span widths X-direction [m]								
Y-Span		6	7	8	9	10	11	12
	6	374,33	399,79	422,84	462,88	496,52	564,27	629,89
	7	378,58	412,88	437,03	474,19	511,84	588,44	659,33
	8	384,14	423,55	439,03	482,71	540,30	609,44	690,63
	9	385,17	426,69	453,87	495,95	569,37	637,21	694,55
	10	394,21	440,20	466,05	543,88	664,02	755,61	850,21
	11	399,97	451,39	576,30	689,30	795,66	834,74	874,61
	12	413,30	491,77	680,81	768,72	808,85	851,18	888,48

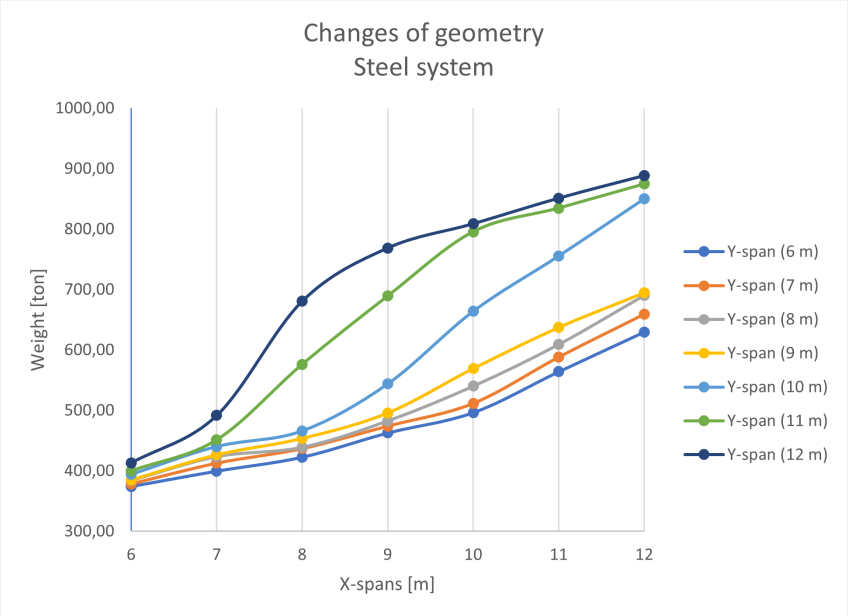

Figure 5.7: *Weight of steel element as a function of different span widths, by Johanna Nilsson 2023*

As previously explained, the procedure involves optimising two aspects and selecting the mass from the case that requires the most material. Figure 5.8 provides an illustration of the various combinations and which aspect, Utilisation (UTIL) or Displacement (DISP), was the determining factor in the dimensioning process. The blue colour highlights instances where certain elements need to be larger than the

largest selectable in the cross-section range or have a different cross-section than the chosen one. This indicates that either the utilisation exceeds 80 % or the displacement is greater than L/300.

Analys Steel Span width Y-axis [m]	Span width X-axis [m]						
	6	7	8	9	10	11	12
6	DISP	UTIL	UTIL	UTIL	UTIL	DISP	UTIL
7	DISP	UTIL	UTIL	DISP	UTIL	DISP	UTIL
8	UTIL	UTIL	UTIL	UTIL	DISP	UTIL	UTIL
9	UTIL	UTIL	UTIL	UTIL	DISP	UTIL	DISP*
10	DISP	UTIL	DISP	DISP	DISP*	DISP*	DISP*
11	UTIL	DISP	DISP	DISP*	DISP*	DISP*	DISP*
12	DISP	DISP	DISP*	DISP*	DISP*	DISP*	DISP*

*) Blue parts: unable to meet the criteria

Figure 5.8: *Illustration of the dimensional factor for each span iteration, by Johanna Nilsson 2023*

To investigate the possibility of different strengthening technics, the same illustration is presented, but with a focus on how the outcome have been if only utilisation was the determining factor. This is illustrated in figure 5.9

Analys Steel Span width Y-axis [m]	Span width X-axis [m]						
	6	7	8	9	10	11	12
6							
7							
8							
9							0 DISP, 4 UTIL
10					5 DISP, 0 UTIL	7 DISP, 0 UTIL	9 DISP, 4 UTIL
11				7 DISP, 0 UTIL	18 DISP, 0 UTIL	19 DISP, 1 UTIL	20 DISP, 4 UTIL
12			7 DISP, 0 UTIL	19 DISP, 0 UTIL	19 DISP, 0 UTIL	19 DISP, 4 UTIL	20 DISP, 4 UTIL

Widths where its unable to meet the criteria. Note the blue part there both DISP and UTIL fall
The numbers correspond to the number of cross-sectional groups that fail.

Figure 5.9: *Illustration of how long the cross-section range is sufficient for the two different dimensional factors, by Johanna Nilsson 2023*

The results obtained from this case study are not valid for the timber system. By altering the spans, a significant discrepancy is observed between the overall system's utilisation result and the utilisation result for individual elements, rendering it unacceptable. A thorough discussion addressing this issue and investigating potential reasons will be presented in Chapter 6, *Discussion*.

5.3 Result from varying of the numbers of floors

Table 5.9, together with figure 5.10 and 5.11, present the outcome from examining the behaviour of the steel system under changes in the numbers of floors. The case study and the analyis input are stated in section 4.7.3.

Table 5.9: Total weight of structural system for imposed load 2 kN/m^2 with different numbers of floors, Steel system

Number of floors	Total weight of steel system [ton]
4	253,33
5	344,59
6	437,03
7	530,60
8	635,95
9	730,40
10	856,21
11	995,01
12	1173,14
13	1547,65
14	1756,37
15	1953,12

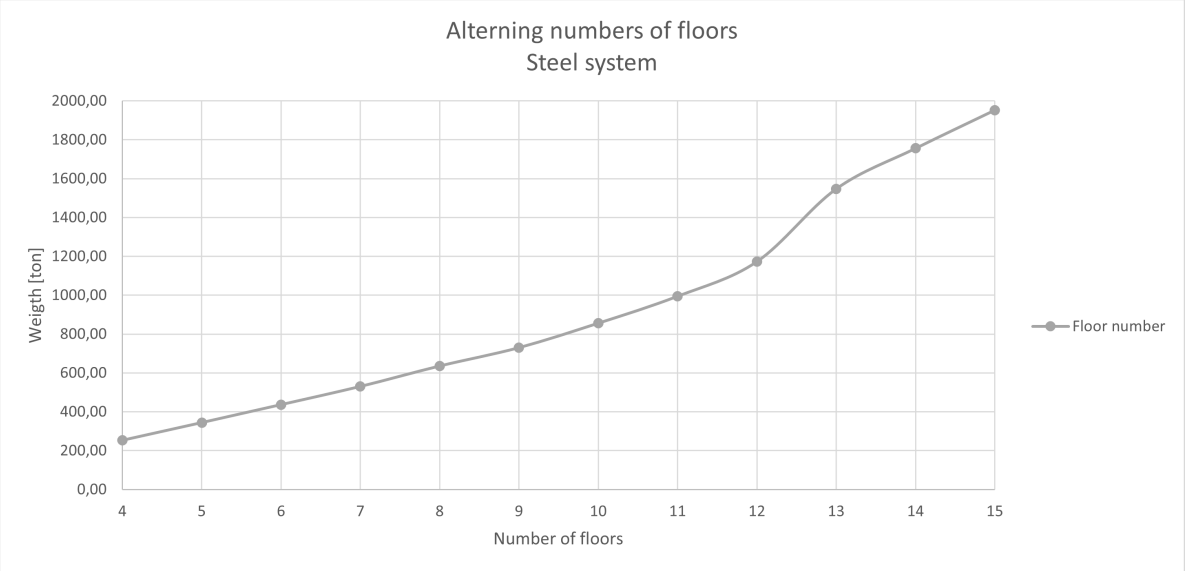

Figure 5.10: *Weigth of the steel system as a function of the number of floors, by Johanna Nilsson 2023*

As can be seen in figure 5.11, optimisation with regards to displacement are covering most of the different floor iterations, for the steel system. The blue colour indicates

instances where there is a change in cross-section type or when larger cross-sections need to be assigned, as mentioned previously in section 5.2.

Number of floors	Weight [ton]	Dimensioned section
4	253,33	UTIL
5	344,59	UTIL
6	437,03	UTIL
7	530,60	UTIL
8	635,95	DISP
9	730,40	DISP
10	856,21	DISP
11	995,01	DISP
12	1173,14	DISP
13	1547,65	DISP*
14	1756,37	DISP*
15	1953,12	DISP*

*) Blue part: unable to meet the criteria

Figure 5.11: *Illustration of the most critical case for the case study of the number of floors, by Johanna Nilsson 2023*

The optimization procedure described in 4.6.2 was also implemented for the timber system in this case study. It is evident that the system's weight is linear and aligns with the prognosis. Figure 5.13 demonstrates that, in contrast to the result derived from the steel system, the dimensional parameter for timber system is utilisation. The iteration where the utilisation surpassing the maximum limit of 80% is indicated by the blue colour. A thorough discussion regarding this matter will be conducted in Chapter 6.

Table 5.10: Total weight of structural system for imposed load 2 kN/m^2 with different numbers of floors, Timber system

Number of floors	Total weight of Timber system [ton]
4	208,18
5	279,75
6	352,02
7	424,72
8	498,21
9	572,04
10	645,79
11	720,70
12	796,20
13	872,25
14	949,23
15	1027

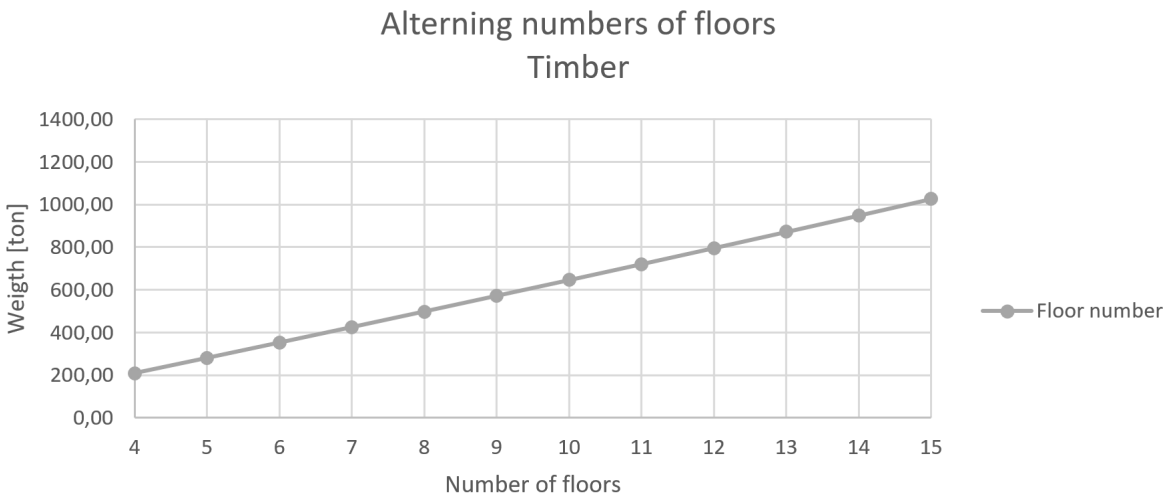

Figure 5.12: *Weigth of the timber system as a function of the number of floors, done by Johanna Nilsson 2023*

Number of floors	Weight [ton]	Dimensioned section
4	208,18	UTIL
5	279,75	UTIL
6	352,02	UTIL
7	424,72	UTIL
8	498,21	UTIL
9	572,04	UTIL*
10	645,79	UTIL*
11	720,70	UTIL*
12	796,20	UTIL*
13	872,25	UTIL*
14	949,23	UTIL*
15	1027,00	UTIL*

*) Blue part: unable to meet the criteria

Figure 5.13: *Weigth of the timber element as a function of the number of floors, by Johanna Nilsson 2023*

Another observation made was that the ratio between the actual value and max limit for displacement decreased with an increasing number of floors, while the utilization increased with the increasing number of floors. This is illustrated in the equation below, equation 5.1, 5.2, respective 5.3, 5.4.

$$\eta_{Util.4} = 78,98\%$$

$$\eta_{Util.max} = 80,00\%$$

$$ratio_{Util.4} = \frac{\eta_{Util.4}}{\eta_{Util.max}} = 98,73 \tag{5.1}$$

$$\eta_{Disp.4} = 86\%$$

$$\eta_{Disp.max} = 100\%$$

$$ratio_{Disp.4} = \frac{\eta_{Disp.4}}{\eta_{Disp.max}} = 86 \tag{5.2}$$

$$\eta_{Util.15} = 83,55\%$$

$$\eta_{Util.max} = 80,00\%$$

$$ratio_{Util.15} = \frac{\eta_{Util.15}}{\eta_{Util.max}} = 104,44 \tag{5.3}$$

$$\eta_{Disp.15} = 58\%$$

$$\eta_{Disp.max} = 100\%$$

$$ratio_{Disp.15} = \frac{\eta_{Disp.15}}{\eta_{Disp.max}} = 58 \tag{5.4}$$

5.4 Changes in utilisation

When examining the steel system and varying the magnitude of the imposed load, the investigation revealed the following results regarding the most critical elements. The column's buckling resistance was crucial due to the significant compression force it experienced. The steel column had a utilisation of 1,28, and the verification calculations are presented below in the provided equation. It's important to note that these calculations are based on the highest tested load of 7 kN/m^2.The calculations are also based on the extracted values from the steel model.

$$N_{Ed} = -3889,04kN$$

$$N_{Rd} = 3816,00kN$$

$$\chi_z = 0,7943$$

$$\eta_N = \frac{N_{Ed}}{\frac{N_{Rd}}{\chi_z}} = 1,28 \rightarrow 128\% \tag{5.5}$$

Worth mentioning is that the investigated column only carries the load in compression and therefore, for this model, all the other sectional forces are zero.

As expected, the X-beams were most fragile to bending and lateral torsional buckling. The beams showed utilisation of 1,17, with the largest variation of 43% observed between the element subjected to the reference load and the element under the highest load. See equation 5.6 for validation of the result.

$$M_{Y.Ed} = 698,84kNm$$

$$M_{Y.Rd} = 829,58kNm$$

$$\chi_{LT} = 0,7222$$

$$\eta_{M_Y} = \frac{M_{Y.Ed}}{\frac{M_{Y.Rd}}{\chi_{LT}}} = 1,17 \rightarrow 117\% \tag{5.6}$$

For the X-beam, the load is also carried in shear in the z-direction for this specific beam element and load case. However, the utilisation in shear is well below the limiting value. The calculations of the shear force are stated below. The other sectional forces can be considered negligible.

$$V_{Z.Ed} = 446,68kN$$

$$V_{Z.Rd} = 848,01,58kN$$

$$\eta_{V_Z} = \frac{V_{Z.Ed}}{v_{Z.Rd}} = 0,53 \rightarrow 53\% \tag{5.7}$$

Significant changes were observed in the timber system, surpassing those of the steel system. Similar to the steel system, the most critical column primarily fails due to insufficient buckling capacity. The following summary represents the calculations conducted for the timber column, see equation 5.8. Since Beaver software does not provide resistance values and only displays the calculated utilisation and the sectional forces, additional hand calculations were performed to validate these results. See appendix F for complete calculations.

$$N_{Ed} = 2580kN$$

$$N_{Z.Rd} = f_{c.0.d} \cdot K_c \cdot A = 1453kN$$

$$\eta_N = \frac{N_{Ed}}{N_{Rd}} = 1.776 \rightarrow 178\% \tag{5.8}$$

The timber X-beam, *Beam X1.1.0.3*, surpassed the maximum utilisation of 80 % for almost every failing mode, especially for the failing modes correlated to rotation and lateral-torsional stability. The most critical failure mode was the failure mode categorized as *Compression and bending, beam* in Beaver. This showed results of an experienced utilisation rate of 510 %. However, when performing hand calculations to validate this significant utilisation, it appears that this result should not be included since the hand calculation and the model didn't correspond. When performing hand calculations on the other failing modes in Beaver, these aliens with the result obtained in the model. Hand calculation is attached in appendix G, and a discussion about the difference between the hand calculations and the utilisation provided from the model, will be examined in chapter 6, *Discussion*.

For the same reason as for the timber column, the result is presented in a summarising below and the extended calculations are attached in appendix G. Not that the values defined below are not for *Beam X1.1.0.3*, as when the *Compression and bending, beam* failing mode were neglected, *Beam X0.3.0.1* where the most critical in compression and bending and *Beam X0.4.0.1* in biaxial bending. Note that all failure mode was significantly higher than the maximum limit.

Compression and bending accordingly to EN 1995-1-1 6.2.4

$$\sigma_{m.y.d} = 31.745\ MPa$$

$$\sigma_{m.z.d} = 8.0 \cdot 10^{-}4\ MPa$$

$$\sigma_{c.0.d} = 1.12 \cdot 10^{-}5\ MPa$$

$$\eta_{Compresionandbending.y} = (\frac{\sigma_{c.0.d}}{f_{c.0.d}}) + \frac{\sigma_{m.y.d}}{f_{m.y.d}} + k_c \cdot \frac{\sigma_{m.z.d}}{f_{m.z.d}} = 1.653 \rightarrow 165\% \tag{5.9}$$

Compression and bending accordingly to EN 1995-1-1 6.1.6

$$\sigma_{m.y.d} = 34.98\ MPa$$

$$\sigma_{m.z.d} = 9.0 \cdot 10^{-}5\ MPa$$

$$\eta_{biaxialbending.y} = \frac{\sigma_{m.y.d}}{f_{m.y.d}} + k_c \cdot \frac{\sigma_{m.z.d}}{f_{m.z.d}} = 1.82 \rightarrow 182\% \tag{5.10}$$

6

Discussion

The discussion of this master thesis is based on the results obtained from the four case studies (section 4.7), and are complemented with theory and implementation strategies outlined in the theory chapter (2), particularly focusing on section 2.4. However, to ensure greater validity and provide a comprehensive overview, additional investigations and analyses demand further. It is crucial to acknowledge that the results and discussions presented may not be directly applicable. Instead, they serve to broaden perspectives, foster innovative thinking, and lay the groundwork for design and early-stage development. The discussion revolves around a comprehensive analysis of the comparative results obtained from various alternative outcomes achieved through repurposing, for each of the two systems individually. The focus lies on exploring and evaluating the distinctions between these alternatives and their respective outcomes. The outcomes resulting from the changes due to the repurposing of the steel and timber systems will also be compared with each other. This analysis examines and evaluates the respective outcomes of both systems and identifies any variations or similarities between them.

Furthermore, in practises when designing structural systems, the aspect of stabilisation is an essential part of structural analysis and design. Therefore it is essential to acknowledge that the relationship between optimisation and permitted flexibility within the vertical load-bearing system might not align or correspond with the correlation between optimisation and flexibility within the stabilization system.

6.1 Optimisation procedure

The master thesis involves optimisation. The optimisation procedure is for the two systems, developed in two different ways, but striving for the same result, material optimisation. The steel system is optimised, as detailed in subsection 4.6.1, utilizing the optimization component within Karamba 3D. The timber optimisation, in contrast to the steel system, is done using an optimisation procedure specifically developed by the author of this master thesis, which is deeper described in subsection 4.6.2. It is essential to recognise this disparity in procedures since the result between the two systems is compared, despite not sharing the exact same optimisation approach.

6.2 Structural adjustments as a result of repurposing

In this segment, the result from the four case studies is presented. The respective case studies and results can be found in chapter 4, *Parametric model procedure*, and chapter 5, *Result*.

6.2.1 Modification of imposed load

When analysing the effects of varying the magnitude of the imposed load, as described in section 5.1, the results demonstrate an evident linear trend in the total weight difference, for the two systems. Notably, the timber system presents a more evenly progressive weight increase compared to the steel system, emphasising the impact of repurposing.

The diagram represented in Figure 5.1 exposes a notable characteristic concerning the cumulative weight of the steel system. Notably, the diagram exhibits a series of steps. Distinguishing it from the timber system, where the cross-section varies in terms of width and height, the steel system varies more in the form of choice of cross-section types, such as HEA, HEB, or IPE, along with dimensional variations within each cross-section type. In contrast, the timber system offers a broader selection of 149 cross-sectional alternatives, while the steel system presents 48 options for columns and 42 options for X-beams. Consequently, the disparity in cross-sections, concerning material and volume, is much more significant in the steel system. Furthermore, it is possible for two steel cross-sections to possess similar volumes but exhibit significant variations in capacity. Given that the optimisation process prioritises material and is limited to a maximum of 10 iterations for determining the optimal solution for the steel system, such discontinuities may arise. Similarly, the inverse scenario may occur, where different volumes correspond to approximately equal capacities.

This could clarify the reason behind the timber system presenting a more linear curve compared to the graph representing the steel system. Having more alternatives allows for smaller increments between various load scenarios.

Investigating the steel system a bit further, it can be seen that the columns tend to have a consistent prognosis, while the X-beams have a more spread shape. This can be assumed depending on the same theory as before, the columns iterate between HEA and HEB, which is two cross-sections types with similar visual appearance and form factor, resulting in similar volume for the same profile height, while the X-beams iterate between IPE and HEA, demonstrating significant differences in their respective forms. This is illustrated in figure 5.3. Regarding the number of elements undergoing modifications, as shown in Figure 5.4, it is shown, essentially, the same elements are being adjusted when increasing the imposed load. The exception lies with the elements on the 4th floor, which only is loaded with the snow load and remain unchanged throughout the case study.

For this figure, it can also be seen that more alterations are occurring between the scenarios of a 4 kN/m^2 and 5 kN/m^2 imposed load compared to the other load scenarios. This can be explained by the varying reduction factor between these particular scenarios as specified by the Eurocode. This result is unique to this case study as displacement is the covering factor. See appendix E for all results obtained.

For the timber system, the difference in weight is, as previously described, linear. Similar to the steel analysis, specific columns undergo consistent adjustments throughout the entire case study. However, in difference, X-beams on the 4th floor also experience changes. This can be assumed to be due to the deflection criteria for these beams, as deflection is often a more significant concern for timber beams. Additionally, in the final analysis, where the highest load,7 kN/m^2, is applied, Y-beams for floors 0-3 also undergo modifications in the timber system. This is due to that some load, that should be carried only by the X-beams, are transferred to the Y-beams. This can be a consequence of combining Karamba 3D connections with Beaver. However, discussions with the developers of Beaver indicate that this issue will be addressed and rectified in the forthcoming version update of Beaver.

Upon examining the comparison between *Optimisation* and *Over-dimensioning* for enhanced flexibility, the results reveal a notable trend: the relationship between material, volume, and applied load exhibits a demonstrates near linearity. Consequently, it becomes evident that excessive over-dimensioning does not yield significant benefits unless there is prior knowledge of future repurposing.

6.2.2 Modification of the geometry

When examining the impact of varying span widths in the X-and Y-directions for the steel system, it can be seen that the behaviour tends to follow a relatively linear trend for span widths from 6 up to 9 meters in both directions. As could be seen in figure 5.8, for these spans, the primary governing factor is the utilisation of different elements, although there are some exceptions.

One such exception arises when considering the displacement analysis for a 6x6 span width. In this case, the displacement operates as the critical parameter. When optimising exclusively for utilisation, the resulting cross-sections become relatively small. However, due to the tight maximum displacement limit of L/300, 2 cm for the small span widths, these smaller cross-sections are unable to meet the required criteria. As a result, cross-sections that optimise for the displacement requirement are chosen instead. It is important to note that the variation between the two solutions, specifically for this case, is not significant. However, the change in cross-sections leads to a lower ratio between the displacement limit and the actual value, thus fulfilling the displacement requirement more effectively. Figure 6.1, illustrates the result obtained from the analysis of 6-9 m span widths, extracted from the figure 5.7.

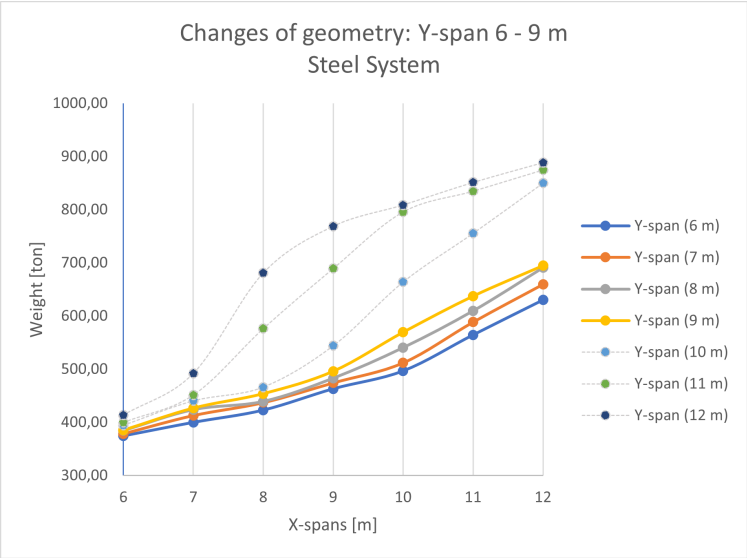

Figure 6.1: *Weight of steel element as a function of span widths between 6-9 m, by Johanna Nilsson 2023*

For span widths ranging from 10 m to 12 m, a change of character can be seen. For these longer spans, displacement is the covering factor, influencing the weight and leading to an increase in the weight gradient. As can be seen in figures 6.2 and 6.3, a demonstration of this relationship, where weight increases as displacement becomes the governing parameter and then stabilises when the elements have reached their maximum allowed cross-section. The blue colour in the figure 6.3 indicates instances where the largest cross-sections are insufficient in restricting the maximum utilisation below 80% or keeping the displacement below $L/300$. Figure 6.3 illustrates how many cross-section groups that need to be bigger. Note that due to the grouping of elements in the optimisations, this applies to the entire group, regardless of whether there are one or multiple elements within that group that require larger cross-sections.

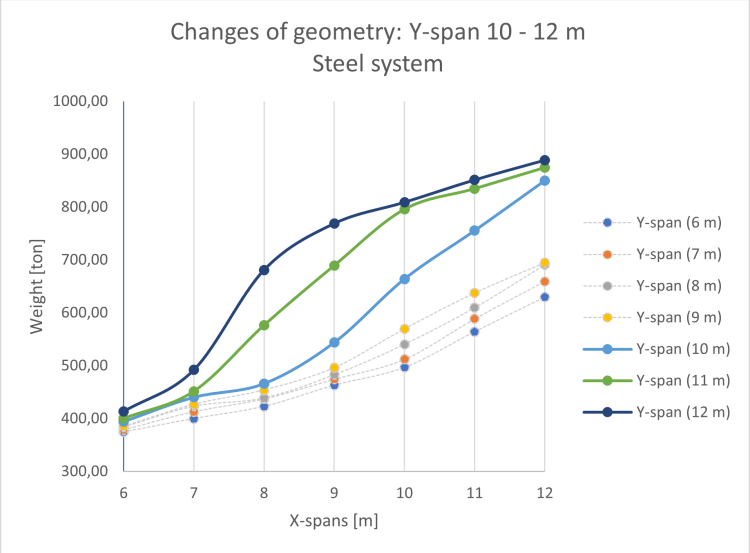

Figure 6.2: *Weight of steel element as a function of span widths between 10-12 m, by Johanna Nilsson 2023*

Analys Steel Span width Y-axis [m]	Span width X-axis [m]						
	6	7	8	9	10	11	12
6							
7							
8							
9							0 DISP, 4 UTIL
10					5 DISP, 0 UTIL	7 DISP, 0 UTIL	9 DISP, 4 UTIL
11				7 DISP, 0 UTIL	18 DISP, 0 UTIL	19 DISP, 1 UTIL	20 DISP, 4 UTIL
12			7 DISP, 0 UTIL	19 DISP, 0 UTIL	19 DISP, 0 UTIL	19 DISP, 4 UTIL	20 DISP, 4 UTIL

Widths where its unable to meet the criteria. Note the blue part there both DISP and UTIL fall
The numbers correspond to the number of cross-sectional groups that fail.

Figure 6.3: *Illustration of how long the cross-section range is sufficient for the two different dimensional factors and how many groups are insufficient, by Johanna Nilsson 2023*

In addition, it should be stated that the utilisation slightly increases in the final solution due to the inclusion of the self-weight of the new elements. When completing the optimisation, and assembling the system, it can be seen that the utilisation increase, and in cases where the systems and span widths require larger cross-sections, the utilisation may even surpass the maximum limit of 80 %.

As observed from figure 6.3, the range of selectable cross-sections for the elements becomes insufficient for the displacement criteria faster than for the utilisation criteria. This observation indicates that by strengthening the beams that do not meet the criteria against deflection, there is a potential to extend span widths further. Consequently, this enhances the future potential for increased flexibility. The strengthening methods described in 2.4.1 can be utilised, where some examples are, single flange steel plate or using CFRP on the tension side.

As previously mentioned, the timber system model demonstrated an issue with assigning the appropriate cross-sections to the corresponding elements when the load was increased. Although manual control of the model ensured the correct assignment of elements and cross-sections, the final analysis revealed that the utilisation rate of the facade X-beams was significantly higher. Since the underlying cause of this phenomenon remains unidentified, timber has been excluded from this particular case study.

6.2.3 Modification of the numbers of floors

The results obtained from analysing the variation in the number of floors for the steel system show a similar pattern to the observed when altering the span widths. Displacement is the dimensional factor mainly, and it is noteworthy that the character of the curve changes when the selectable range of cross-sections is insufficient. This is illustrated in figure 5.10, as the increase of slope between iteration with 12 floors and 13 floors.

At 13 floors, the normal force applied on the columns, particularly those on the ground floor, becomes so substantial that the required cross-section exceeds the maximum selectable size within this analysis. This can be predicted, since the load on the column amplifies with the number of floors, while the X-beams load stays near constant. This is indicated with blue in figure 5.11

The optimisation for displacement becomes the dimensional case for the steel system, for floor number 8 to 15. In contrast to the steel system, the dimensional factor for the timber system is utilisation. This is a consequence of the inconsistency of selected way of modelling the displacement. As the steel system is modelled with a displacement that are analysed globally, this affects the result. This choice of modelling results in if a column deforms due to high axial load, the X-beams appear to have a greater deflection than they actually possess. This is due to the deformation of the columns and the deflection of the X-beams combine and are attributed to the X-beams. Consequently, the X-beams undergo a deformation of x mm from their original position. An illustration of how the column deform can be seen in figure 6.4

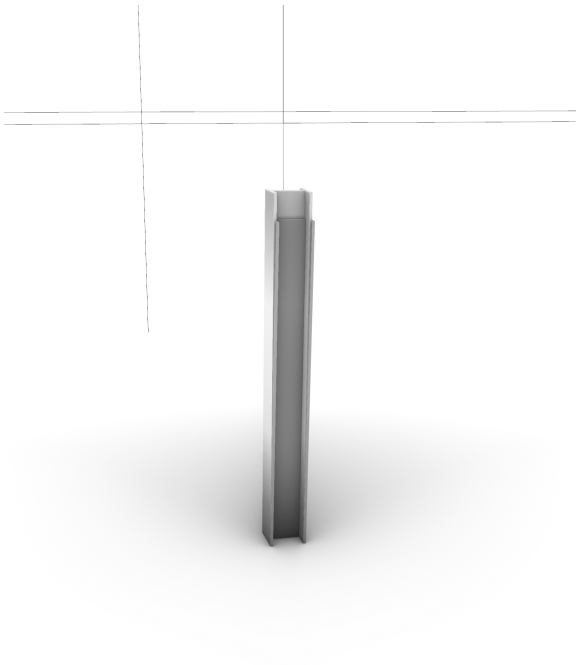

Figure 6.4: *Columns deformation between 2 kN/m^2 and 7 kN/m^2 , by Johanna Nilsson 2023*

The optimisation for displacement for the timber system, however, are done locally. This results in that the utilisation instead becomes the covering factor, as the columns experience high axial load and therefore needs to iterative enlarge the choice of cross-section. Nevertheless, the X-beams carry approximately the same load for all the different scenarios, resulting in that they remain constant throughout the process. This theory is also strengthened by the derivation of the result of how the ratio between the maximum limit and the actual value for the two dimensional criteria, UTIL and DISP, change.

For the sake of being able to compare the two results, it would have been advantageous to analyze the displacement using similar methodologies. Since they serve different purpose, the project-specific outcome should be stated before deciding which modelling approach that should be used.

From the results discussed above, the analysis of the steel and timber systems, it can be concluded that these two systems possess distinct critical factors. Consequently, in order to achieve the same desired outcome, which is to enhance future flexibility, they should be strengthened according to their respective critical requierment.

6.2.4 Changes in utilisation

The result derived from the case study, which is further detailed in section 4.7.4, demonstrated the most significant disparity between the two systems. The results can be seen in section 5.4.

The most critical steel column experienced utilisation of 128 %, leading to failure as a consequence of excessive axial force and thereby causing buckling failure. As this result is obtained from the analysis using the highest tested load, 7 kN/m^2, it signifies favourable opportunities for implementing strengthening strategies. For example by utilise double symmetrical steel plates to increase the moment of inertia and the cross-section area and thereby increase the buckling resistance, or using CFRP laminates. Additional potential strengthening techniques are outlined in section 2.4.1. The primary failure mode for the steel X-beam is lateral-torsional buckling, which results in a utilization of 117 %. Here are strengthening techniques using both steel plates or CRFP applicable also. These methods can effectively enhance the beam's resistance to lateral-torsional buckling and increase its overall strength.

An essential aspect and significant outcome is the relatively low utilization, which highlights the effectiveness of strengthening strategies for both columns and beams. These strategies have demonstrated the ability to decrease utilisation to a level below 100 % in these cases. While achieving a utilization below 80 % may present challenges, achieving a utilization below 100 % can be considered acceptable after increasing the load with a factor of three. This also aligns with the principles of the third carbon reduction potential step, *Built clever, Specify enough material and no more.*

The critical element for the timber system, however, undergo a more extended change in utilisation between the reference load and the highest applied load. The timber column, encounters a utilisation of 178 %, similar to the steel column, failing in buckling. This indicates the need for potential strengthening measures, although it may pose challenges. One approach to achieve this is by enlarging the column's cross-section with additional timber or reinforcing it with steel rods, as further elaborated in section 2.4.3.

Among all the structural elements in both systems, the timber X-beam exhibited the highest utilisation, reaching 510 %. Almost every failure mode was over-utilized in this case. The specific failure mode responsible for the 510 % utilisation was the lack of lateral-torsional stability along the weak axis. The disparity between the hand calculations and the utilisation values obtained from the models appears to arise from the program's computation of lateral-torsional stability along the weaker axis and its comparison to the maximum applied flexural load. Due to this discrepancy, this failure mode is neglected. This failing mode is dimensional for the cross-section optimisation for only a few elements, and therefore the discussion about over-dimensioning as a good solution is still considered reasonable.

The utilisation, when neglecting the non-validated failing mode, is still well above the limited value of 80 %, showing 182 % for biaxial bending, respective 165 % for compression and bending. As these utilisation rates can be seen as considerably above the maximum limit, a combination between over-dimensioning and strengthening can be a beneficial solution.

6.2.5 Stabilisation

Although the stabilisation isn't apart of this study, it serves a crucial role in the overall integrity of the structural system. Therefore, when preforming structural analysis and design, the stabilisation should always be include and accounted for. Different stabilisation strategies are stated in the section 2.3.4 and these provides a good understanding of how to adopt the stabilisation system in the vertical load bearing system.

Then preforming a stabilisation study, where the wind load and untended inclination were included in the case-study *Modification of imposed load*,some observations could be done. The cross-sections wheren't optimise for these additional horisontal load, instead, the previously selected cross-sections were applied for respective increase of imposed load. the result presented that the uplift was the most critical part, and this could be derived from that utilisation for the reference load where higher than for the highest load. As the cross-sections are optimised for only the vertical load for each load scenario, the elements for the reference load tend to be slender and more influenced by the horisontal loads. Higher vertical load are also preferable for the uplift as it counteracting effect. Therefore, higher imposed load resulting in lower utilisation, as can be seen in the equation stated below.

$$3kN/m^2 \rightarrow 1.04 \rightarrow 104\%$$

$$7kN/m^2 \rightarrow 0.94 \rightarrow 94\%$$

This particular study is not included in the results but serves as a complementary analysis to the other studies. The reason for this is the complexity of the connections required to analyze both vertical and horizontal loads within the same model. To address this complexity, it is advantageous to create separate models for vertical and horizontal load analyses in order to accurately capture the true behavior of the structure.

7
Conclusion

The aim of the thesis was to examine the current design methods for two structural systems of buildings and their consequences in future modifications due to repurposing. Additionally develop an design process that allows for greater flexibility in the future while still maintaining the current focus on optimization and cost-effectiveness. With this in mind, and based on the result and the discussion after analysing different consequences of respourposing, some final conclusions could been drawn:

- When analysing a fixed structural system with varying magnitude of applied imposed load, it was observed that the optimal chosen cross-sections and its weight is in direct correlation to the applied load. Failure due to sectional forces is the determining factor in terms of dimensions.

- For increasing span widths, the deflection of the beams becomes the critical factor for optimisation of the elements cross-section dimensions. By implementing strengthening measures specifically aimed at addressing deflection, the structural system can be effectively utilised for longer span widths.

- The dimensions of the structural system's columns are directly influenced by the number of floors. By utilise strengthening techniques to reduce the axial force, improved results can be achieved, allowing for smaller cross-sections to be implemented or valid longer.

When assessing the best solution for improved future flexibility, the following conclusions could be stated based on the discussion:

- To enhance future flexibility in the steel system, simply over-dimensioning the structural system does not provide significant benefits. However, optimising the system for current purposes and implementing strengthening strategies for potential future repurposing demonstrates promising possibilities. There are various strategies for strengthening that can serve this purpose, with particular emphasis on increasing buckling capacity and resistance to lateral torsional buckling in the steel elements. Hence, it is crucial to design for strengthening in order to facilitate the strengthening process. This involves ensuring sufficient access on the sides of the columns as well as access to the beams.

- When aiming for future flexibility in the timber system, over-dimensioning proves to be a more suitable solution. This is because the utilisation rates

tend to reach significant levels even with the application of strengthening techniques alone. Another approach is to incorporate a certain degree of over-dimensioning and then focus on strengthening the most critical elements, as there are validated and effective solutions and strengthening techniques available. Due to the substantially lower environmental impact of timber compared to steel, the consequences of over-dimensioning are not as significant in the case of timber systems.

The most important learning from this study is the crucial aspect of proactively considering and planning for the potential of repurposing and enhancing future flexibility in the early stages of a project. This has been demonstrated throughout the process, highlighting the significant requirement for various strengthening techniques and the complexity involved in strengthening a structure. However, despite the challenges, these strategies and implementations are essential in mitigating the negative environmental impact caused by the construction and building sector. By adopting such approaches, it becomes possible to reduce the adverse effects on the climate and promote sustainable practices within the industry.

References

Agenda 21-kommittén. (1995). Retrieved from https://www.riksdagen.se/sv/dokument-lagar/dokument/kommittedirektiv/agenda-21-kommitten_GJB134#Bakgrund

Agrawal, A., Sanghai, S., & Dabhekar, K. (2021). Comparative studies between precast and conventional cast-in-situ structural systems. In *Iop conference series: Materials science and engineering* (Vol. 1197, p. 012062).

Al-Emrani, M., Engström, B., Johansson, M., & Johansson, P. (2013). *Bärande konstruktioner: Del 1.* Chalmers Tekniska Högskola.

Almusallam, A. A. (2001). Effect of degree of corrosion on the properties of reinforcing steel bars. *Construction and Building Materials*, *15*(8), 361-368. Retrieved from https://www.sciencedirect.com/science/article/pii/S0950061801000095 doi: https://doi.org/10.1016/S0950-0618(01)00009-5

American Institute of Steel Construction. (2018, March). *Design of strengthening for existing steel members.* Webinar. Retrieved from https://www.aisc.org/education/continuingeducation/education-archives/design-of-strengthening-for-existing-steel-members/ (Accessed on 22nd March 2018)

Associates, R. M. . (n.d.). *Rhinoceros: Background.* Retrieved from https://www.rhino3d.com/mcneel/about/

Athanasiadis, M., & Al Sahi, H. (2018). *Val av stomsystem för en offentlig lokal: Fallstudie avseende entreprenadformen partnering och beaktade av miljöperspektiv.*

Bekhet, A. K., & Zauszniewski, J. A. (2012). Methodological triangulation: An approach to understanding data. *Nurse researcher*, *20*(2).

Benaim, R. (2007). *The design of prestressed concrete bridges: concepts and principles.* CRC Press.

Bength Strandberg, A. B. (2015). *Bygga hus: Illustrerad bygglära* (No. 2). Studentlitteratur.

Blaß, H. J., & Sandhaas, C. (2017). *Timber engineering-principles for design.* KIT Scientific Publishing.

Boverket. (Accessed on 2023-06-12). *Om klimatdeklaration.* https://www.boverket.se/sv/klimatdeklaration/om-klimatdeklaration/.

Boverket. (Accessed on 2023-06-13). *Klimatdatabas.* https://www.boverket.se/sv/klimatdeklaration/klimatdatabas/klimatdatabas/.

Carolin, A. (2001). *Strengthening of concrete structures with cfrp: shear strengthening and full scale applications* (Unpublished doctoral dissertation). Luleå

tekniska universitet.

Carolin, A. (2003). *Carbon fibre reinforced polymers for strengthening of structural elements* (Unpublished doctoral dissertation). Luleå tekniska universitet.

CEN, E. (2002). *Eurocode: Actions on structures-general actions-densities, self-weigth, imposed loads of buildings.* CEN-European Committee for Standardization.

CEN, E. (2003). *Eurocode: Actions on structures-part 1-3: General actions-snow load.* CEN-European Committee for Standardization.

CEN, E. (2005a). *Eurocode 1: Actions on structures - part 1-4:general actions-wind actions.* CEN-European Committee for Standardization.

CEN, E. (2005b). *Eurocode 2: Design of concrete structures-part 1-1: General rules and rules for buildings.* CEN-European Committee for Standardization.

Chang, W.-S. (2015). Repair and reinforcement of timber columns and shear walls – a review. *Construction and Building Materials*, *97*, 14-24. Retrieved from `https://www.sciencedirect.com/science/article/pii/S0950061815300246` (Special Issue: Reinforcement of Timber Structures) doi: https://doi.org/10.1016/j.conbuildmat.2015.07.002

Chong, E. K., & Zak, S. H. (2013). *An introduction to optimization* (Vol. 75). John Wiley & Sons.

Colombo, A., Ferrara, L., Negro, P., & Toniolo, G. (2004). Precast vs. cast-in-situ reinforced concrete industrial buildings under earthquake loading: an assessment via pseudodynamic tests. In *13th world conference on earthquake engineering, vancouver, bc canada* (Vol. 743).

Davidson, S. (n.d.). *Grasshopper.* Retrieved from `https://www.grasshopper3d.com/`

Davison, B., & Owens, G. W. (2012). *Steel designers' manual.* John Wiley & Sons.

Deng, D., & Murakawa, H. (2008). Prediction of welding distortion and residual stress in a thin plate butt-welded joint. *Computational Materials Science*, *43*(2), 353–365.

Dowswell, B. (2014). *Steelwise: Reinforcing the point.* `https://www.aisc.org/globalassets/modern-steel/steelwise/steelwise-january-2014.pdf`. (Modern Steel Construction, January 2014)

Dwivedi, D. K., & Dwivedi, D. K. (2022). Design of welded joints: Weld failure modes, welding symbols: Type of welds, joints, welding position. *Fundamentals of Metal Joining: Processes, Mechanism and Performance*, 327–342.

Engström, B. (2011). *Design and analysis of prestressed concrete structures* (7th ed.). Department of Architecture and Civil Engineering, Chalmers University of Technology.

Falkner, R. (2016, 08). The Paris Agreement and the new logic of international climate politics. *International Affairs*, *92*(5), 1107-1125. Retrieved from `https://doi.org/10.1111/1468-2346.12708` doi: 10.1111/1468-2346.12708

Fernandez, I. (2021). *structural system and response: Timber.*

Food4Rhino. (Accessed 2023). *Beaver.* `https://www.food4rhino.com/en/app/beaver`.

Fu, F. (2018). *6.6.1 what is parametric modeling.* Elsevier. Retrieved from https://app.knovel.com/hotlink/khtml/id:kt011PDD01/design-analysis-tall/what-is-parametric-modeling

Hasth, A. (2022). *The act of climate declaration of buildings: A study of construction engineers' approach and competence for implementation of the act.*

Hu, D. (2022). Chapter 1 - basic concepts of prestressed concrete. In D. Hu (Ed.), *Analysis and design of prestressed concrete* (p. 1-13). Elsevier. Retrieved from https://www.sciencedirect.com/science/article/pii/B9780128244258000014 doi: https://doi.org/10.1016/B978-0-12-824425-8.00001-4

Isaksson, T., Mårtensson, A., & Thelandersson, S. (2010). *Byggkonstruktion* (No. 2). Studentlitteratur AB.

Jack Porteous, A. K. (2013). *Structural timber design to eurocode 5.* John Wiley & Sons, Incorporated. Retrieved from http://ebookcentral.proquest.com/lib/chalmers/detail.action?docID=1174133

Jacob, J., & Barragán, O. L. G. (2007). *Flexural strengthening of glued laminated timber beams with steel and carbon fiber reinforced polymers.* Chalmers tekniska högskola.

Karamba 3d. (n.d.). Retrieved from https://www.karamba3d.com/

Karamba3D. (2021). *Basic properties of materials.* https://manual.karamba3d.com/appendix/a.4-background-information/a.4.1-basic-properties-of-materials.

Karlsson, M. (2007). *Cfrp strengthening of existing building structures.*

Keykha, A. H., Nekooei, M., & Rahgozar, R. (2015). Experimental and theoretical analysis of hollow steel columns strengthening by cfrp. *Civil Engineering Dimension*, *17*(2), 101–107.

Liang, Q. Q. (2015). *Analysis and design of steel and composite structures.* Taylor & Francis. Retrieved from https://www.taylorfrancis.com/books/mono/10.1201/9781315274843/analysis-design-steel-composite-structures-qing-quan-liang

Lindberg, J. (2013). *Comparative study on load-bearing systems: Framework or column and truss/beam system.*

Linghoff, D., Haghani, R., & Al-Emrani, M. (2009). Carbon-fibre composites for strengthening steel structures. *Thin-Walled Structures*, *47*(10), 1048-1058. Retrieved from https://www.sciencedirect.com/science/article/pii/S0263823108002255 (FRP Strengthened Metallic Structures) doi: https://doi.org/10.1016/j.tws.2008.10.019

Mather, B. (2004). Concrete durability. *Cement and Concrete Composites*, *26*(1), 3–4.

Moynihan, M. C., & Allwood, J. M. (2014). Utilization of structural steel in buildings. *Proceedings of the Royal Society A: Mathematical, Physical and Engineering Sciences*, *470*(2168), 20140170.

Orr, J., M.Cooke, Ibell, T. J., Smith, C., Watson, N., Algaard, W., ... Roynon, J. (2021). *Design for zero.* The Institution of Structural Engineers.

Owojori, O. M., Okoro, C. S., & Chileshe, N. (2021). Current status and emerging trends on the adaptive reuse of buildings: A bibliometric analysis. *Sustain-*

ability, *13*(21). Retrieved from https://www.mdpi.com/2071-1050/13/21/11646 doi: 10.3390/su132111646

Plos, H. B. . K. L. . M. (2008). *A guide to non-linear finite element modelling of shear and torsion in concrete bridges*. Gothenburg: Challmers University Of Technology.

Preisinger, C., & Heimrath, M. (2014). Karamba—a toolkit for parametric structural design. *Structural Engineering International*, *24*(2), 217-221. Retrieved from https://doi.org/10.2749/101686614X13830790993483 doi: 10.2749/101686614X13830790993483

Programme, U. N. E. (2022). 2022 global status report for buildings and construction- towards a zero-emission,efficient and resilient buildings and construction sector [Report].

Rezaei, H. (2022). *En jämförelse mellan regelsystem och pelar-balksystem.* Linköpings university.

Ripple, W. J., Wolf, C., Gregg, J. W., Levin, K., Rockström, J., Newsome, T. M., ... Lenton, T. M. (2022, 10). World Scientists' Warning of a Climate Emergency 2022. *BioScience*, *72*(12), 1149-1155. Retrieved from https://doi.org/10.1093/biosci/biac083 doi: 10.1093/biosci/biac083

Ripple, W. J., Wolf, C., Newsome, T. M., Galetti, M., Alamgir, M., Crist, E., ... 15, . s. s. f. . c. (2017, 11). World Scientists' Warning to Humanity: A Second Notice. *BioScience*, *67*(12), 1026-1028. Retrieved from https://doi.org/10.1093/biosci/bix125 doi: 10.1093/biosci/bix125

Rowley, J., & Slack, F. (2004). Conducting a literature review. *Management research news*, *27*(6), 31–39.

Sawantt, S. (n.d.). *Grasshopper 3d: A modeliing software redefining the design process.* Retrieved from https://parametric-architecture.com/grasshopper-3d-a-modeling-software-redefining-the-design-process/

Shafigh, P., Asadi, I., & Mahyuddin, N. B. (2018). Concrete as a thermal mass material for building applications-a review. *Journal of Building Engineering*, *19*, 14–25.

Sitarz, D. (1993, 1). Agenda 21: The earth summit strategy to save our planet. Retrieved from https://www.osti.gov/biblio/6289330

Slaughter, E. S. (2001). Design strategies to increase building flexibility. *Building Research & Information*, *29*(3), 208-217. Retrieved from https://doi.org/10.1080/09613210010027693 doi: 10.1080/09613210010027693

Strängbetong. (2015). *Strängbetong.* Retrieved 2023, from https://strangbetong.se/

Svenskt trä. (2015). *Dimensionering av träkonstruktioner:del1.* Stockholm: Sveriges skogsindustrier.

Svenskt trä. (2019). *The clt handbook.* Stockholm: Sveriges skogsindustrier.

Taheri, F., Nagaraj, M., & Khosravi, P. (2009). Buckling response of glue-laminated columns reinforced with fiber-reinforced plastic sheets. *Composite Structures*, *88*(3), 481–490.

Teng, J., Yu, T., & Fernando, D. (2012). Strengthening of steel structures with fiber-reinforced polymer composites. *Journal of constructional steel research*, *78*, 131–143.

trä, S. (2015). *Hållfasthetsklasser för limträ.* https://www.svenskttra.se/siteassets/5-publikationer/pdfer/hallfasthetsklasser-for_limtra.pdf.

UNFCCC. (2015). Paris agreement. In *Paris Climate Change Conference: Paris Agreement* (pp. 2–25). Paris, France.

University, C. (n.d.-a). *Flexibility.* Retrieved from https://dictionary.cambridge.org/dictionary/english/flexibility

University, C. (n.d.-b). *Optimization.* Retrieved from https://dictionary.cambridge.org/dictionary/english/optimization

University, C. (n.d.-c). *Repurposing.* Retrieved from https://dictionary.cambridge.org/dictionary/english/repurposing

Valluzzi, M. R., Garbin, E., & Modena, C. (2007). Flexural strengthening of timber beams by traditional and innovative techniques. *Journal of Building Appraisal*, *3*, 125–143.

Viola, S., & Diano, D. (2019). Repurposing the built environment: Emerging challenges and key entry points for future research. *Sustainability*, *11*(17). Retrieved from https://www.mdpi.com/2071-1050/11/17/4669 doi: 10.3390/su11174669

Wang, Q., Cheng, J. C. P., & Sohn, H. (2015). Automated quality inspection of precast concrete elements with irregular shapes using terrestrial laser scanner and bim technology. In *Isarc. proceedings of the international symposium on automation and robotics in construction* (Vol. 32, p. 1).

A

Verification of structural analysis

Verification of parametric model: Structural analysis

This calculation is performed to validate the parametric model. It is important to note that the calculations are conducted on individual elements rather than on the entire set of elements. The selected elements will be visually represented in a figure, indicating their respective positions.

1. Moment verification steel system

Input:

Chosen element: Beam X.0.0.0.4

$m_{HEA400} := 125\ \frac{kg}{m}$ — Weigth for cross-section HEA400

$g_{HEA400} := g \cdot m_{HEA400} = 1.226\ \frac{kN}{m}$ — Self-weight for Beam X.0.0.0.4

$g_{HDF} := 5.34 \cdot \frac{kN}{m^2}$ — Self-weigth for HDF slab

$Q_{Imp} := 7 \cdot \frac{kN}{m^2}$ — Magnitude for imposed load

$s_{y\_axis} := 7\ m$ — Span-width in Y-direction

$s_{x\_axis} := 8.0\ m$ — Span-width in X-direction

$k_s := -0.1071$ — Constant for continuous beam, see figure below.

Appendix E1: Continuous beams with uniformly-distributed loads

Sectional forces

load case	max. field moment (factor: qL^2)					support moment (factor: qL^2)				reaction forces (factor: qL)				
	M_1	M_2	M_3	M_4	M_5	M_B	M_C	M_D	M_E	A	B_A B_B	C_B C_C	D_C D_D	E_D E_E
2 spans	0,0703	0,0703				0,1250				0,3750	0,6250 0,6250	0,3750		
	0,0957					−0,0625				0,4375	0,5625 0,0625	−0,0625		
3 spans	0,0800	0,0250	0,0800			−0,1000	−0,1000			0,4000	0,6000 0,5000	0,5000 0,6000	0,4000	
	0,1013		0,1013			−0,0500	0,0500			0,4500	0,5500 0	0 0,5500	0,4500	
		0,0750				−0,0500	−0,0500			−0,0500	0,0500 0,5000	0,5000 0,0500	0,0500	
	0,0755	0,0535				−0,1167	−0,0333			0,3833	0,6167 0,5834	0,4166 0,0333	−0,0333	
	0,0939					−0,0667	+0,0167			0,4333	0,5667 0,0834	−0,0834 −0,0167	0,0167	
4 spans	0,0772	0,0364	0,0364	0,0772		−0,1071	−0,0714	−0,1071		0,3929	0,6071 0,5357	0,4643 0,4643	0,5357 0,6071	0,3929
	0,0996		0,0805			−0,0536	−0,0357	−0,0536		0,4464	0,5536 0,0179	−0,0179 0,4821	0,5179 0,0536	−0,0536
	0,0720	0,0610		0,0977		−0,1205	0,0179	0,0580		0,3795	0,6205 0,6076	0,3974 0,0401	0,0401 0,5580	0,4420
		0,0561	0,0561			−0,0357	−0,1072	−0,0357		−0,0357	0,0357 0,4285	0,5715 0,5715	0,4285 0,0357	−0,0357
	0,0940					−0,0665	+0,0179	−0,0045		0,4335	0,5665 0,0844	−0,0844 0,0224	0,0224 0,0045	0,0045
		0,0737				−0,0491	−0,0536	+0,0134		−0,0491	0,0491 0,4955	0,5045 0,0670	−0,0670 −0,0134	0,0134

September 2019

Design load :

$$q_d := \left(1.2 \cdot \left(g_{HDF} \cdot \frac{s_{y\_axis}}{2} + g_{HEA400}\right) + 1.5 \cdot 0.8 \cdot Q_{Imp} \cdot \frac{s_{y\_axis}}{2}\right) = 53.299 \ \boldsymbol{m} \cdot \frac{\boldsymbol{kN}}{\boldsymbol{m}^2}$$

$$M_s := k_s \cdot q_d \cdot s_{x\_axis}{}^2 = -365.333 \ \boldsymbol{kN} \cdot \boldsymbol{m}$$

Verification

Comparison with the load observed in the parametric model

$$M_{s.model} := 351.65 \ \boldsymbol{kN} \cdot \boldsymbol{m}$$

$$\text{abs}\left(\frac{M_s}{M_{s.model}}\right) = 1.039$$

4% diffrence. The variance between hand calculations and the parametric model can be seen as tolerable.

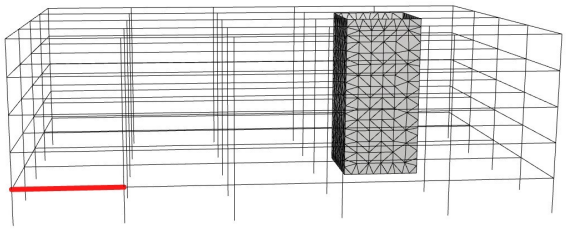

2. Moment verification timber system

Input:

Chosen element: Beam X.0.0.0.4

$\rho_{GL30} := 4800 \frac{N}{m^3}$ — Desity for GL30, provided from karamba

$A_{GL30.672} := 0.06728\ m^2$

$g_{GL30} := A_{GL30.672} \cdot \rho_{GL30} = 0.323 \frac{kN}{m}$ — Self-weight for Beam X.0.0.0.4

$g_{CLT} := 1.275 \cdot \frac{kN}{m^2}$ — Self-weigth for CLT slab

$Q_{Imp} := 7 \cdot \frac{kN}{m^2}$ — Magnitude for imposed load

$s_{y\_axis} := 7\ m$ — Span-width in Y-direction

$s_{x\_axis} := 8.0\ m$ — Span-width in X-direction

$k_s := -0.1071$ — Constant for continuous beam, see figure below.

Appendix E1: Continuous beams with uniformly-distributed loads

Sectional forces

load case	max. field moment (factor: qL^2)					support moment (factor: qL^2)				reaction forces (factor: qL)				
	M_1	M_2	M_3	M_4	M_5	M_B	M_C	M_D	M_E	A	B_R B_h	C_R C_h	D_R D_h	E_R E_h
2 spans	0,0703	0,0703				0,1250				0,3750	0,6250 0,6250	0,3750		
	0,0957					−0,0625				0,4375	0,5625 0,0625	−0,0625		
3 spans	0,0800	0,0250	0,0800			−0,1000	−0,1000			0,4000	0,6000 0,5000	0,5000 0,6000	0,4000	
	0,1013		0,1013			−0,0500	0,0500			0,4500	0,5500 0	0 0,5500	0,4500	
		0,0750				−0,0500	−0,0500			−0,0500	0,5000 0,5000	0,5000 0,5000	0,0500	
	0,0755	0,0535				−0,1167	−0,0333			0,3833	0,6167 0,5834	0,4166 0,0333	−0,0333	
	0,0939					−0,0667	+0,0167			0,4333	0,5667 0,0834	−0,0834 −0,0167	0,0167	
4 spans	0,0772	0,0364	0,0364	0,0772		−0,1071	−0,0714	−0,1071		0,3929	0,6071 0,5357	0,4643 0,4643	0,5357 0,6071	0,3929
	0,0996		0,0805			−0,0536	−0,0357	−0,0536		0,4464	0,5536 0,0179	−0,0179 0,4821	0,5179 0,0536	−0,0536
	0,0720	0,0610		0,0977		−0,1205	0,0179	0,0580		0,3795	0,6205 0,6076	0,3974 −0,0401	0,0401 0,5580	0,4420
		0,0561	0,0561			−0,0357	−0,1072	−0,0357		−0,0357	0,0357 0,4285	0,5715 0,5715	0,4285 0,0357	−0,0357
	0,0940					−0,0665	+0,0179	−0,0045		0,4335	0,5665 0,0844	−0,0844 −0,0224	0,0224 0,0045	0,0045
		0,0737				−0,0491	−0,0536	+0,0134		−0,0491	0,0491 0,4955	0,5045 0,0670	−0,0670 −0,0134	0,0134

Design load :

$$q_d := \left(1.2 \cdot \left(g_{CLT} \cdot \frac{s_{y\_axis}}{2} + g_{GL30}\right) + 1.5 \cdot 0.8 \cdot Q_{Imp} \cdot \frac{s_{y\_axis}}{2}\right) = 35.143\ m \cdot \frac{kN}{m^2}$$

$$M_s := k_s \cdot q_d \cdot s_{x\_axis}^{\ 2} = -240.881\ kN \cdot m$$

Verification

Comparison with the load observed in the parametric model

$$M_{s.model} := 224.4\ kN \cdot m$$

$$\mathrm{abs}\left(\frac{M_s}{M_{s.model}}\right) = 1.073$$

7% diffrence. The variance between hand calculations and the parametric model can be seen as tolerable.

3. Reaction force verification steel system

Input:

Chosen element: Column4.2.0

$m_{HEA100} := 16.7 \frac{kg}{m}$ Weigth for cross-section HEA100

$m_{HEA160} := 30.4 \frac{kg}{m}$ Weigth for cross-section HEA160

$m_{HEA220} := 50.5 \frac{kg}{m}$ Weigth for cross-section HEA220

$m_{HEA260} := 68.2 \frac{kg}{m}$ Weigth for cross-section HEA260

$m_{HEB240} := 83.2 \frac{kg}{m}$ Weigth for cross-section HEB240

$l_{Column} := 2.7\ m$ Length of column4.2.0

$g_{Column} := g \cdot (m_{HEB240} + m_{HEA100} + m_{HEA220} + m_{HEA160} + m_{HEA100}) \cdot l_{Column} = 5.229\ kN$

Self-weight for Column4.2.0

$n_{HDF} := 5$ Four floors with HDF slabs. the roof is in this model assumed to be the same as the floors:
Total number of HDF:5

$g_{HDF} := 5.34 \cdot \frac{kN}{m^2}$ Self-weigth for HDF slab

$g_{HDF} := g_{HDF} \cdot n_{HDF} = 26.7 \frac{kN}{m^2}$

$n_{Imp} := 4$ Number of floors with imposed load

$Q_{Imp} := 7 \cdot \frac{kN}{m^2}$ Magnitude for imposed load

$Q_s := 1.2 \frac{kN}{m^2}$ Magnitude for snow load.

$s_{y\_axis} := 7\ m$ Span-width in Y-direction

$s_{x\_axis} := 8.0\ m$ Span-width in X-direction

$k_v := 0.5357$ Constant for continuous beam, for calculation Rv and Rh, see figure below.

$k_h := 0.6071$

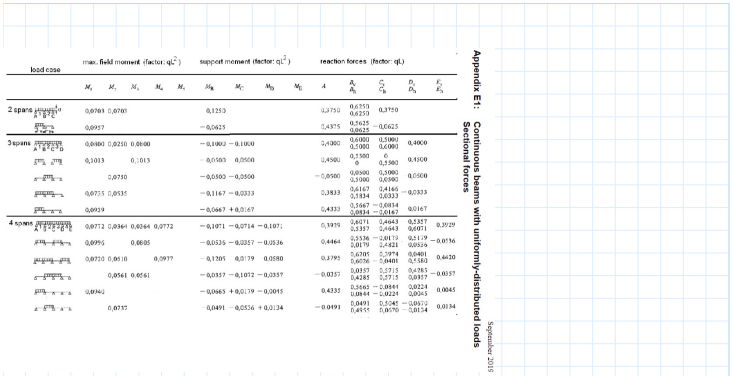

Design load :

$q_d := \left(1.2\ g_{HDF} + \left(1.5 \cdot 0.8 \cdot n_{Imp} \cdot Q_{Imp}\right) + 1.5 \cdot 0.6 \cdot Q_s\right) = 66.72\ \frac{kN}{m^2}$

$N_{steel} := \left(s_{x\_axis} \cdot s_{y\_axis}\right) \cdot q_d + g_{Column} = \left(3.742 \cdot 10^3\right)\ kN$

$R_v := k_v \cdot N_{steel} = \left(2.004 \cdot 10^3\right)\ kN$

$R_h := k_h \cdot N_{steel} = \left(2.271 \cdot 10^3\right)\ kN$

$R := R_v + R_h = \left(4.276 \cdot 10^3\right)\ kN$

Verification

Comparison with the load observed in the parametric model

$R_{model} := 3860.33\ kN$

$\mathrm{abs}\left(\frac{R}{R_{model}}\right) = 1.108$

11% diffrence. The variance between hand calculations and the parametric model can be seen as tolerable.

4. Reaction force verification timber system

Input:

Chosen element: Column4.2.0

$\rho_{GL30} := 4800 \frac{N}{m^3}$ — Density for GL30

There are 5 columns ontop of each other.

$A_{GL30.207} := 0.021\ m^2$ — Area for cross-section Column 4.2.4

$A_{GL30.297} := 0.0297\ m^2$ — Area for cross-section Column 4.2.3

$A_{GL30.513} := 0.0513\ m^2$ — Area for cross-section Column 4.2.2

$A_{GL30.769.5} := 0.0769\ m^2$ — Area for cross-section Column 4.2.1

$A_{GL30.967.5} := 0.0967\ m^2$ — Area for cross-section Column 4.2.0

$l_{Column} := 2.7\ m$ — Length of column4.2.0

$g_{Column.timber} := \left(A_{GL30.967.5} + A_{GL30.769.5} + A_{GL30.513} + A_{GL30.297} + A_{GL30.207}\right) \cdot \rho_{GL30} \cdot l_{Column} = 3.572\ kN$

Self-weigth for column 4.2.0

$n_{CLT} := 5$ — Four floors with HDF slabs. the roof is in this model assumed to be the same as the floors:
Total number of HDF:5

$g_{CLT} := 1.275 \cdot \frac{kN}{m^2}$ — Self-weigth for HDF slab

$g_{CLT} := g_{CLT} \cdot n_{CLT} = 6.375 \frac{kN}{m^2}$

$n_{Imp} := 4$ — Number of floors with imposed load

$Q_{Imp} := 7 \cdot \frac{kN}{m^2}$ — Magnitude for imposed load

$Q_s := 1.2 \frac{kN}{m^2}$ — Magnitude for snow load.

$s_{y\_axis} := 7\ m$ — Span-width in Y-direction

$s_{x\_axis} := 8.0\ m$ — Span-width in X-direction

$k_v := 0.5357$

$k_h := 0.6071$ — Constant for continuous beam, for calculation Rv and Rh, see figure below.

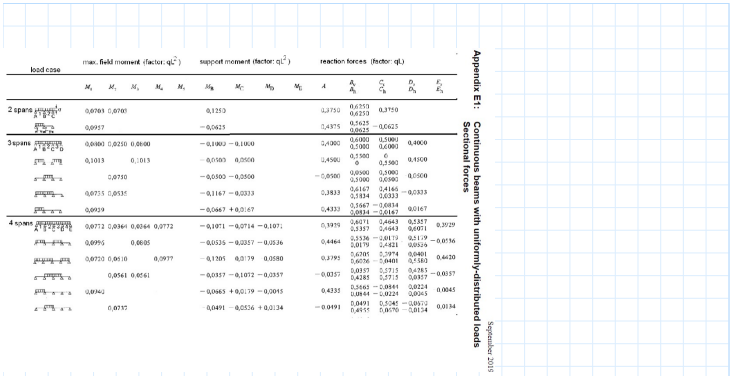

Appendix E1: Continuous beams with uniformly-distributed loads
Sectional forces
September 2015

Design load :

$q_d := \left(1.2\ g_{CLT} + \left(1.5 \cdot 0.8 \cdot n_{Imp} \cdot Q_{Imp}\right) + 1.5 \cdot 0.6 \cdot Q_s\right) = 42.33\ \frac{kN}{m^2}$

$N_{timber} := \left(s_{x\_axis} \cdot s_{y\_axis}\right) \cdot q_d + g_{Column} = \left(2.376 \cdot 10^3\right)\ kN$

$R_v := k_v \cdot N_{timber} = \left(1.273 \cdot 10^3\right)\ kN$

$R_h := k_h \cdot N_{timber} = \left(1.442 \cdot 10^3\right)\ kN$

$R := R_v + R_h = \left(2.715 \cdot 10^3\right)\ kN$

Verification
Comparison with the load observed in the parametric model

$R_{model} := 2513\ kN$

$\mathrm{abs}\left(\frac{R}{R_{model}}\right) = 1.08$

8% diffrence. The variance between hand calculations and the parametric model can be seen as tolerable.

B

Verification of structural design

Verification of parametric model: Structural design

This calculation is performed to validate the parametric model. It is important to note that the calculations are conducted on individual elements rather than on the entire set of elements. The selected elements will be visually represented in a figure, indicating their respective positions.

1. Buckling resistance timber column

Input:

Chosen element: Column 4.2.0

$f_{c0k} := 24.5\ MPa$ — Characteristic compression strength for GL30

$E_{0.05} := 10800\ MPa$ — Modulus of elasticity

$\gamma_M := 1.25$ — Partial factor timber

$k_{mod} := 0.8$ — Climate and load reductionfactor

$\beta_c := 0.1$ — Straightness factor

$L_{cr} := 2.7\ m \cdot 0.9 = 2.43\ m$ — Critical buckling length

$N_{Ed} := 2715\ kN$

$b := 215\ mm$ — Width of beam 4.2.0

$h := 450\ mm$ — Heigth of beam 4.2.0

$f_{c0d} := \frac{f_{c0k} \cdot k_{mod}}{\gamma_M} = 15.68\ MPa$ — Design strength for GL30

$I := \frac{h \cdot b^3}{12} = \left(3.727 \cdot 10^{-4}\right)\ m^4$ — Moment of inertia

$A := b \cdot h = 0.097\ m^2$ — Area of beam 4.2.0

$i := \sqrt{\frac{I}{A}} = 0.062\ m$

$\lambda := \frac{L_{cr}}{i} = 39.152$

$\lambda_{rel} := \frac{\lambda}{\pi} \cdot \sqrt{\frac{f_{c0k}}{E_{0.05}}} = 0.594$ — Relative slenderness

$k := 0.5 \cdot \left(1 + \beta_c \cdot \left(\lambda_{rel} - 0.3\right) + {\lambda_{rel}}^2\right) = 0.691$

$k_c := \frac{1}{k + \sqrt{k^2 - {\lambda_{rel}}^2}} = 0.958$ — Magnification factor that takes load direction into account

$N_{Rd} := f_{c0d} \cdot k_c \cdot A = \left(1.453 \cdot 10^3\right)$ kN

$\eta_b := \frac{N_{Ed}}{N_{Rd}} = 1.869$

Verification

Comparison with the load observed in the parametric model

$\eta_{b.model} := 1.78$

$\text{abs}\left(\frac{\eta_b}{\eta_{b.model}}\right) = 1.05$

5 % diffrence. The variance between hand calculations and the parametric model can be seen as tolerable.

2. Buckling resistance steel column

Input:

Chosen element: Column 4.2.0

$E := 210\ \mathit{GPa}$ — Modulus of elasticity

$f_y := 355\ \mathit{MPa}$

$\gamma_{M1} := 1$ — Partial factor steel

$A := 10600\ \mathit{mm}^2$ — Cross-section area HEB240

$I_y := 112.6 \cdot 10^6\ \mathit{mm}^4$ — Moment of inertia

$L := 2.7\ \mathit{m}$ — Length of column 4.2.0

$\beta := 1$ — Simply supported

$$\lambda := \frac{\beta \cdot L}{\pi \cdot \sqrt{\frac{I_y}{A}}} \cdot \sqrt{\frac{f_y}{E}} = 0.343$$ — Slenderness

$\alpha := 0.34$ — Imperfection factor: Buckling curve b

$$\varphi := 0.5 \cdot \left(1 + \alpha \cdot \lambda + \lambda^2\right) = 0.617$$

$$\chi := \frac{1}{\varphi + \sqrt{\varphi^2 - \lambda^2}} = 0.885$$

$$N_{Rd} := \chi \cdot A \cdot \frac{f_y}{\gamma_{M1}} = \left(3.33 \cdot 10^3\right)\ \mathit{kN}$$ — Buckling resistance

$N_{Ed} := 4276\ \mathit{kN}$

$$\eta_b := \frac{N_{Ed}}{N_{Rd}} = 1.284$$

Verification

Comparison with the load observed in the parametric model

$\eta_{b.model} := 1.27$

$$\mathrm{abs}\left(\frac{\eta_b}{\eta_{b.model}}\right) = 1.011$$

0.9% diffrence. The variance between hand calculations and the parametric model can be seen as tolerable.

3. Lateral torsional stability resistance timber beam

Input:

Chosen element: Beam X.0.0.0.4

$f_{m.k} := 30\ \mathit{MPa}$ — Characteristic bending strength for GL30

$k_{mod} := 0.8$ — Climate and load reductionfactor

$\gamma_M := 1.25$ — Partial factor timber

$f_{m.d} := \frac{f_{m.k} \cdot k_{mod}}{\gamma_M} = 19.2\ \mathit{MPa}$ — Design bending stength

$E_{0.05} := 10800\ \mathit{MPa}$ — Modulus of elasticity

$b_{BeamX0.0.0.4} := 115\ \mathit{mm}$ — Width of beam X0.0.0.4

$h_{BeamX0.0.0.4} := 585\ \mathit{mm}$ — Height of beam X0.0.0.4

$l_{BeamX0.0.0.4} := 8\ \mathit{m}$ — Length of beam X0.0.0.4

$l_{ef} := l_{BeamX0.0.0.4} \cdot 0.9 = 7.2\ \mathit{m}$ — Effectiv length of beam X0.0.0.4

Balktyp	Lasttyp	k_{ef}
Fritt upplagd	Konstant moment	1,0
	Jämnt utbredd last	0,9
	Koncentrerad last mitt på spannet	0,8
Konsol	Jämnt utbredd last	0,5
	Koncentrerad last vid den fria änden	0,8

* Förhållandet mellan den effektiva längden ℓ_{ef} och spännvidden ℓ gäller för en balk med vridstyvt upplagda ändar belastad i tvärsnittets tyngdpunkt. Om lasten angriper i balkens tryckta kant bör ℓ_{ef} ökas med beloppet $2h$. Om lasten angriper i den dragna kanten får den effektiva längden ℓ_{ef} minskas med beloppet $0.5h$.

Rectangular beam--›A simplified method can be used according to EN 1995-1-1:2004

$\sigma_{m.crit} := \frac{0.78 \cdot b_{BeamX0.0.0.4}^{\ 2}}{h_{BeamX0.0.0.4} \cdot l_{ef}} \cdot E_{0.05} = 26.45\ \mathit{MPa}$ — Critical bending stress, simplidied method (equ:6.32)

$\lambda_{rel.m} := \sqrt{\frac{f_{m.k}}{\sigma_{m.crit}}} = 1.065$ — Relative slenderness ratio

$k_{crit} := 1.56 - 0.75 \cdot \lambda_{rel.m} = 0.761$ — Factor that considerate lateral stability

$f_{m.d} \cdot k_{crit} = 14.616\ \mathit{MPa}$ — Lateral torsional buckling resistance for BeamX.0.0.0.4

$M_y := 240.888\ \mathit{kN \cdot m}$

$W_y := \frac{h_{BeamX0.0.0.4}^{\ 2} \cdot b_{BeamX0.0.0.4}}{4} = 0.01\ \mathit{m}^3$

$\sigma_m := \frac{M_y}{W_y} = 24.483\ \mathit{MPa}$

Verification

Comparison with the load observed in the parametric model

$$\eta_{LT} := \frac{\sigma_m}{f_{m.d} \cdot k_{crit}} = 1.675$$

$$\eta_{LT.model} := 1.82$$

$$\text{abs}\left(\frac{\eta_{LT}}{\eta_{LT.model}}\right) = 0.92$$

8 % diffrence. The variance between hand calculations and the parametric model can be seen as tolerable.

4. Lateral torsional buckling resistance steel beam

Input:

Chosen element: Beam X.0.0.0.4

Cross-section class: 1

$h_{HEA400} := 390\ mm$ — Height cross-section

$b_{HEA400} := 300\ mm$ — Width cross-section

$t_{HEA400} := 19\ mm$ — Thickness flange

$d_{HEA400} := 11\ mm$ — Thickness web

$L := 8 \cdot m$ — Length Beam X0.0.0.4

$I_z := 8564 \cdot 10^4\ mm^4$

$I_t := 1.9 \cdot 10^6\ mm^4$

$I_w := 2940 \cdot 10^9\ mm^6$

$W_{pl} := 2560 \cdot 10^3\ mm^3$

$f_y := 355\ MPa$ — Yeild strength

$E := 210\ GPa$ — Modulus of elasticity

$G := 80.77\ GPa$ — Shear module

$\gamma_{M1} := 1$

$\varepsilon := \sqrt{\frac{235\ MPa}{f_y}} = 0.814$

$C_1 := 1.127$ — Conservatively: assum simply sypported

$k := 1$ — No rotational restrain

$k_w := 1$ — No warping restrain

Critical moment: From NCCI: Elastic critical moment for lateral torsional buckling

$$M_{Cr} := C_1 \cdot \frac{\pi^2 \cdot E \cdot I_z}{(k \cdot L)^2} \cdot \sqrt{\left(\frac{k}{k_w}\right)^2 \cdot \frac{I_w}{I_z} + \frac{(k \cdot L)^2 \cdot G \cdot I_t}{\pi^2 \cdot E \cdot I_z}} = 935.937\ kN \cdot m$$

$W_y := W_{pl}$ For cross-section class 1 and 2

$\lambda_{LT} := \sqrt{\frac{W_y \cdot f_y}{M_{Cr}}} = 0.985$

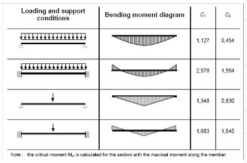

$\frac{h_{HEA400}}{b_{HEA400}} = 1.3$

$\alpha_{LT} := 0.21$ Buckling curve a

$\phi_{LT} := 0.5 \left(1 + \alpha_{LT} \cdot \left(\lambda_{LT} - 0.2\right) + {\lambda_{LT}}^2\right) = 1.068$

$\chi_{LT} := \frac{1}{\phi_{LT} + \sqrt{{\phi_{LT}}^2 - {\lambda_{LT}}^2}} = 0.676$ $\chi_{LT} < 1$

$k_c := 0.91$

$f := 1 - 0.5 \cdot \left(1 - k_c\right) \cdot \left(1 - 2.0 \cdot \left(\lambda_{LT} - 0.8\right)^2\right) = 0.958$

$\chi_{LT\_mod} := \frac{\chi_{LT}}{f} = 0.705$

$M_{b.Rd} := \chi_{LT\_mod} \cdot W_y \cdot \frac{f_y}{\gamma_{M1}} = 641.026\ \mathbf{kN \cdot m}$

$M_s := 365.33\ \mathbf{kN \cdot m}$ Obtained from the structural analysis

$\eta_{LT} := \frac{M_s}{M_{b.Rd}} = 0.57$

Verification

Comparison with the load observed in the parametric model

$\eta_{LT.model} := 0.5364$

$\mathrm{abs}\left(\frac{\eta_{LT}}{\eta_{LT.model}}\right) = 1.062$

6.2% diffrence. The variance between hand calculations and the parametric model can be seen as tolerable.

Calculation of self-weight for slabs

Since the slabs aren't modeled as structural element in the case studys, *Modification of imposed load, changes of span widths and altering number of floors*, there self-weigth aren't included in the karamba komponent for sel-weigth. Therefor, the slabs self-weigth needs to be calculated manally

1. Self-weigth for HDF

$d_{concrete} := 50\ mm$ Assumed concrete layers

$g_{concrete} := 25\ \frac{kN}{m^3}$ Assumed self-weigth for concrete

Provided input data from stängbetong for two diffrent HD27, with diffrent sizing of the ducts. See figure below for mer information

$b := 1197\ mm$

$g_{FI84} := 361\ \frac{kg}{m^2}$

$g_{FI55} := 457\ \frac{kg}{m^2}$

$g := 10\ \frac{m}{s^2}$

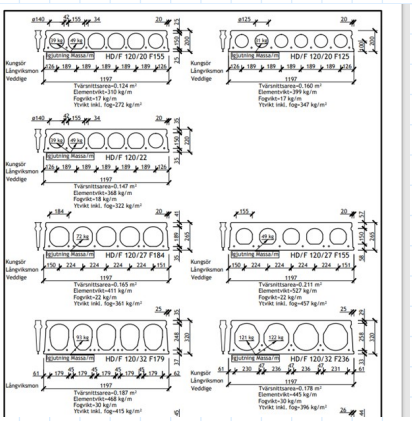

The gravity is set to 10 m/s2 since that is the value used for the component load (Gravity) in Karamaba 3D

$g_{FI84} := g_{FI84} \cdot g + \langle d_{concrete} \cdot g_{concrete} \rangle = 4.86\ \frac{kN}{m^2}$

$g_{FI55} := g_{FI55} \cdot g + \langle d_{concrete} \cdot g_{concrete} \rangle = 5.82\ \frac{kN}{m^2}$

$g_{mean} := \frac{g_{FI84} + g_{FI55}}{2} = 5.34\ \frac{kN}{m^2}$

2. Self-weigth for CLT

$h_{CLT} := 0.250\ m$ Asumed heigth of CLT slabs. This to have similar geometry as for the HFD slab

$\rho_{CLT} := 5100\ \frac{N}{m^3}$ Providen desity from Beaver.

$g_{CLT} := h_{CLT} \cdot \rho_{CLT} = 1.275\ \frac{kN}{m^2}$

C

Self weight och effective height

Calkculation of the effective heigth of HD27

Provioded information from strängbetong, see figure below.

$I_{HD27} := 1716424301\ mm^4$ Inertia of a rectangular

$b := 1197\ mm$

$I := \frac{b \cdot h^3}{12}$

$h_{eff} := \left(\frac{I_{HD27} \cdot 12}{b}\right)^{\frac{1}{3}} = 0.258\ m$

Model of a representative rectangular concrete cross-section

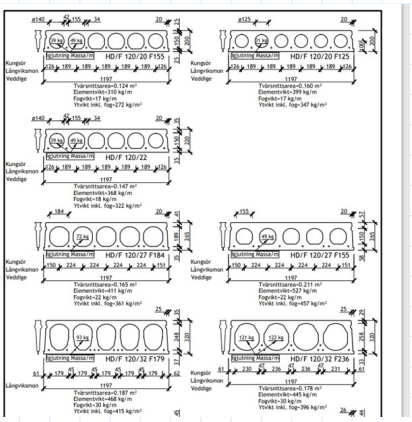

D

Beaver material

Column1	Column2	Column3	Column4	Column5	Column6	Column7	Column8	Column10
Bredd b (mm)	42	56	66	78	90	115	140	165
Höjd h(mm)								
90	GL28hs	GL28hs	GL28hs	GL28hs	GL30h	GL30h	GL30h	GL30h
115						GL30h	GL30h	GL30h
135	GL28hs	GL28hs	GL28hs	GL28hs	GL30h	GL30h	GL30h	GL30h
140							GL30h	
160								
165								GL30h
180	GL28cs	GL28cs	GL28cs	GL28cs	GL30c	GL30c	GL30c	GL30c
225	GL28cs	GL28cs	GL28cs	GL28cs	GL30c	GL30c	GL30c	GL30c
270	GL28cs	GL28cs	GL28cs	GL28cs	GL30c	GL30c	GL30c	GL30c
315	GL28cs	GL28cs	GL28cs	GL28cs	GL30c	GL30c	GL30c	GL30c
360	GL28cs*	GL28cs	GL28cs	GL28cs	GL30c	GL30c	GL30c	GL30c
405	GL28cs*	GL28cs	GL28cs	GL28cs	GL30c	GL30c	GL30c	GL30c
450		GL28cs	GL28cs	GL28cs	GL30c	GL30c	GL30c	GL30c
495		GL28cs*	GL28cs	GL28cs	GL30c	GL30c	GL30c	GL30c
540		GL28cs*	GL28cs*	GL28cs	GL30c	GL30c	GL30c	GL30c
585			GL28cs*	GL28cs	GL30c	GL30c	GL30c	GL30c
630			GL28cs*	GL28cs*	GL30c	GL30c	GL30c	GL30c
675				GL28cs*	GL30c	GL30c	GL30c	GL30c
720				GL28cs*	GL30c	GL30c	GL30c	GL30c
765				GL28cs*	GL30c	GL30c	GL30c	GL30c
810					GL30c	GL30c	GL30c	GL30c
855					GL30c	GL30c	GL30c	GL30c
900					GL30c	GL30c	GL30c	GL30c
945						GL30c	GL30c	GL30c
990						GL30c	GL30c	GL30c
1 035						GL30c	GL30c	GL30c
1 080						GL30c	GL30c	GL30c
1 125						GL30c	GL30c	GL30c
1 170							GL30c	GL30c
1 215							GL30c	GL30c
1 260							GL30c	GL30c
1 305							GL30c	GL30c
1 350							GL30c	GL30c
1 395							GL30c	GL30c
1 440								GL30c
1 485								GL30c
1 530								GL30c
1 575								GL30c
1 620								GL30c

Column11	Column12
190	215
GL30h	GL30h
GL30h	GL30h
GL30h	GL30h
GL30c	GL30c
GL30c	GL30c
GL30c	GL30c
GL30c	GL30c
GL30c	GL30c
GL30c	GL30c
GL30c	GL30c
GL30c	GL30c
GL30c	GL30c
GL30c	GL30c
GL30c	GL30c
GL30c	GL30c
GL30c	GL30c
GL30c	GL30c
GL30c	GL30c
GL30c	GL30c
GL30c	GL30c
GL30c	GL30c
GL30c	GL30c
GL30c	GL30c
GL30c	GL30c
GL30c	GL30c
GL30c	GL30c
GL30c	GL30c
GL30c	GL30c
GL30c	GL30c
GL30c	GL30c
GL30c	GL30c
GL30c	GL30c
GL30c	GL30c
GL30c	GL30c
GL30c	GL30c
GL30c	GL30c

name, type, fmk [MPa], ft0k [MPa], ft90k [MPa], fc0k [MPa], fc90k [MPa], fvk [MPa],frk [MPa], E0mean
C14,Softwood,14.,7.2,0.4,16.,2.,3.,0.8,7000,4700,230,154,440,295.5,2900,3500,0.00
C16,Softwood,16.,8.5,0.4,17.,2.2,3.2,0.8,8000,5400,270,181,500,337.5,3100,3700,0.00
C18,Softwood,18.,10.,0.4,18.,2.2,3.4,0.8,9000,6000,300,201,560,373.4,3200,3800,0.00
C20,Softwood,20.,11.5,0.4,19.,2.3,3.6,0.8,9500,6400,320,214,590,397.5,3300,4000,0.00
C22,Softwood,22.,13.,0.4,20.,2.4,3.8,0.8,10000,6700,330,221,630,422.1,3400,4100,0.00
C24,Softwood,24.,14.5,0.4,21.,2.5,4.,0.8,11000,7400,370,248,690,464.2,3500,4200,0.00
C27,Softwood,27.,16.5,0.4,22.,2.5,4.,0.8,11500,7700,380,255,720,482.1,3600,4300,0.00
C30,Softwood,30.,19.,0.4,24.,2.7,4.,0.8,12000,8000,400,268,750,500.0,3800,4600,0.00
C35,Softwood,35.,22.5,0.4,25.,2.7,4.,0.8,13000,8700,430,288,810,542.1,3900,4700,0.00
C40,Softwood,40.,26.,0.4,27.,2.8,4.,0.8,14000,9400,470,315,880,590.9,4000,4800,0.00
C45,Softwood,45.,30.,0.4,29.,2.9,4.,0.8,15000,10100,500,335,940,633.0,4100,4900,0.00
C50,Softwood,50.,33.5,0.4,30.,3.,4.,0.8,16000,10700,530,355,1000,668.8,4300,5200,0.00
D30,Hardwood,30.,18.,0.6,24.,5.3,3.9,1.2,11000,9200,730,489,690,577.1,5300,6400,0.00
D35,Hardwood,35.,21.,0.6,25.,5.4,4.1,1.2,12000,10100,800,536,750,631.3,5400,6500,0.00
D40,Hardwood,40.,24.,0.6,27.,5.5,4.2,1.2,13000,10900,870,583,810,679.2,5500,6600,0.00
D50,Hardwood,50.,30.,0.6,29.,6.2,4.5,1.2,14000,11800,930,623,880,741.8,6200,7400,0.00
D60,Hardwood,60.,36.,0.6,33.,10.5,4.8,1.2,17000,14300,1130,757,1060,891.7,7000,8400,0.00
D70,Hardwood,70.,42.,0.6,36.,12.,5.,1.2,20000,16800,1330,891,1250,1050.0,8000,9600,0.00
GL20h,Glulam h,20.,16.,0.5,20.,2.5,3.5,1.,8400,7000,300,250,650,540.0,3400,3700,0.00
GL22h,Glulam h,22.,17.6,0.5,22.,2.5,3.5,1.,10500,8800,300,250,650,540.0,3700,4100,0.00
GL24h,Glulam h,24.,19.2,0.5,24.,2.5,3.5,1.,11500,9600,300,250,650,540.0,3850,4200,0.00
GL26h,Glulam h,26.,20.8,0.5,26.,2.5,3.5,1.,12100,10100,300,250,650,540.0,4050,4450,0.00
GL28h,Glulam h,28.,22.3,0.5,28.,2.5,3.5,1.,12600,10500,300,250,650,540.0,4250,4600,0.00
GL30h,Glulam h,30.,24.,0.5,30.,2.5,3.5,1.,13600,11300,300,250,650,540.0,4300,4800,0.00
GL32h,Glulam h,32.,25.6,0.5,32.,2.5,3.5,1.,14200,11800,300,250,650,540.0,4400,4900,0.00
GL20c,Glulam c,20.,15.,0.5,18.5,2.5,3.5,1.,10400,8600,300,250,650,540.0,3550,3900,0.00
GL22c,Glulam c,22.,16.,0.5,20.,2.5,3.5,1.,10400,8600,300,250,650,540.0,3550,3900,0.00
GL24c,Glulam c,24.,17.,0.5,21.5,2.5,3.5,1.,11000,9100,300,250,650,540.0,3650,4000,0.00
GL26c,Glulam c,26.,19.,0.5,23.5,2.5,3.5,1.,12000,10000,300,250,650,540.0,3850,4200,0.00
GL28c,Glulam c,28.,19.5,0.5,24.,2.5,3.5,1.,12500,10400,300,250,650,540.0,3900,4200,0.00
GL30c,Glulam c,30.,19.5,0.5,24.5,2.5,3.5,1.,13000,10800,300,250,650,540.0,3900,4300,0.00
GL32c,Glulam c,32.,19.5,0.5,24.5,2.5,3.5,1.,13500,11200,300,250,650,540.0,4000,4400,0.00
Kerto-S,LVL,44.,35.,0.8,35.,6.,4.1,0.5,13800,11600,1,1,600,400.0,4800,5100,0.00
Kerto-Q,LVL,32.,26.,6.,26.,9.,4.5,0.5,10500,8800,1,1,600,400.0,4800,5100,0.00

Analys Steel New imposed	Numbers of elements that changes [-]	Difference in weight [ton]
2 kN/m^2	0	0,00
3 kN/m^2	83	3,93
4 kN/m^2	187	14,09
5 kN/m^2	216	24,35
6 kN/m^2	216	29,54
7 kN/m^2	216	30,88

Analys Steel New imposed	Numbers of Columns that changes [-]	Diffrence in weight Columns [ton]
2 kN/m^2	0	0
3 kN/m^2	58	1,04
4 kN/m^2	87	2,54
5 kN/m^2	116	5,75
6 kN/m^2	116	6,14
7 kN/m^2	116	7,48

E

Result:Steel System and Timber system

Analys Steel New imposed	Numbers of X beams that changes [-]	Diffrence in weight X beams [ton]
2 kN/m^2	0	0
3 kN/m^2	25	2,89
4 kN/m^2	100	11,55
5 kN/m^2	125	18,60
6 kN/m^2	100	23,40
7 kN/m^2	100	23,40

Analys Steel Columns	Number of Column that changes:				
New imposed	Floor 0	Floor 1	Floor 2	Floor 3	Floor 4
2 kN/m^2	0	0	0	0	0
3 kN/m^2	29	29	0	0	0
4 kN/m^2	29	29	29	0	0
5 kN/m^2	29	29	29	29	0
6 kN/m^2	29	29	29	29	0
7 kN/m^2	29	29	29	29	0

Analys Steel X-beams	Number of X-beams that changes:				
New imposed	Floor 0	Floor 1	Floor 2	Floor 3	Floor 4
2 kN/m^2	0	0	0	0	0
3 kN/m^2	25	0	0	0	0
4 kN/m^2	25	25	25	25	0
5 kN/m^2	25	25	25	25	25
6 kN/m^2	25	25	25	25	0
7 kN/m^2	25	25	25	25	0

Analys Steel Columns	Number of Columns that changes/ floor				
Floor	Analys 1---> Analys 1 2 kN/m^2 -->2 kN/m^2	Analys 1---> Analys 2 2 kN/m^2 -->3 kN/m^2	Analys 1---> Analys 3 2 kN/m^2 -->4 kN/m^2	Analys 1---> Analys 4 2 kN/m^2 -->5 kN/m^2	Analys 1---> Analys 5 2 kN/m^2 -->6 kN/m^2
0	0	29	29	29	29
1	0	29	29	29	29
2	0	0	29	29	29
3	0	0	0	29	29
4	0	0	0	0	0

Analys Steel X-beams	Number of X-beams that changes/ floor				
Floor	Analys 1---> Analys 1 2 kN/m^2 -->2 kN/m^2	Analys 1---> Analys 2 2 kN/m^2 -->3 kN/m^2	Analys 1---> Analys 3 2 kN/m^2 -->4 kN/m^2	Analys 1---> Analys 4 2 kN/m^2 -->5 kN/m^2	Analys 1---> Analys 5 2 kN/m^2 -->6 kN/m^2
0	0	25	25	25	25
1	0	0	25	25	25
2	0	0	25	25	25
3	0	0	25	25	25

4	0	0	0	25	0

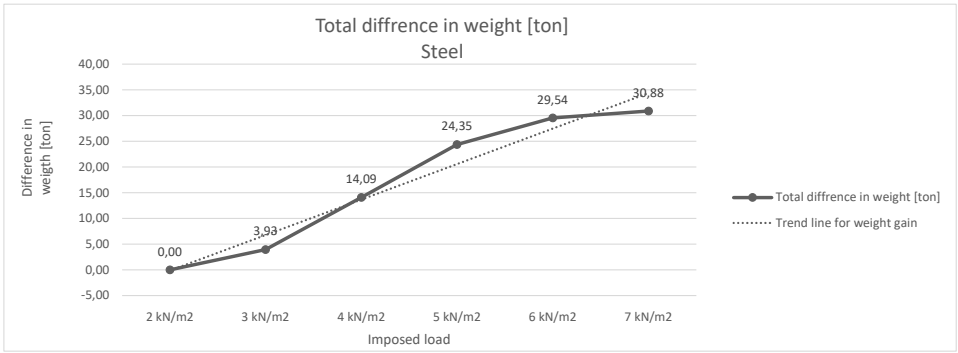
Total diffrence in weight [ton]
Steel
Difference in weigth [ton]
40,00
35,00
30,00
25,00
20,00
15,00
10,00
5,00
0,00
-5,00
0,00
3,93
14,09
24,35
29,54
30,88
2 kN/m2
3 kN/m2
4 kN/m2
5 kN/m2
6 kN/m2
7 kN/m2
Imposed load
Total diffrence in weight [ton]
Trend line for weight gain

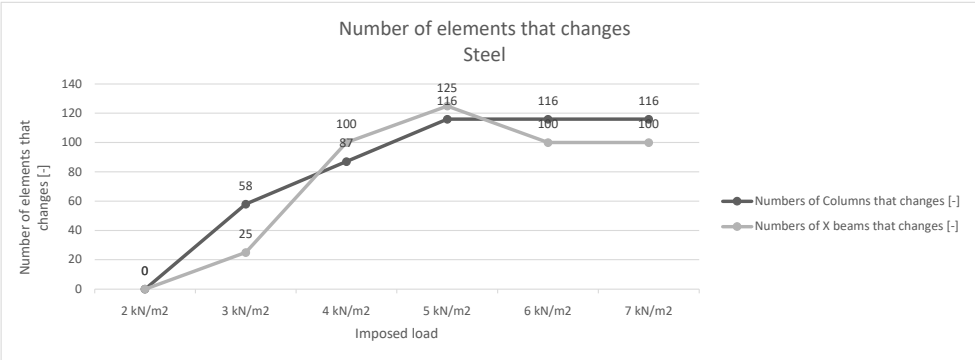
Number of elements that changes
Steel
Number of elements that changes [-]
140
120
100
80
60
40
20
0
0
58
100
116
116
116
25
87
125
100
100
2 kN/m2
3 kN/m2
4 kN/m2
5 kN/m2
6 kN/m2
7 kN/m2
Imposed load
Numbers of Columns that changes [-]
Numbers of X beams that changes [-]

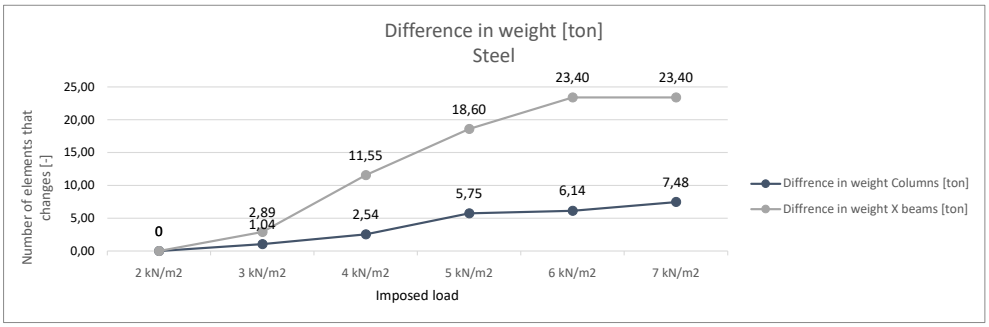
Difference in weight [ton]
Steel
Number of elements that changes [-]
25,00
20,00
15,00
10,00
5,00
0,00
0
1,04
2,89
2,54
11,55
5,75
18,60
6,14
23,40
7,48
23,40
2 kN/m2
3 kN/m2
4 kN/m2
5 kN/m2
6 kN/m2
7 kN/m2
Imposed load
Diffrence in weight Columns [ton]
Diffrence in weight X beams [ton]

Analys 1---> Analys 6 2 kN/m^2 -->7 kN/m^2
29
29
29
29
0

Analys 1---> Analys 6 2 kN/m^2 -->7 kN/m^2
25
25
25
25

Analys Steel geometry Span width Y-axis [m]	Span width X-axis [m]						
	6	7	8	9	10	11	12
6	374,33	399,79	422,85	462,89	496,53	564,27	629,90
7	378,58	412,88	437,03	474,20	511,84	588,44	659,34
8	384,14	423,56	439,04	482,72	540,30	609,44	690,64
9	385,17	426,69	453,87	495,96	569,37	637,21	694,55
10	394,21	440,20	466,05	543,89	664,02	755,61	850,22
11	399,98	451,40	576,30	689,31	795,66	834,74	874,62
12	413,31	491,78	680,81	768,72	808,85	851,18	888,48

Analys Steel Span width Y-axis [m]	Span width X-axis [m]							
	6	7	8	9	10	11	12	
6	DISP	UTIL	UTIL	UTIL	UTIL	DISP	UTIL	
7	DISP	UTIL	UTIL	DISP	UTIL	DISP	UTIL	
8	UTIL	UTIL	UTIL	UTIL	DISP	UTIL	UTIL	
9	UTIL	UTIL	UTIL	UTIL	DISP	UTIL	DISP*	9
10	DISP	UTIL	DISP	DISP	DISP*	DISP*	DISP*	10
11	UTIL	DISP	DISP	DISP*	DISP*	DISP*	DISP*	11
12	DISP	DISP	DISP*	DISP*	DISP*	DISP*	DISP*	12

*) Blue parts: unable to meet the criteria

Number of floors	Weight [ton]	Dimensioned section
4	253,33	UTIL
5	344,59	UTIL
6	437,03	UTIL
7	530,60	UTIL
8	635,95	DISP
9	730,40	DISP
10	856,21	DISP
11	995,01	DISP
12	1173,14	DISP
13	1547,65	DISP*
14	1756,37	DISP*
15	1953,12	DISP*

*) Blue part: unable to meet the criteria

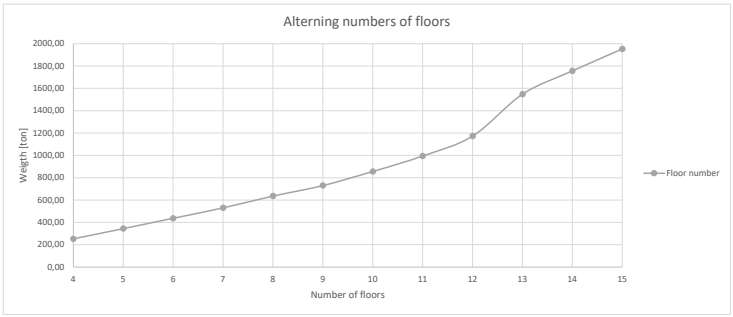

Analys Steel	Span width X-axis [m]						
Span width Y-axis [m]	6	7	8	9	10	11	12
6							
7							
8							
9							0 DISP, 4 UTIL
10					5 DISP, 0 UTIL	7 DISP, 0 UTIL	9 DISP, 4 UTIL
11				7 DISP, 0 UTIL	18 DISP, 0 UTIL	19 DISP, 1 UTIL	20 DISP, 4 UTIL
12			7 DISP, 0 UTIL	19 DISP, 0 UTIL	19 DISP, 0 UTIL	19 DISP, 4 UTIL	20 DISP, 4 UTIL

Widths where its unable to meet the criteria. Note the blue part there both DISP and UTIL fall
The numbers correspond to the number of cross-sectional groups that fail.

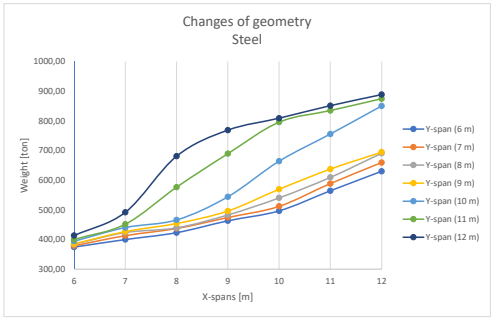
Changes of geometry
Steel
Weight [ton]
1000,00
900,00
800,00
700,00
600,00
500,00
400,00
300,00
6
7
8
9
10
11
12
X-spans [m]
Y-span (6 m)
Y-span (7 m)
Y-span (8 m)
Y-span (9 m)
Y-span (10 m)
Y-span (11 m)
Y-span (12 m)

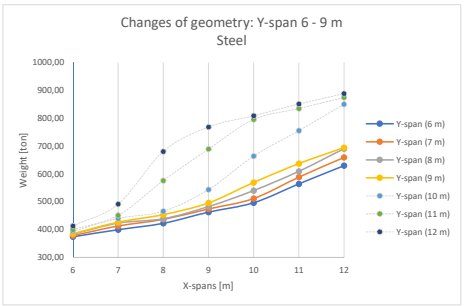
Changes of geometry: Y-span 6 - 9 m
Steel
Weight [ton]
1000,00
900,00
800,00
700,00
600,00
500,00
400,00
300,00
6
7
8
9
10
11
12
X-spans [m]
Y-span (6 m)
Y-span (7 m)
Y-span (8 m)
Y-span (9 m)
Y-span (10 m)
Y-span (11 m)
Y-span (12 m)

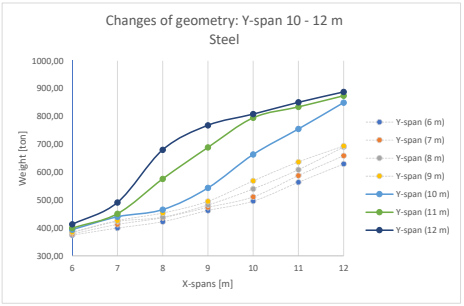
Changes of geometry: Y-span 10 - 12 m
Steel
Weight [ton]
1000,00
900,00
800,00
700,00
600,00
500,00
400,00
300,00
6
7
8
9
10
11
12
X-spans [m]
Y-span (6 m)
Y-span (7 m)
Y-span (8 m)
Y-span (9 m)
Y-span (10 m)
Y-span (11 m)
Y-span (12 m)

Analys Timber New imposed	Numbers of elements that changes [-]	Difference in weight [ton]
2 kN/m^2	0	0
3 kN/m^2	221	9,48
4 kN/m^2	221	19,14
5 kN/m^2	221	30,10
6 kN/m^2	221	39,71
7 kN/m^2	258	49,84

Analys Timber New imposed	Total weight [ton]
2 kN/m^2	352,02
3 kN/m^2	361,50
4 kN/m^2	371,16
5 kN/m^2	382,13
6 kN/m^2	391,73
7 kN/m^2	401,86

Analys Timber New imposed	Numbers of Columns that changes [-]	Diffrence in weight Columns [ton]
2 kN/m^2	0	0
3 kN/m^2	116	9,50
4 kN/m^2	116	11,48
5 kN/m^2	116	13,44
6 kN/m^2	116	15,51
7 kN/m^2	116	17,60

Changes of imposed load

Analys Timber New imposed	Numbers of X beams that changes [-]	Diffrence in weight X beams [ton]
2 kN/m^2	0	0
3 kN/m^2	105	36,98
4 kN/m^2	105	44,77
5 kN/m^2	105	52,80
6 kN/m^2	105	60,47
7 kN/m^2	110	69,83

Analys Timber New imposed	Numbers of Y beams that changes [-]	Diffrence in weight Y beams [ton]
2 kN/m^2	0	0
3 kN/m^2	0	0,00
4 kN/m^2	0	0,00
5 kN/m^2	0	0,00
6 kN/m^2	0	0,00
7 kN/m^2	32	3,16

Analys Timber Columns	Number of Column that changes:				
New imposed	Floor 0	Floor 1	Floor 2	Floor 3	Floor 4
2 kN/m^2	0	0	0	0	0
3 kN/m^2	29	29	29	29	0
4 kN/m^2	29	29	29	29	0
5 kN/m^2	29	29	29	29	0
6 kN/m^2	29	29	29	29	0
7 kN/m^2	29	29	29	29	0

Changes of imposed load

Analys Timber X-beams	Number of X-beam that changes:				
New imposed	Floor 0	Floor 1	Floor 2	Floor 3	Floor 4
2 kN/m^2	0	0	0	0	0
3 kN/m^2	25	25	25	25	5
4 kN/m^2	25	25	25	25	5
5 kN/m^2	25	25	25	25	5
6 kN/m^2	25	25	25	25	5
7 kN/m^2	25	25	25	25	10

Analys Timber Y-beams	Number of Y-beam that changes:				
New imposed	Floor 0	Floor 1	Floor 2	Floor 3	Floor 4
2 kN/m^2	0	0	0	0	0
3 kN/m^2	0	0	0	0	0
4 kN/m^2	0	0	0	0	0
5 kN/m^2	0	0	0	0	0
6 kN/m^2	0	0	0	0	0
7 kN/m^2	8	8	8	8	0

Changes of imposed load

Analys Timber Columns	Number of Columns that changes/ floor				
	Analys 1---> Analys 1	Analys 1---> Analys 2	Analys 1---> Analys 3	Analys 1---> Analys 4	Analys 1---> Analys 5
Floor	2 kN/m^2 -->2 kN/m^2	2 kN/m^2 -->3 kN/m^2	2 kN/m^2 -->4 kN/m^2	2 kN/m^2 -->5 kN/m^2	2 kN/m^2 -->6 kN/m^2
0	0	29	29	29	29
1	0	29	29	29	29
2	0	29	29	29	29
3	0	29	29	29	29
4	0	0	0	0	0

Analys Timber X-beams	Number of X-beams that changes/ floor				
	Analys 1---> Analys 1	Analys 1---> Analys 2	Analys 1---> Analys 3	Analys 1---> Analys 4	Analys 1---> Analys 5
Floor	2 kN/m^2 -->2 kN/m^2	2 kN/m^2 -->3 kN/m^2	2 kN/m^2 -->4 kN/m^2	2 kN/m^2 -->5 kN/m^2	2 kN/m^2 -->6 kN/m^2
0	0	25	25	25	25
1	0	25	25	25	25
2	0	25	25	25	25
3	0	25	25	25	25
§	0	5	5	5	5

Analys Timber Y-beams	Number of Y-beams that changes/ floor				
	Analys 1---> Analys 1	Analys 1---> Analys 2	Analys 1---> Analys 3	Analys 1---> Analys 4	Analys 1---> Analys 5
Floor	2 kN/m^2 -->2 kN/m^2	2 kN/m^2 -->3 kN/m^2	2 kN/m^2 -->4 kN/m^2	2 kN/m^2 -->5 kN/m^2	2 kN/m^2 -->6 kN/m^2
0	0	0	0	0	0
1	0	0	0	0	0
2	0	0	0	0	0
3	0	0	0	0	0
4	0	0	0	0	0

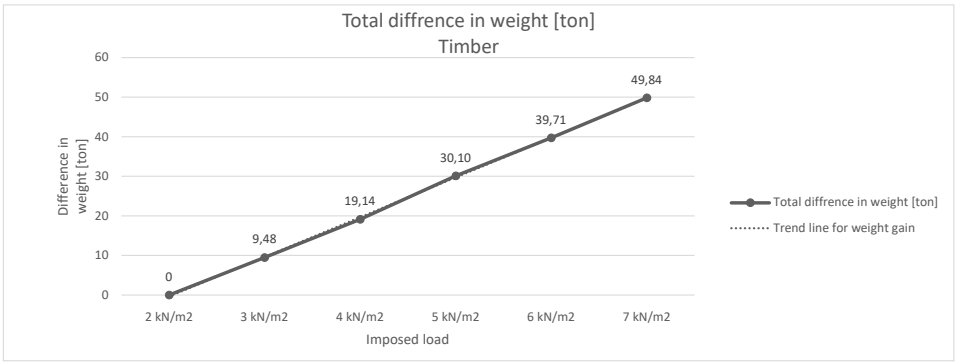
Total diffrence in weight [ton]
Timber
Difference in weight [ton]
60
50
40
30
20
10
0
49,84
39,71
30,10
19,14
9,48
0
2 kN/m2
3 kN/m2
4 kN/m2
5 kN/m2
6 kN/m2
7 kN/m2
Imposed load
Total diffrence in weight [ton]
Trend line for weight gain

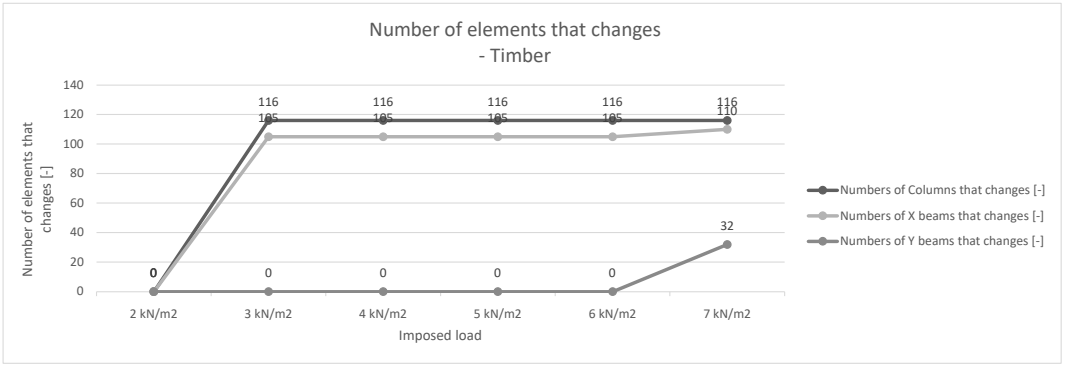
Number of elements that changes
- Timber
Number of elements that changes [-]
140
120
100
80
60
40
20
0
116
116
116
116
116
105
105
105
105
110
32
0
0
0
0
0
2 kN/m2
3 kN/m2
4 kN/m2
5 kN/m2
6 kN/m2
7 kN/m2
Imposed load
Numbers of Columns that changes [-]
Numbers of X beams that changes [-]
Numbers of Y beams that changes [-]

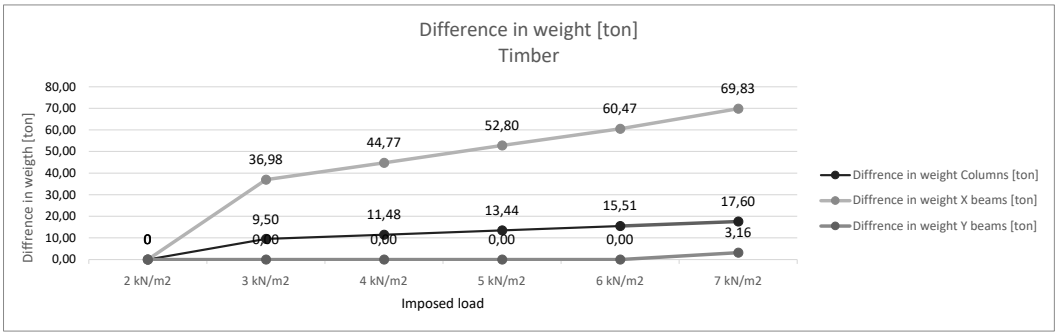
Difference in weight [ton]
Timber
Diffrence in weigth [ton]
80,00
70,00
60,00
50,00
40,00
30,00
20,00
10,00
0,00
0
36,98
44,77
52,80
60,47
69,83
9,50
11,48
13,44
15,51
17,60
0,00
0,00
0,00
0,00
3,16
2 kN/m2
3 kN/m2
4 kN/m2
5 kN/m2
6 kN/m2
7 kN/m2
Imposed load
Diffrence in weight Columns [ton]
Diffrence in weight X beams [ton]
Diffrence in weight Y beams [ton]

Analys 1---> Analys 6 2 kN/m^2 -->7 kN/m^2
29
29
29
29
0

Analys 1---> Analys 6 2 kN/m^2 -->7 kN/m^2
25
25
25
25
10

Analys 1---> Analys 6 2 kN/m^2 -->7 kN/m^2
8
8
8
8
0

Number of floors	Weight [ton]	Dimensioned section
4	208,18	UTIL
5	279,75	UTIL
6	352,02	UTIL
7	424,72	UTIL
8	498,21	UTIL
9	572,04	UTIL*
10	645,79	UTIL*
11	720,70	UTIL*
12	796,20	UTIL*
13	872,25	UTIL*
14	949,23	UTIL*
15	1027,00	UTIL*

*) Blue part: unable to meet the criteria

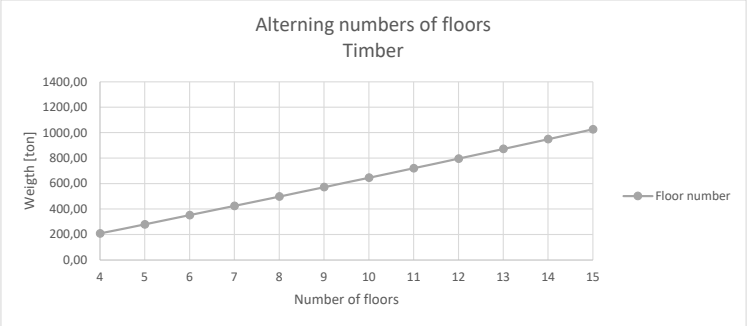

F

Verification of result of critical timber column

Most critical timber element: Column 3.4.0

This calculation is performed to validate the parametric model, and give bases to section 5.4. The element that experienced highest utilisation are here analysed and compared to the model result.

1. Buckling resistance timber column — According to EN 1995-1-1 6.3.2

Input:

Chosen element: Column 3.4.0

$f_{c0k} := 24.5\ MPa$ — Characteristic compression strength for GL30

$E_{0.05} := 10800\ MPa$ — Modulus of elasticity

$\gamma_M := 1.25$ — Partial factor timber

$k_{mod} := 0.8$ — Climate and load reductionfactor

$\beta_c := 0.1$ — Straightness factor

$L_{cr} := 2.7\ m \cdot 0.9 = 2.43\ m$ — Critical buckling length

$N_{Ed} := 2580\ kN$ — Value provide drom model

$b := 215\ mm$ — Width of column 3.4.0

$h := 450\ mm$ — Heigth of column 3.4.0

$f_{c0d} := \frac{f_{c0k} \cdot k_{mod}}{\gamma_M} = 15.68\ MPa$ — Design strength for GL30

$I := \frac{h \cdot b^3}{12} = \left(3.727 \cdot 10^{-4}\right)\ m^4$ — Moment of inertia

$A := b \cdot h = 0.097\ m^2$ — Area of column 3.4.0

$i := \sqrt{\frac{I}{A}} = 0.062\ m$

$\lambda := \frac{L_{cr}}{i} = 39.152$

$\lambda_{rel} := \frac{\lambda}{\pi} \cdot \sqrt{\frac{f_{c0k}}{E_{0.05}}} = 0.594$ — Relative slenderness

$k := 0.5 \cdot \left(1 + \beta_c \cdot \left(\lambda_{rel} - 0.3\right) + {\lambda_{rel}}^2\right) = 0.691$

$$k_c := \frac{1}{k + \sqrt{k^2 - \lambda_{rel}^{\ 2}}} = 0.958$$

Magnification factor that takes load direction into account

$$N_{Rd} := f_{c0d} \cdot k_c \cdot A = \left(1.453 \cdot 10^3\right)\ \textit{kN}$$

$$\eta_b := \frac{N_{Ed}}{N_{Rd}} = 1.776$$

Verification

Comparison with the load observed in the parametric model

$$\eta_{b.model} := 1.78$$

$$\text{abs}\left(\frac{\eta_b}{\eta_{b.model}}\right) = 0.998$$

‹1 % diffrence. The variance between hand calculations and the parametric model can be seen as tolerable.

G

Hand calculations for verifying most critical X-beam

Verification of parametric model: Critical timber element

This calculation is performed to validate the parametric model. The element that experienced highest utilisation are here analysed and compared to the model result.

Biaxial bending — According to EN 1995-1-1, 6.1.6

Input:

Chosen element: Beam X.1.1.0.3

$f_{m.k} := 30\ MPa$ — Characteristic bending strength for GL30

$k_{mod} := 0.8$ — Climate and load reductionfactor

$\gamma_M := 1.25$ — Partial factor timber

$f_{m.y.d} := \frac{f_{m.k} \cdot k_{mod}}{\gamma_M} = 19.2\ MPa$ — Design bending stength

$E_{0.05} := 10800\ MPa$ — Modulus of elasticity

$f_{m.z.d} := \frac{f_{m.k} \cdot k_{mod}}{\gamma_M} = 19.2\ MPa$ — Design bending stength

$E_{90.05} := 300\ MPa$ — Modulus of elasticity

$b_{BeamX1.1.0.3} := 115\ mm$ — Width of Beam X.1.1.0.3

$h_{BeamX1.1.0.3} := 990\ mm$ — Height of Beam X.1.1.0.3

$l_{BeamX1.1.0.3} := 8\ m$ — Length of Beam X.1.1.0.3

$l_{ef} := l_{BeamX1.1.0.3} \cdot 0.9 = 7.2\ m$ — Effectiv length of Beam X.1.1.0.3

$M_y := 412\ kN \cdot m$ — Provided from the model

$W_y := \frac{h_{BeamX1.1.0.3}^{\ 2} \cdot b_{BeamX1.1.0.3}}{6} = 0.019\ m^3$

$\sigma_{m.y.d} := \frac{M_y}{W_y} = 21.932\ MPa$ — Design bending stress around the strong axis

$M_z := 0.12\ N \cdot m$ — Provided from the model

$W_z := \frac{b_{BeamX1.1.0.3}^{\ 2} \cdot h_{BeamX1.1.0.3}}{6} = 0.002\ m^3$

$\sigma_{m.z.d} := \frac{M_z}{W_z} = \left(5.499 \cdot 10^{-5}\right) MPa$ — Design bending stress around the week axis

$k_c := 0.7$

$$\eta_{biaxial} := \frac{\sigma_{m.y.d}}{f_{m.y.d}} + k_c \cdot \frac{\sigma_{m.z.d}}{f_{m.z.d}} = 1.142$$

Verification

Comparison with the load observed in the parametric model

$$\eta_{b.model} := 1.17$$

$$\text{abs}\left(\frac{\eta_{biaxial}}{\eta_{b.model}}\right) = 0.976$$

‹3 % diffrence. The variance between hand calculations and the parametric model can be seen as tolerable.

Compression and bending — According to EN 1995-1-1, 6.2.4

Input:

Chosen element: Beam X.1.1.0.3

$f_{m.k} := 30\ MPa$ — Characteristic bending strength for GL30

$k_{mod} := 0.8$ — Climate and load reductionfactor

$\gamma_M := 1.25$ — Partial factor timber

$f_{m.y.d} := \frac{f_{m.k} \cdot k_{mod}}{\gamma_M} = 19.2\ MPa$ — Design bending stength

$E_{0.05} := 10800\ MPa$ — Modulus of elasticity

$f_{m.z.d} := \frac{f_{m.k} \cdot k_{mod}}{\gamma_M} = 19.2\ MPa$ — Design bending stength

$f_{c.0.k} := 24.5\ MPa$

$f_{c.0.d} := \frac{f_{c.0.k} \cdot k_{mod}}{\gamma_M} = 15.68\ MPa$

$E_{90.05} := 300\ MPa$ — Modulus of elasticity

$b_{BeamX1.1.0.3} := 115\ mm$ — Width of Beam X.1.1.0.3

$h_{BeamX1.1.0.3} := 990\ mm$ — Height of Beam X.1.1.0.3

$A_{beamX1.1.0.3} := h_{BeamX1.1.0.3} \cdot b_{BeamX1.1.0.3} = 0.114\ m^2$

$l_{BeamX1.1.0.3} := 8\ m$ — Length of Beam X.1.1.0.3

$l_{ef} := l_{BeamX1.1.0.3} \cdot 0.9 = 7.2\ m$ — Effectiv length of Beam X.1.1.0.3

$M_y := 412\ kN \cdot m$ — Provided from the model

$W_y := \frac{{h_{BeamX1.1.0.3}}^2 \cdot b_{BeamX1.1.0.3}}{6} = 0.019\ m^3$

$\sigma_{m.y.d} := \frac{M_y}{W_y} = 21.932\ MPa$ — Design bending stress around the strong axis

$M_z := 0.12\ N \cdot m$ — Provided from the model

$W_z := \frac{{b_{BeamX1.1.0.3}}^2 \cdot h_{BeamX1.1.0.3}}{6} = 0.002\ m^3$

$\sigma_{m.z.d} := \frac{M_z}{W_z} = \left(5.499 \cdot 10^{-5}\right) MPa$ — Design bending stress around the week axis

$k_c := 0.7$

$N_{axial} := 0.19\ \boldsymbol{N}$ Provided from the model

$\sigma_{c.0.d} := \frac{N_{axial}}{A_{beamX1.1.0.3}} = \langle 1.669 \cdot 10^{-6} \rangle\ \boldsymbol{MPa}$

$\eta_{compresionandbendning} := \left(\frac{\sigma_{c.0.d}}{f_{c.0.d}}\right)^2 + \frac{\sigma_{m.y.d}}{f_{m.y.d}} + k_c \cdot \frac{\sigma_{m.z.d}}{f_{m.z.d}} = 1.142$

Verification

Comparison with the load observed in the parametric model

$\eta_{b.model} := 1.17$

$\mathrm{abs}\left(\frac{\eta_{compresionandbendning}}{\eta_{b.model}}\right) = 0.976$

3 % diffrence. The variance between hand calculations and the parametric model can be seen as tolerable.

Compresion and bending, beam — According to EN 1995-1-1 6.3.2

Strong axis

Input:

Chosen element: Beam X.1.1.0.3

$f_{m.k} := 30\ MPa$ — Characteristic bending strength for GL30

$k_{mod} := 0.8$ — Climate and load reductionfactor

$\gamma_M := 1.25$ — Partial factor timber

$f_{m.d} := \frac{f_{m.k} \cdot k_{mod}}{\gamma_M} = 19.2\ MPa$ — Design bending stength

$E_{0.05} := 10800\ MPa$ — Modulus of elasticity

$b_{BeamX1.1.0.3} := 115\ mm$ — Width of Beam X.1.1.0.3

$h_{BeamX1.1.0.3} := 990\ mm$ — Height of Beam X.1.1.0.3

$l_{BeamX1.1.0.3} := 8\ m$ — Length of Beam X.1.1.0.3

$l_{ef} := l_{BeamX1.1.0.3} \cdot 0.9 = 7.2\ m$ — Effectiv length of Beam X.1.1.0.3

Balktyp	Lasttyp	k_{ef}
Fritt upplagd	Konstant moment	1,0
	Jämnt utbredd last	0,9
	Koncentrerad last mitt på spannet	0,8
Konsol	Jämnt utbredd last	0,5
	Koncentrerad last vid den fria änden	0,8

* Förhållandet mellan den effektiva längden l_{ef} och spännvidden l gäller för en balk med vridstyvt upplagda ändar belastad i tvärsnittets tyngdpunkt. Om lasten angriper i balkens tryckta kant bör l_{ef} ökas med beloppet $2h$. Om lasten angriper i den dragna kanten får den effektiva längden l_{ef} minskas med beloppet $0,5h$.

Rectangular beam-->A simplified method can be used according to EN 1995-1-1:2004

$\sigma_{m.crit} := \frac{0.78 \cdot b_{BeamX1.1.0.3}^{2}}{h_{BeamX1.1.0.3} \cdot l_{ef}} \cdot E_{0.05} = 15.63\ MPa$ — Critical bending stress, simplidied method (equ:6.32)

$\lambda_{rel.m} := \sqrt{\frac{f_{m.k}}{\sigma_{m.crit}}} = 1.385$ — Relative slenderness ratio

$k_{crit} := 1.56 - 0.75 \cdot \lambda_{rel.m} = 0.521$ — Factor that considerate lateral stability

$f_{m.d} \cdot k_{crit} = 10.002\ MPa$ — Lateral torsional buckling resistance for Beam X.1.1.0.3

$M_y := 374011\ N \cdot m$ — Provided from the model

$$W_y := \frac{h_{BeamX1.1.0.3}^{\ 2} \cdot b_{BeamX1.1.0.3}}{4} = 0.028\ m^3$$

$$\sigma_m := \frac{M_y}{W_y} = 13.273\ MPa$$

Verification

Comparison with the load observed in the parametric model

$$\eta_{compresionandbending.beam} := \frac{\sigma_m}{f_{m.d} \cdot k_{crit}} = 1.327$$

Verification

Comparison with the load observed in the parametric model

$$\eta_{b.model} := 5.1$$

$$\mathrm{abs}\left(\frac{\eta_{compresionandbending.beam}}{\eta_{b.model}}\right) = 0.26$$

78 % diffrence. The variance between hand calculations and the parametric model can be seen as NOT tolerable.

Compresion and bending, beam — According to EN 1995-1-1 6.3.2

Strong axis

Input:

Chosen element: Beam X.1.1.0.3

$f_{m.k} := 30\ MPa$ — Characteristic bending strength for GL30

$k_{mod} := 0.8$ — Climate and load reductionfactor

$\gamma_M := 1.25$ — Partial factor timber

$f_{m.d} := \frac{f_{m.k} \cdot k_{mod}}{\gamma_M} = 19.2\ MPa$ — Design bending stength

$E_{0.05} := 10800\ MPa$ — Modulus of elasticity

$b_{BeamX1.1.0.3} := 115\ mm$ — Width of Beam X.1.1.0.3

$h_{BeamX1.1.0.3} := 990\ mm$ — Height of Beam X.1.1.0.3

$l_{BeamX1.1.0.3} := 8\ m$ — Length of Beam X.1.1.0.3

$l_{ef} := l_{BeamX1.1.0.3} \cdot 0.9 = 7.2\ m$ — Effectiv length of Beam X.1.1.0.3

Balktyp	Lasttyp	k_{ef}
Fritt upplagd	Konstant moment	1,0
	Jämnt utbredd last	0,9
	Koncentrerad last mitt på spannet	0,8
Konsol	Jämnt utbredd last	0,5
	Koncentrerad last vid den fria änden	0,8

* Förhållandet mellan den effektiva längden l_{ef} och spännvidden l gäller för en balk med vridstyvt upplagda ändar belastad i tvärsnittets tyngdpunkt. Om lasten angriper i balkens tryckta kant bör l_{ef} ökas med beloppet $2h$. Om lasten angriper i den dragna kanten får den effektiva längden l_{ef} minskas med beloppet $0,5h$.

Rectangular beam-->A simplified method can be used according to EN 1995-1-1:2004

$\sigma_{m.crit} := \frac{0.78 \cdot h_{BeamX1.1.0.3}^{2}}{b_{BeamX1.1.0.3} \cdot l_{ef}} \cdot E_{0.05} = \langle 9.971 \cdot 10^{3} \rangle\ MPa$ — Critical bending stress, simplidied method (equ:6.32)

$\lambda_{rel.m} := \sqrt{\frac{f_{m.k}}{\sigma_{m.crit}}} = 0.055$ — Relative slenderness ratio

$k_{crit} := 1$ — Factor that considerate lateral stability

$f_{m.d} \cdot k_{crit} = 19.2\ MPa$ — Lateral torsional buckling resistance for Beam X.1.1.0.3

$M_y := 374011\ N \cdot m$ — Provided from the model

$W_y := \frac{b_{BeamX1.1.0.3}^{2} \cdot h_{BeamX1.1.0.3}}{4} = 0.003\ m^3$

$\sigma_m := \frac{M_y}{W_y} = 114.265\ MPa$

Verification

Comparison with the load observed in the parametric model

$\eta_{Icompresionandbending.beam} := \frac{\sigma_m}{f_{m.d} \cdot k_{crit}} = 5.951$

Verification

Comparison with the load observed in the parametric model

$\eta_{b.model} := 5.1$

$\text{abs}\left(\frac{\eta_{compresionandbending.beam}}{\eta_{b.model}}\right) = 1.167$

16 % diffrence. The variance between hand calculations and the parametric model can be seen as tolerable but arent calculated in the typical way.

Verification of parametric model: Critical timber element

This calculation is performed to validate the parametric model. The element that experienced highest utilisation are here analysed and compared to the model result.

Compression and bending

According to EN 1995-1-1, 6.2.4

Input:

Chosen element: Beam X.0.3.0.1

$f_{m.k} := 30\ \boldsymbol{MPa}$ — Characteristic bending strength for GL30

$k_{mod} := 0.8$ — Climate and load reductionfactor

$\gamma_M := 1.25$ — Partial factor timber

$f_{m.y.d} := \frac{f_{m.k} \cdot k_{mod}}{\gamma_M} = 19.2\ \boldsymbol{MPa}$ — Design bending stength

$E_{0.05} := 10800\ \boldsymbol{MPa}$ — Modulus of elasticity

$f_{m.z.d} := \frac{f_{m.k} \cdot k_{mod}}{\gamma_M} = 19.2\ \boldsymbol{MPa}$ — Design bending stength

$E_{90.05} := 300\ \boldsymbol{MPa}$ — Modulus of elasticity

$f_{c.0.k} := 24.5\ \boldsymbol{MPa}$

$f_{c.0.d} := \frac{f_{c.0.k} \cdot k_{mod}}{\gamma_M} = 15.68\ \boldsymbol{MPa}$

$b_{BeamX0.3.0.1} := 165\ \boldsymbol{mm}$ — Width of Beam X.0.3.0.1

$h_{BeamX0.3.0.1} := 720\ \boldsymbol{mm}$ — Height of Beam X.0.3.0.1

$l_{BeamX0.3.0.1} := 8\ \boldsymbol{m}$ — Length of Beam X.0.3.0.1

$l_{ef} := l_{BeamX0.3.0.1} \cdot 0.9 = 7.2\ \boldsymbol{m}$ — Effectiv length of Beam X.0.3.0.1

$A_{beamX0.3.0.1} := h_{BeamX0.3.0.1} \cdot b_{BeamX0.3.0.1} = 0.119\ \boldsymbol{m^2}$

$M_y := 452557\ \boldsymbol{N \cdot m}$ — Provided from the model

$W_y := \frac{h_{BeamX0.3.0.1}^{\ 2} \cdot b_{BeamX0.3.0.1}}{6} = 0.014\ \boldsymbol{m^3}$

$\sigma_{m.y.d} := \frac{M_y}{W_y} = 31.745\ \boldsymbol{MPa}$ — Design bending stress around the strong axis

$M_z := 2.64\ \boldsymbol{N \cdot m}$ Provided from the model

$W_z := \frac{b_{BeamX0.3.0.1}^{\ 2} \cdot h_{BeamX0.3.0.1}}{6} = 0.003\ \boldsymbol{m^3}$

$\sigma_{m.z.d} := \frac{M_z}{W_z} = \left(8.081 \cdot 10^{-4}\right)\ \boldsymbol{MPa}$ Design bending stress around the week axis

$k_c := 0.7$

$N_{axial} := 1.33\ \boldsymbol{N}$ Provided from the model

$\sigma_{c.0.d} := \frac{N_{axial}}{A_{beamX0.3.0.1}} = \left(1.12 \cdot 10^{-5}\right)\ \boldsymbol{MPa}$

$\eta_{compresionandbendning.y} := \left(\frac{\sigma_{c.0.d}}{f_{c.0.d}}\right)^2 + \frac{\sigma_{m.y.d}}{f_{m.y.d}} + k_c \cdot \frac{\sigma_{m.z.d}}{f_{m.z.d}} = 1.653$

$\eta_{compresionandbendning.z} := \left(\frac{\sigma_{c.0.d}}{f_{c.0.d}}\right)^2 + k_c \cdot \frac{\sigma_{m.y.d}}{f_{m.y.d}} + \frac{\sigma_{m.z.d}}{f_{m.z.d}} = 1.157$

Verification

Comparison with the load observed in the parametric model

$\eta_{b.model} := 1.65$

$\mathrm{abs}\left(\frac{\eta_{compresionandbendning.y}}{\eta_{b.model}}\right) = 1.002$

<2 % diffrence. The variance between hand calculations and the parametric model can be seen as tolerable.

Biaxial bending — According to EN 1995-1-1, 6.1.6

Input:

Chosen element: Beam X.0.3.0.1

$f_{m.k} := 30\ MPa$ — Characteristic bending strength for GL30

$k_{mod} := 0.8$ — Climate and load reductionfactor

$\gamma_M := 1.25$ — Partial factor timber

$f_{m.y.d} := \frac{f_{m.k} \cdot k_{mod}}{\gamma_M} = 19.2\ MPa$ — Design bending stength

$E_{0.05} := 10800\ MPa$ — Modulus of elasticity

$f_{m.z.d} := \frac{f_{m.k} \cdot k_{mod}}{\gamma_M} = 19.2\ MPa$ — Design bending stength

$E_{90.05} := 300\ MPa$ — Modulus of elasticity

$b_{BeamX0.3.0.1} := 165\ mm$ — Width of Beam X.0.3.0.1

$h_{BeamX0.3.0.1} := 720\ mm$ — Height of Beam X.0.3.0.1

$l_{BeamX0.3.0.1} := 8\ m$ — Length of Beam X.0.3.0.1

$l_{ef} := l_{BeamX0.3.0.1} \cdot 0.9 = 7.2\ m$ — Effectiv length of Beam X.0.3.0.1

$A_{beamX0.3.0.1} := h_{BeamX0.3.0.1} \cdot b_{BeamX0.3.0.1} = 0.119\ m^2$

$M_y := 452557\ N \cdot m$ — Provided from the model

$W_y := \frac{h_{BeamX0.3.0.1}^{\ 2} \cdot b_{BeamX0.3.0.1}}{6} = 0.014\ m^3$

$\sigma_{m.y.d} := \frac{M_y}{W_y} = 31.745\ MPa$ — Design bending stress around the strong axis

$M_z := 2.64\ N \cdot m$ — Provided from the model

$W_z := \frac{b_{BeamX0.3.0.1}^{\ 2} \cdot h_{BeamX0.3.0.1}}{6} = 0.003\ m^3$

$\sigma_{m.z.d} := \frac{M_z}{W_z} = \left(8.081 \cdot 10^{-4}\right) MPa$ — Design bending stress around the week axis

$k_c := 0.7$

$$\eta_{biaxial.y} := \frac{\sigma_{m.y.d}}{f_{m.y.d}} + k_c \cdot \frac{\sigma_{m.z.d}}{f_{m.z.d}} = 1.653$$

$$\eta_{biaxial.z} := k_c \cdot \frac{\sigma_{m.y.d}}{f_{m.y.d}} + \frac{\sigma_{m.z.d}}{f_{m.z.d}} = 1.157$$

Verification

Comparison with the load observed in the parametric model

$\eta_{b.model} := 1.65$

$$\text{abs}\left(\frac{\eta_{biaxial.y}}{\eta_{b.model}}\right) = 1.002$$

<2 % diffrence. The variance between hand calculations and the parametric model can be seen as tolerable.

Verification of parametric model: Critical timber element

This calculation is performed to validate the parametric model. The element that experienced highest utilisation are here analysed and compared to the model result.

Biaxialbending

According to EN 1995-1-1, 6.2.4

Input:

Chosen element: Beam X.0.4.0.1

$f_{m.k} := 30\ \boldsymbol{MPa}$ — Characteristic bending strength for GL30

$k_{mod} := 0.8$ — Climate and load reductionfactor

$\gamma_M := 1.25$ — Partial factor timber

$f_{m.y.d} := \frac{f_{m.k} \cdot k_{mod}}{\gamma_M} = 19.2\ \boldsymbol{MPa}$ — Design bending stength

$E_{0.05} := 10800\ \boldsymbol{MPa}$ — Modulus of elasticity

$f_{m.z.d} := \frac{f_{m.k} \cdot k_{mod}}{\gamma_M} = 19.2\ \boldsymbol{MPa}$ — Design bending stength

$E_{90.05} := 300\ \boldsymbol{MPa}$ — Modulus of elasticity

$b_{BeamX0.4.0.1} := 115\ \boldsymbol{mm}$ — Width of Beam X.0.4.0.1

$h_{BeamX0.4.0.1} := 585\ \boldsymbol{mm}$ — Height of Beam X.0.4.0.1

$l_{BeamX0.3.0.1} := 8\ \boldsymbol{m}$ — Length of Beam X.0.4.0.1

$l_{ef} := l_{BeamX0.3.0.1} \cdot 0.9 = 7.2\ \boldsymbol{m}$ — Effectiv length of Beam X.0.4.0.1

$A_{beamX0.3.0.1} := h_{BeamX0.4.0.1} \cdot b_{BeamX0.4.0.1} = 0.067\ \boldsymbol{m}^2$

$M_y := 229493\ \boldsymbol{N \cdot m}$ — Provided from the model

$W_y := \frac{h_{BeamX0.4.0.1}^{\ 2} \cdot b_{BeamX0.4.0.1}}{6} = 0.007\ \boldsymbol{m}^3$

$\sigma_{m.y.d} := \frac{M_y}{W_y} = 34.987\ \boldsymbol{MPa}$ — Design bending stress around the strong axis

$M_z := 0.12\ \boldsymbol{N \cdot m}$ — Provided from the model

$W_z := \frac{b_{BeamX0.4.0.1}^{\ 2} \cdot h_{BeamX0.4.0.1}}{6} = 0.001\ \boldsymbol{m}^3$

$\sigma_{m.z.d} := \frac{M_z}{W_z} = \left(9.306 \cdot 10^{-5}\right)\ \boldsymbol{MPa}$ — Design bending stress around the week axis

$k_c := 0.7$

$$\eta_{compresionandbendning.y} := \frac{\sigma_{m.y.d}}{f_{m.y.d}} + k_c \cdot \frac{\sigma_{m.z.d}}{f_{m.z.d}} = 1.822$$

$$\eta_{compresionandbendning.z} := k_c \cdot \frac{\sigma_{m.y.d}}{f_{m.y.d}} + \frac{\sigma_{m.z.d}}{f_{m.z.d}} = 1.276$$

Verification

Comparison with the load observed in the parametric model

$$\eta_{b.model} := 1.82$$

$$\text{abs}\left(\frac{\eta_{compresionandbendning.y}}{\eta_{b.model}}\right) = 1.001$$

‹1 % diffrence. The variance between hand calculations and the parametric model can be seen as tolerable.

H

Script for steel analysis

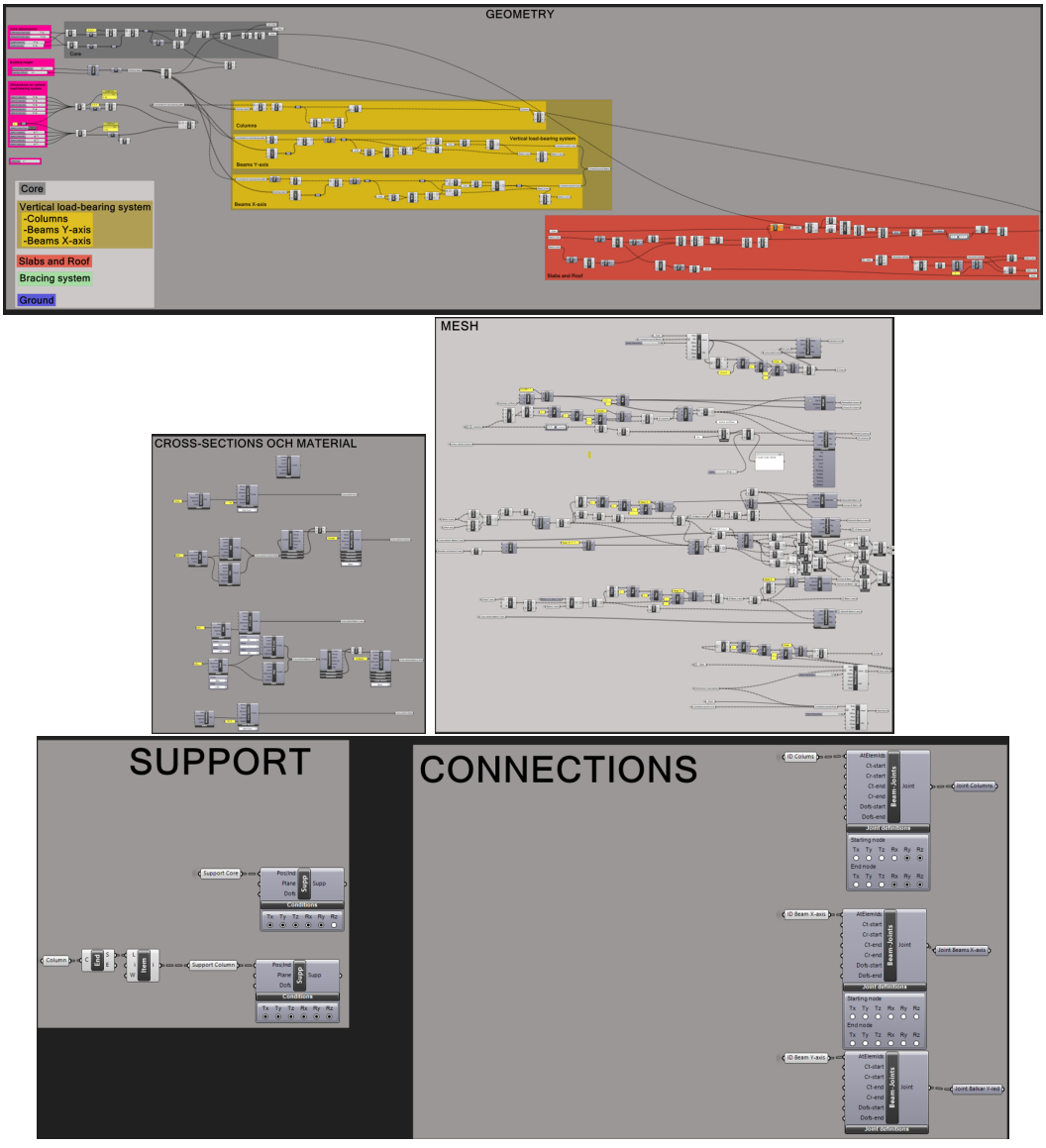

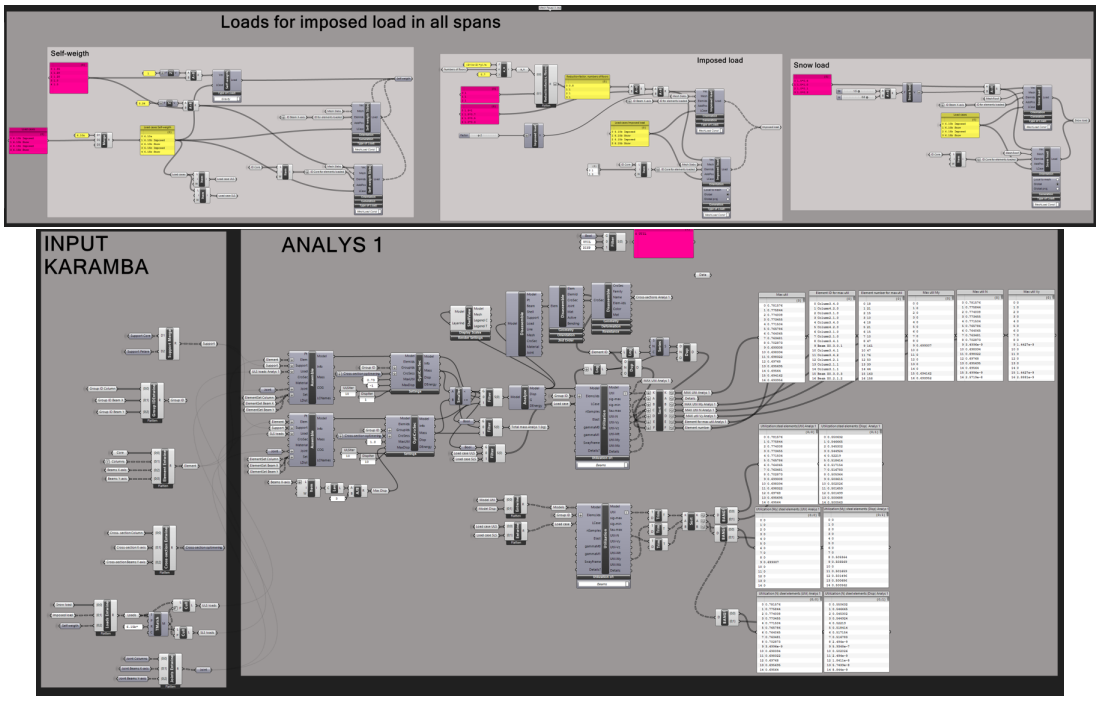
Loads for imposed load in all spans
Self-weigth
Imposed load
Snow load
INPUT
KARAMBA
ANALYS 1

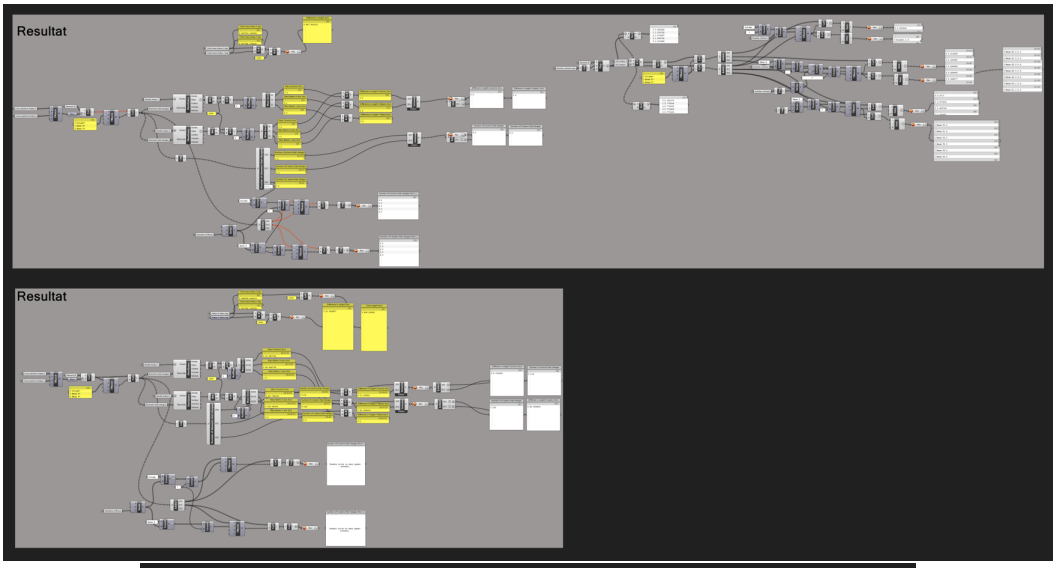
Resultat
Resultat

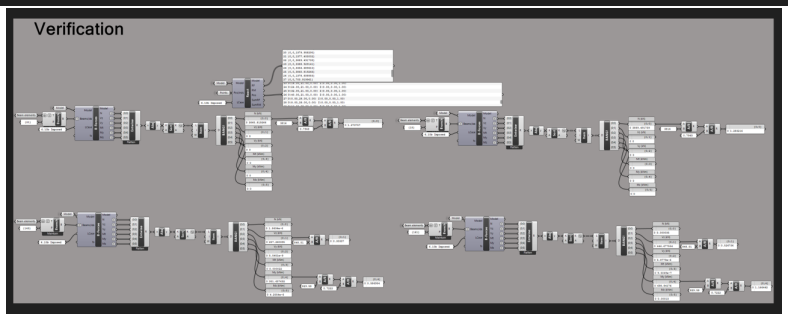
Verification

I

Script for Timber analysis

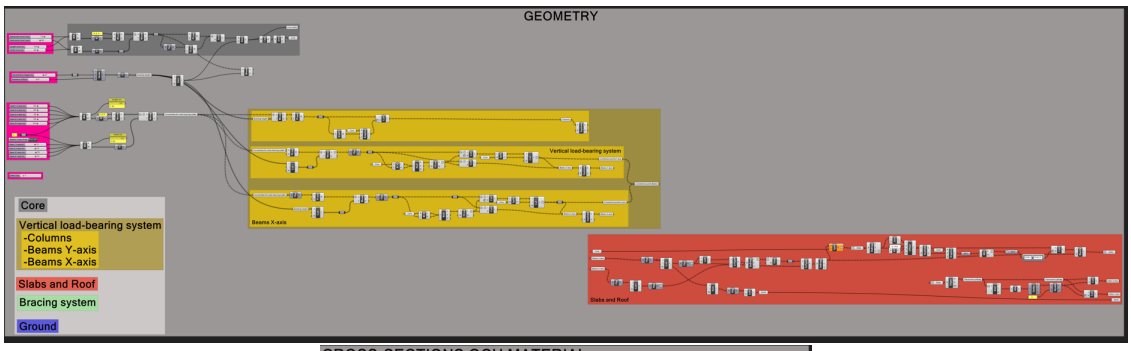

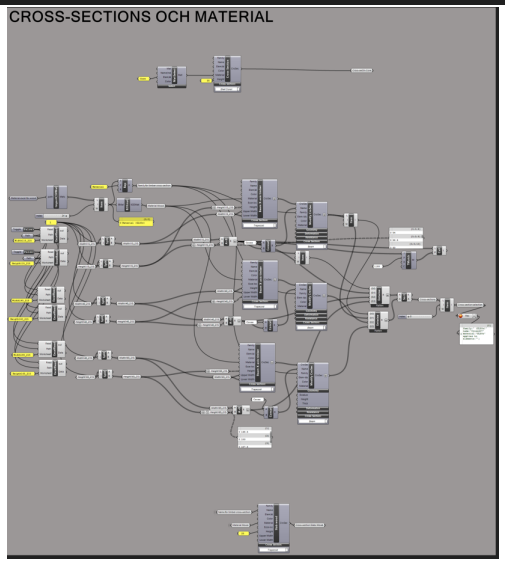

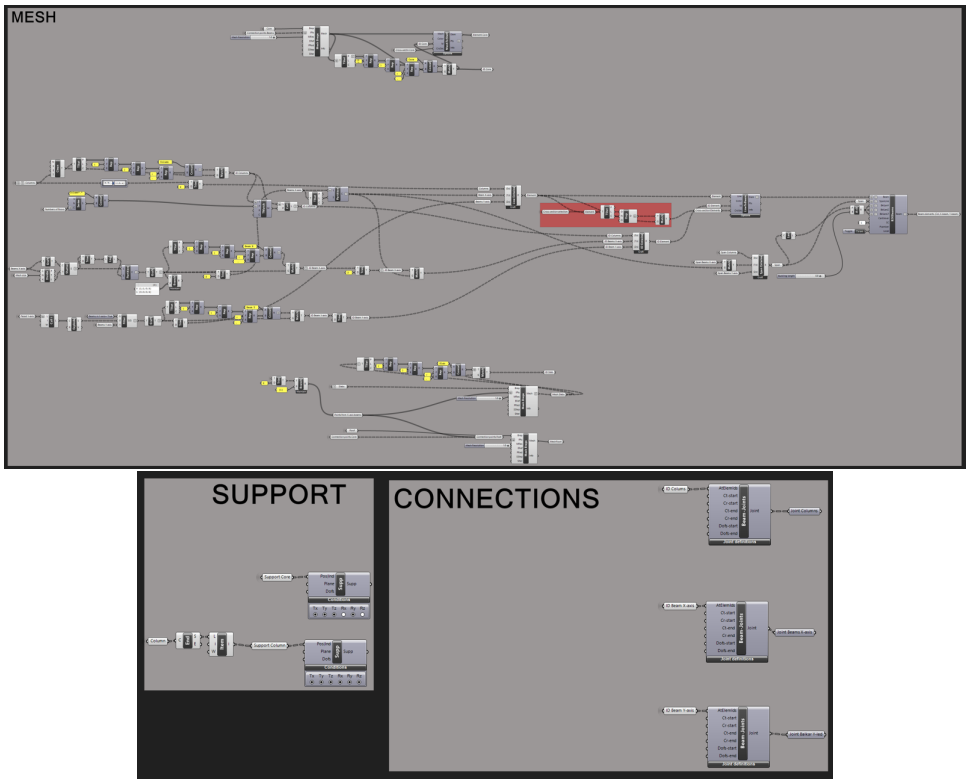
MESH
SUPPORT
CONNECTIONS

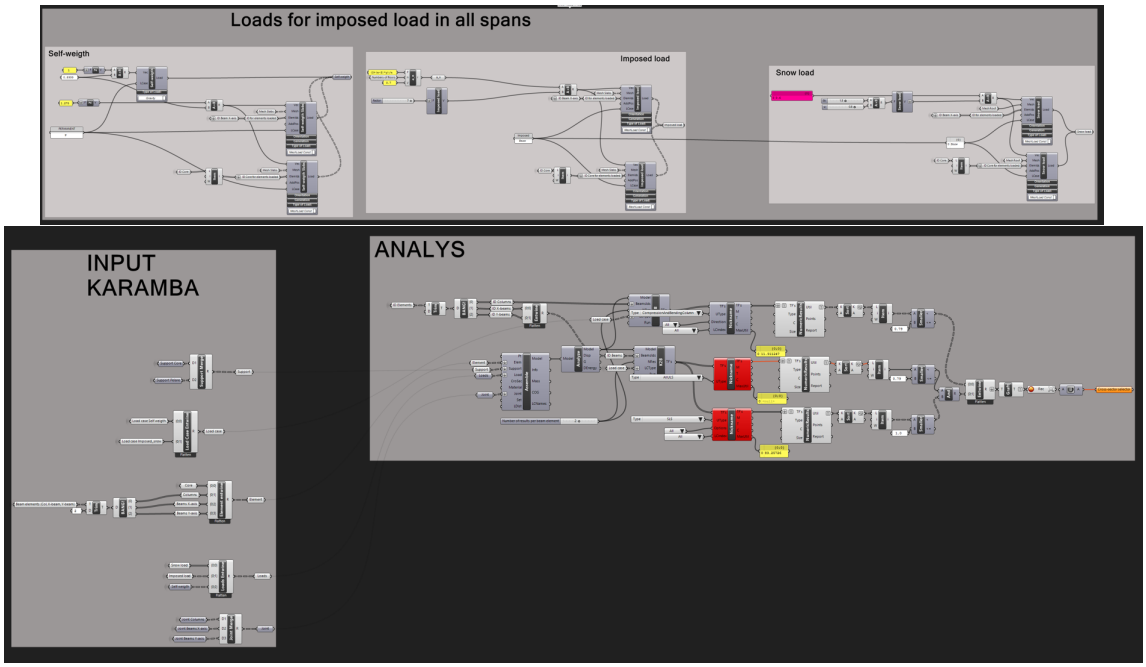
Loads for imposed load in all spans
Self-weigth
Imposed load
Snow load
INPUT
KARAMBA
ANALYS

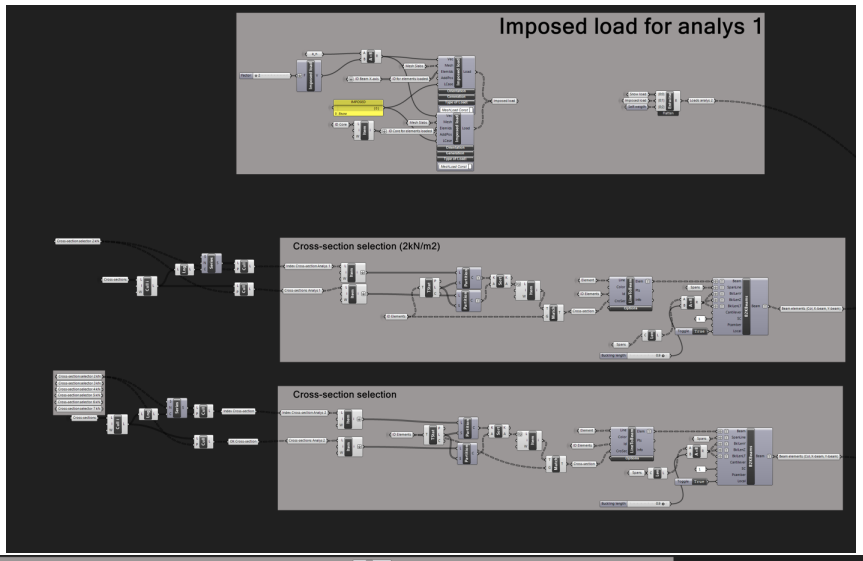
Imposed load for analys 1
Cross-section selection (2kN/m2)
Cross-section selection


ANALYS 1
ANALYS 2

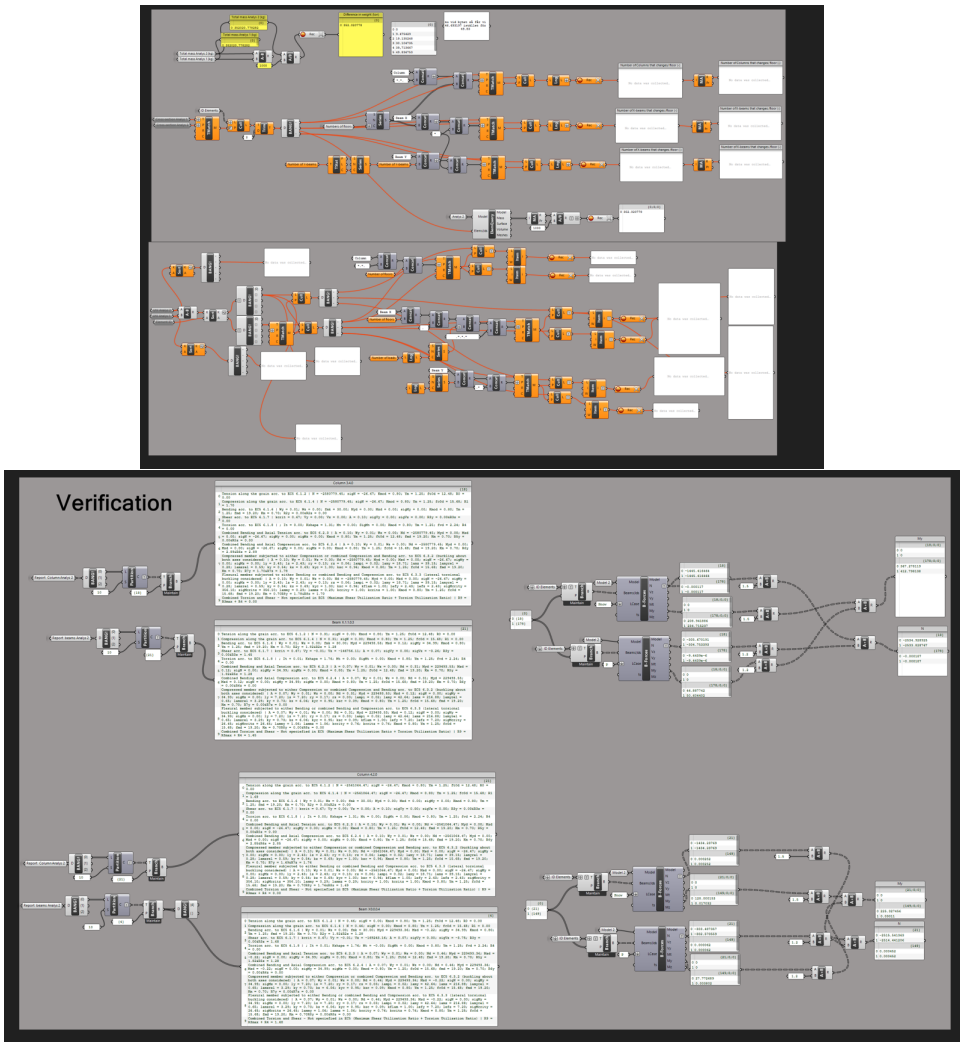
Verification

DEPARTMENT ARCHITECTURE AND CIVIL ENGINEERING
CHALMERS UNIVERSITY OF TECHNOLOGY
Gothenburg, Sweden
www.chalmers.se

CHALMERS
UNIVERSITY OF TECHNOLOGY